universität wien

DIPLOMARBEIT

Titel der Diplomarbeit

„Investigation of the signal transduction mechanisms of activin beta E and its function for malignant growth“

Verfasserin

Emine Sahin

angestrebter akademischer Grad

Magistra der Naturwissenschaften (Mag^{a}.rer.nat.)

Wien, 2011

Studienkennzahl lt. Studienblatt:	A 441
Studienrichtung lt. Studienblatt:	Diplomstudium Genetik-Mikrobiologie (Stzw)
Betreuerin / Betreuer:	Ao. Univ. Prof. Mag. Dr. Wolfgang Mikulits

I dedicate this diploma thesis to my mother Safiye Şahin and my father Osman Şahin, and I would like to express my thankfulness for their love, support, encouragement and care.

Herzaman yanimda olan annem Safiye Şahin ve babam Osman Şahin´e bana gösterdikleri sevgi ve desteklerinden dolayi sonsuz tesekkür ediyorum ve bu tezi onlara armağan ediyorum.

Acknowledgments

I would like to thank

my supervisor ***Dr. Michael Grusch*** for giving me the chance to work on this diploma project and for his never-ending patience,

Dr. Wolfgang Mikulits for appraising this thesis,

Dr. Mir Ali Reza Hoda, Dr. Balazs Hegedüs and Dr. Georg Krupitza for supporting me during my diploma thesis,

my colleagues ***Julia Münzker***, ***Sara Ghassemi*** *and* ***Waltraud Schrottmaier*** who gave me always a helping hand and provided a wonderful working atmosphere.

Furthermore

I would like to thank my whole family who were always supporting me in every phase of my life,

THANK YOU!

Table of contents

1. Abstract

Background:

Activins belong to the extended transforming growth factor beta superfamily of cytokines which play key roles in e.g. embryonic development, inflammation, growth, differentiation and death of cells to mention just some of their functions. Until now the function and signaling mechanism of activin βE, the latest activin subunit to be discovered, which is prominently expressed in the liver, is unclear. Activin E was found downregulated in hepatocellular carcinoma and elevated in multiple leukemia cell lines. The aim of the present study was to investigate activin E signaling in hepatoma and leukemia cell models and how it could contribute to malignancies.

Methods:

A dual approach was conducted in order to investigate activin E functions in malignant cells. For establishment of stable clones with increased activin E level, expression vectors were generated and transfected via lipofection into cell lines with low endogenous activin E levels. At the same time a lentivirus-mediated knockdown of activin βE was performed in cell lines expressing high endogenous levels of activin E. Additionally a baculovirus expression system was used for the production of histidin-tagged activin E, because recombinant activin E is still not available commercially. Phenotypic differences between stable clones and their respective controls were examined by several *in vitro* assays measuring proliferation, viability, migration, anchorage independent growth, clonogenicity and cell cycle distribution. To find potential pathways activin E might be involved in, 4x44k expression arrays were carried out.

Results:

In MTT and proliferation assays no stimulation or inhibition of proliferation and viability were obtained when activin E levels were elevated or decreased. The cell cycle distribution did not differ between stable clones and control cells. In contrast, Activin βE reduced anchorage-indepent growth in three-dimensional soft agar assays and clone size in clonogenic assays. Migration assays revealed a slightly reduced motility in lateral migration and increased ability to pass through pores of transwell membranes when activin E levels were elevated. Baculovirus-produced Histidin-tagged activins were able to dimerize but bioactivity of the recombinant proteins could not be achieved, since the generated recombinant activin A could not activate Smad2/3 phosphorylation. The expression array revealed that several apoptosis-related genes were upregulated in activin E overexpessing cells, and the related cytokine activin A was strongly down-regulated in one of the hepatome cell lines. Several other genes involved in different signalling cascades were regulated and need further investigation.

Conclusion:

Long-term examination of activin E overexpressing cells reveals anti-proliferative effects, especially in *in vivo* like experiments. Activin E crosstalks with multiple signaling cascades but cannot be connected to a certain receptor, thus signaling mechanisms need further investigation.

2. Zusammenfassung

Hintergrund:

Aktivine gehören zur TGF-β Familie an Wachstumsfaktoren und spielen eine wichtige Rolle in der Embryonalentwicklung, in Entzündungsvorgängen, in Wachstum, Differenzierung und Zelltod um nur einige Funktionen zu erwähnen. Bis heute sind die Funktion und der Signaltransduktionsmechanismus von Aktivin βE, der als letztes entdeckten Untereinheit, welcher vor allem in der Leber exprimiert wird, unklar. Aktivin E ist herabreguliert im Leberzellkarzinom und überexprimiert in vielen Leukämie Zelllinien. Das Ziel dieser Studie war, den Signalmechanismus von Aktivin E in Hepatom und Leukämie Zelllinien zu untersuchen und herauszufinden, wie es zum malignen Wachstum beiträgt.

Methoden:

Für die Untersuchung der Funktionen von Aktivin E in malignen Zellen wurde ein Doppelansatz durchgeführt. Für die Etablierung von stabilen Klonen mit erhöhter Aktivin E Expression wurden Expressionsvektoren generiert und durch Lipofektion in Zellen mit niedrigem endogenem Aktivin E transfiziert. Gleichzeitig wurde Aktivin E mittels sh-Lentiviren in Zelllinien mit relativ hoher Aktivin E Expression hinabreguliert. Zusätzlich wurde ein Baculovirus Expressionssystem angewendet, um rekombinantes Aktivin E zu produzieren, welches bis heute noch nicht kommerziell erhältlich ist. Mittels unterschiedlicher *in vitro* Assays wurden stabile Klone mit Kontrollzellen verglichen und auf phänotypische Unterschiede bezüglich Proliferation, Viabilität, Adhäsions-unabhängiges Wachstum, Klonogenität und Zellzyklusphasenverteilung untersucht. Um potentielle Signalkaskaden zu detektieren, in die Aktivin E involviert ist, wurden Expressionsanalysen mit 4x44k Expressionsarrays durchgeführt.

Ergebnisse:

Überexpression oder verminderte Expression von Aktivin E zeigte in MTT- und Proliferationsuntersuchungen keine stimulierende oder inhibierende Wirkung auf die Proliferation oder Viabilität der jeweiligen Zelllinien. Die Verteilung der Zellzyklusphasen war ebenfalls unverändert zwischen stabilen Klonen und Kontrollzellen. Im Gegensatz dazu reduzierte eine Überexpression von Aktivin E die Proliferation im Soft Agar Assay für Adhäsions-unabhägiges Wachstum, und die Größe der Klone im Clonogenic Assay. In Migrationsassays hatten Aktivin E überexprimierende Zellen eine reduzierte laterale Motilität, jedoch eine erhöhte Fähigkeit durch Poren von Membranen zu wandern. Histidin-epitopmarkierte Aktivine konnten dimerisieren, aber eine Bioaktivität konnte nicht nachgewiesen werden, da das produzierte rekombinante Aktivin A keine Smad2/3 Phosphorylierung auslösen konnte. Die Expressionsanalyse zeigte, dass einige in der Apoptose involvierte Gene durch Aktivin E hochreguliert wurden, während das verwandte Zytokin Aktivin A stark herab reguliert war. Diverse andere Gene, die in verschiedene Signalkaskaden involviert sind, waren zusätzlich stark reguliert und sollten weiter untersucht werden.

Schlussfolgerung: Bei Langzeitversuchen mit Aktivin E überexprimierenden Zellen werden anti-proliferative Effekte beobachtet, vor allem in *in vivo* ähnlichen Experimenten. Aktivin E interagiert mit vielen Signalkaskaden ohne bisher einem bestimmten Rezeptor zugeordnet werden zu können.

3. Introduction

3.1. TGF -β family

The transforming growth factor beta (TGF-β), as a multifunctional growth factor, is a member of a superfamily of cytokines including TGF-β isoforms, activins, growth and differentiation factors (GDFs), bone morphogenetic proteins (BMPs), myostatin, Muellerian inhibiting substance (MIS) – and several others- , which are involved in a wide range of cellular processes like proliferation, differentiation and apoptosis (Deli et al., 2008; Nagaraj et al., 2010). Discoveries demonstrate that cytokines of the TGF-β superfamily, which includes more than 40 ligands (Chen et al., 2006) also control embryonic development, wound healing (Zhang et al., 2004) and angiogenesis (Nagaraj et al., 2010). Surely, various other roles in growth and development have yet to be discovered.

3.1.1. TGF-β Signaling

The canonical TGF-β signaling process is relatively simple *(Figure 1)*. TGF-β signals through so called type I and type II serin/threonine kinase receptors (Fischer et al., 2005). Ligand binding to the type II receptor leads to type I receptor recruitment and its phosphorylation due to the intrinsic kinase activity of the receptor (Nagaraj et al., 2010; Zhang et al., 2004). Further on, the type I receptor phosphorylates receptor regulated cytoplasmatic effectors of the SMAD-family (R-SMAD) which then can associate with downstream signaling mediators, the so called Co-SMADs (Massague, 2008). Activation of Co-SMADs through phosphorylation leads to translocation of the R-SMAD-Co-SMAD complex into the nucleus and regulation of the transcription of target genes (Massague, 2008). Through cross-talk with additional proteins,

however, the TGF-β receptors can activate multiple signaling pathways in a SMAD-dependent or independent manner (Nagaraj et al., 2010).

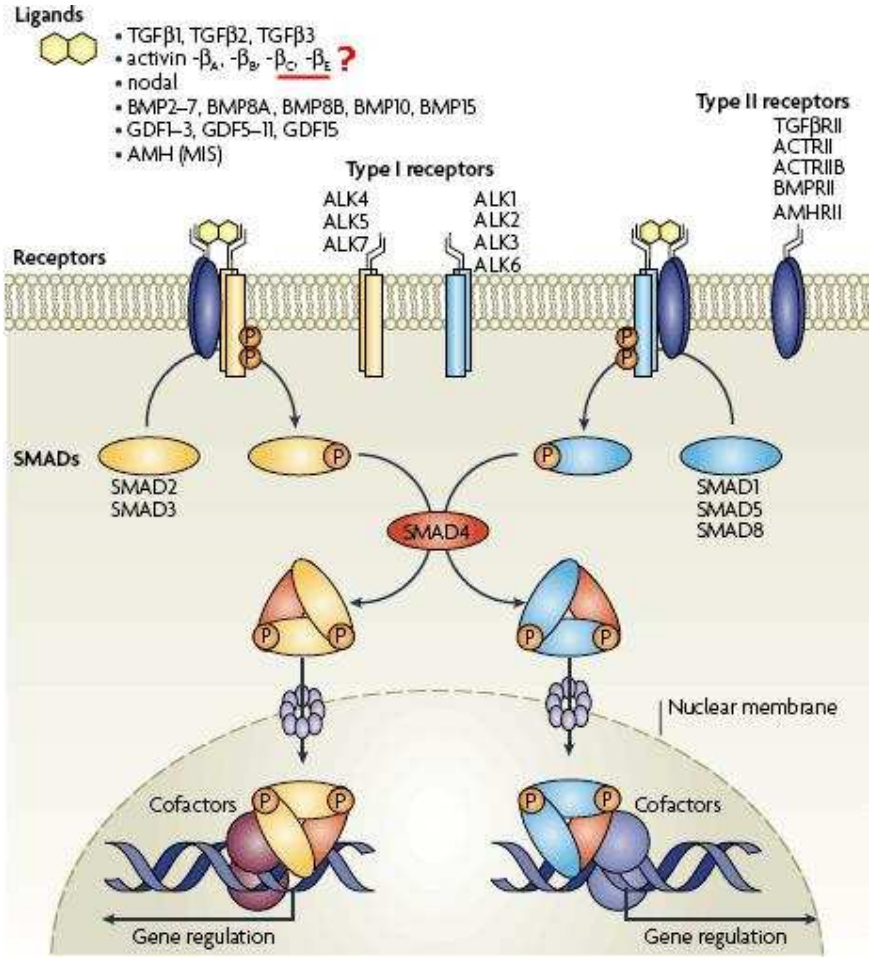

Figure 1: Schematic overview of SMAD-dependent TGF-β signaling (Schmierer et al., 2007).

3.1.2. TGF-β functions in cancer

Activation of TGF-β target genes can lead to pathological events like growth, invasiveness and metastasis of cancer cells (Fischer et al., 2005). It is thought that on the one hand TGF-β acts as a tumor suppressor with a growth inhibitory function in healthy epithelial cells or in early malignant stage by negatively regulating

proliferation (Fischer et al., 2005). In hepatocytes, for instance, TGF-β signaling leads to cell-cycle arrest and apoptosis (Oberhammer et al., 1991; Oberhammer et al., 1992). On the other hand TGF-β acts in a tumor promoting fashion on advanced cancer cells, it stimulates fibroblastoid cells for growth and the production of extracellular matrix. TGF-β, as an angiogenetic factor influences endothelial cells and induces angiogenesis (Fischer et al., 2005). Furthermore it has immunosuppressive properties, for instance through inhibition of T cell proliferation, and in consequence modulates the tumor stroma (Naber et al., 2008). The fact that TGF-β is not found in healthy adult liver, but overexpressed in HCC cells leads to the notion that there is an autocrine stimulation mechanism/machinery of TGF-β signaling (Bedossa et al., 1995).

3.2. Activins and Inhibins

Inhibins and activins are non steroidal dimeric polypeptide hormones (Groome et al., 1993). Gonadal activins play an important role in the production of the structurally unrelated pituitary follicle stimulating hormone FSH and as discoveries meticulously demonstrated also in the maintenance of bone mass and strength (Perrien et al., 2007). Activins were first described as inducers of FSH secretion, the designation "activin" stems from this activity (Harrison et al., 2004). Later multiple other processes were linked to activins, which are structurally related to each other (Woodruff, 1998). In contrast, 1932 another isolated hormone demonstrated suppressing effects on FSH secretion of the anterior pituitary and was designated inhibin (McCullagh, 1932). Inhibins share the β subunits (see below) with activins, but lead to altered activities, when compared with activins (Kingsley, 1994). Previous research results on the expression pattern of activins demonstrate that βA and βB subunits were expressed in almost all tissues, especially in reproductive organs (Vejda et al., 2002). βC and βE expression is especially prominent in the liver, but also occurs at lower levels in a limited number of additional organs (Fang et al., 1997;

Hashimoto et al., 2002; Vejda et al., 2002). High inhibin α mRNA amounts were only detected in adrenal and gonads (Phillips et al., 2009).

3.2.1. Activins - Structure and synthesis

Activins, pluripotent growth factors, which originally were known as reproductive factors, can appear as homo- or heterodimers (Wharton et al., 2009) *(Figure 2)* made up of four different β subunits in mammals (βA, βB, βC, βE), each encoded by its own gene (INHBA, INHBB, INHBC, INHBE). Many possible combinations of homo- (activins A, B, C, E) or heterodimers (AB, AC, AE, BC) can be formed but it is still unclear, how many combinations are actually formed in the body (Kreidl et al., 2009; Wada et al., 2005). There is the opportunity to form activins by dimerization of two β subunits or alternatively, inhibins can be formed by dimerization between one β and one α subunit (Ling et al., 1986). The most common forms are Activin A, B and AB. Additionally, activin βD has been described so far only in Xenopus laevis (Oda et al., 1995) and might play a role in embryogenesis due to axis formative and mesoderm inductive qualities (O'Bryan et al., 2000; Oda et al., 1995). As with other members of the TGF-β family, the same structure with nine conserved cysteines in the mature peptides can be observed in the activin β subunit (Hashimoto et al., 2002). The sixth is used for dimerization, the other eight cysteines are necessary to form intramolecular disulfide bonds, which determine the folding of the peptides (Hashimoto et al., 2002). Activins are secreted as dimers of the mature peptides and no additional processing is necessary in the extracellular space to achieve bioactivity (Mason, 1994). The entire open reading frames of the β subunits of activins encode for precursors with 350-460 amino acids (aa), which weigh between 38 and 50 kDa (Grusch et al., 2008). The NH_2 terminus bears a signal sequence which gives rise to a peptide of 19 hydrophobic amino acids and additional cleavage at a pentabasic cleavage site – aa 232 – 236 - in the ER and in the early Golgi releases the mature

carboxy –terminal peptides with either 115 or 116 aa (Hashimoto et al., 2002; Kingsley, 1994) *(Figure 3).* Also the activin βE subunit has a signal sequence typical for secretion as well as a potential cleavage site indicating its synthesis as a large precursor and subsequent processing. Phylogenetically on the one hand βA and βB can be grouped together and on the other hand βC and βE (Rodgarkia-Dara et al., 2006). The latter two are encoded by closely linked (with respect to chromosome position) genes and most likely developed through tandem duplication (Fang et al., 1997).

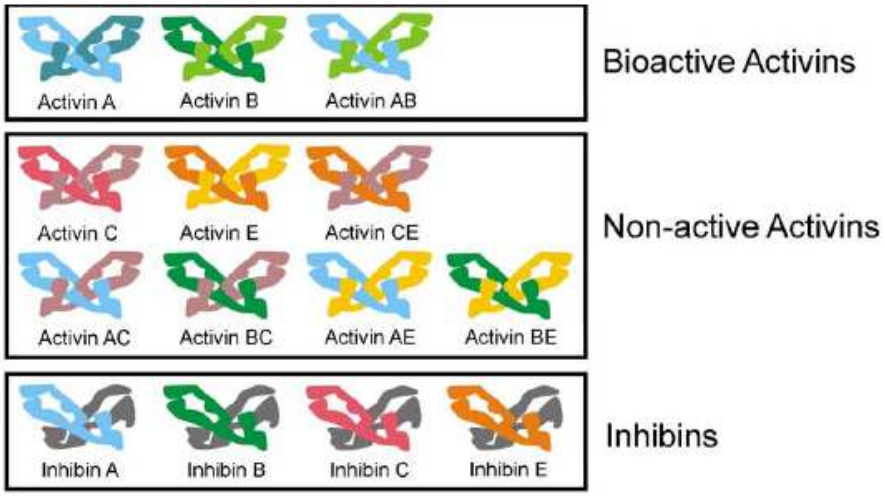

Figure 2: Dimer formation of activins and inhibins: activins are made up of two β subunits; inhibins are formed by dimerization between one β and one α subunit. Adapted from (Phillips et al., 2009).

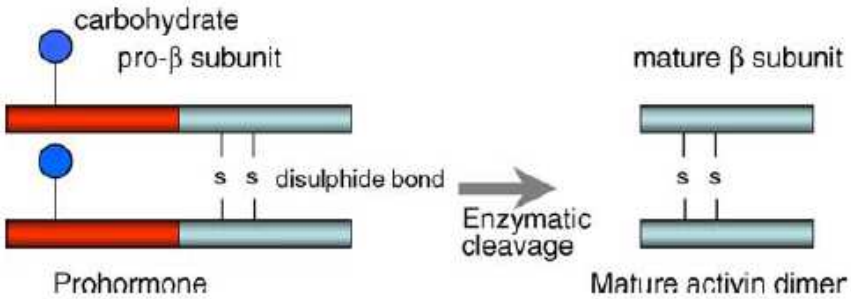

Figure 3: Dimer formation of activin: the dimerized propeptide is enzymatically cleaved to produce the mature peptide (Phillips et al., 2009).

3.2.2. Activins - Signaling

Activins A, B and the heterodimer AB initiate their biological activity, like most members of the TGF-β superfamily, through type I and type II transmembrane serine/threonine kinase receptors whereof various forms exist (Attisano et al., 1996; Pangas et al., 2000). Activin A, the signal transduction of which is best characterized, binds at first a type II receptor, whereof two types were identified ActR-II (A) and ActR-IIB (Abe et al., 2004; Pangas et al., 2000). This binding results in recruitment and phosphorylation of the type I receptor (Attisano et al., 1996) For activin A as ligand, the main receptor is ALK 4 (Activin receptor-like kinase) also called ActR-IB or ACVR1B (Tsuchida et al., 2004). Activins B and AB prefer to signal via ALK7 as type I receptor (Tsuchida et al., 2004). Receptors activated by activin C have not been detected so far. One study demonstrated that activin C was not in a competition with activin A for binding of the receptor (Wada et al., 2004) and chimeric activin containing the receptor binding sequence of βC instead of βA caused indeed type II receptor binding but did not have the ability to recruit ALK 4 (Muenster et al., 2005).
The phosphorylated and activated receptors interact and activate downstream signaling effectors, SMADs, which in turn translocate into the nucleus and regulate transcription (Abe et al., 2004). A distinction is drawn between receptor SMADs (R-SMADs: 1, 2, 3, 5, 8), common mediator SMADs (Co-SMAD 4) and SMADs with inhibitory function (SMADs 6 and 7). Which SMAD molecules get recruited, depends on the activated receptor *(Figure 4).* BMP signaling leads to SMAD 1, 5 and 8 recruitment and activin A and TGF-β receptors have SMADs 2 and 3 as downstream effectors (Heldin et al., 1997; Wharton et al., 2009; Zhang et al., 2004). In spite of this, it has to be kept in mind that SMAD signaling cross talks with other signaling pathways (Wharton et al., 2009). Signal transduction by activin A for instance involves also SMAD-independent pathways like MAP-Kinase and Akt cascades, JNK, RhoA, p38 and MEKK1. There is substantial evidence that activin signaling underlies a tight regulation on the one hand by antagonists of activin signaling, on

the other hand production of activin subunits at the transcriptional or translational level is temporarily and spatially controlled. The glycoprotein follistatin (Fst) which is especially expressed in activin expressing organs, binds mature activin A (Tuuri et al., 1994) with high affinity (Kd 50-680 pM) (Harrington et al., 2006; Schneyer et al., 1994; Sugino et al., 1993), which annuls activin A receptor association and thus signal transduction (de Winter et al., 1996). Besides activin A, early studies show that follistatin binds also to activin E (Hashimoto et al., 2002). To go into detail of Fst action, one activin dimer is clenched by two Fst molecules thus hiding its important parts for receptor binding and other residues (Thompson et al., 2005). Activins A, B, AB, E, and additionally other TGF-β family members such as myostatin, or several BMPs can all act as binding partners for follistatin or follistatin-like 3, which is related to follistatin and shares a similar ability in activin binding (Tsuchida et al., 2000). Receptor binding by various TGF-β superfamily members is not very exclusive. Quite a few of the BMPs and myostatin all signal via ActR-IIB (Rebbapragada et al., 2003). Inhibins use their β subunits to bind type II receptors and additionally they can form a complex with TGFβ type III receptor, also designated betaglycan (Lewis et al., 2000). Due to the fact that the α subunit of inhibin is not capable to bind type I receptors activin signaling is repressed (Cook et al., 2004; Lewis et al., 2000).

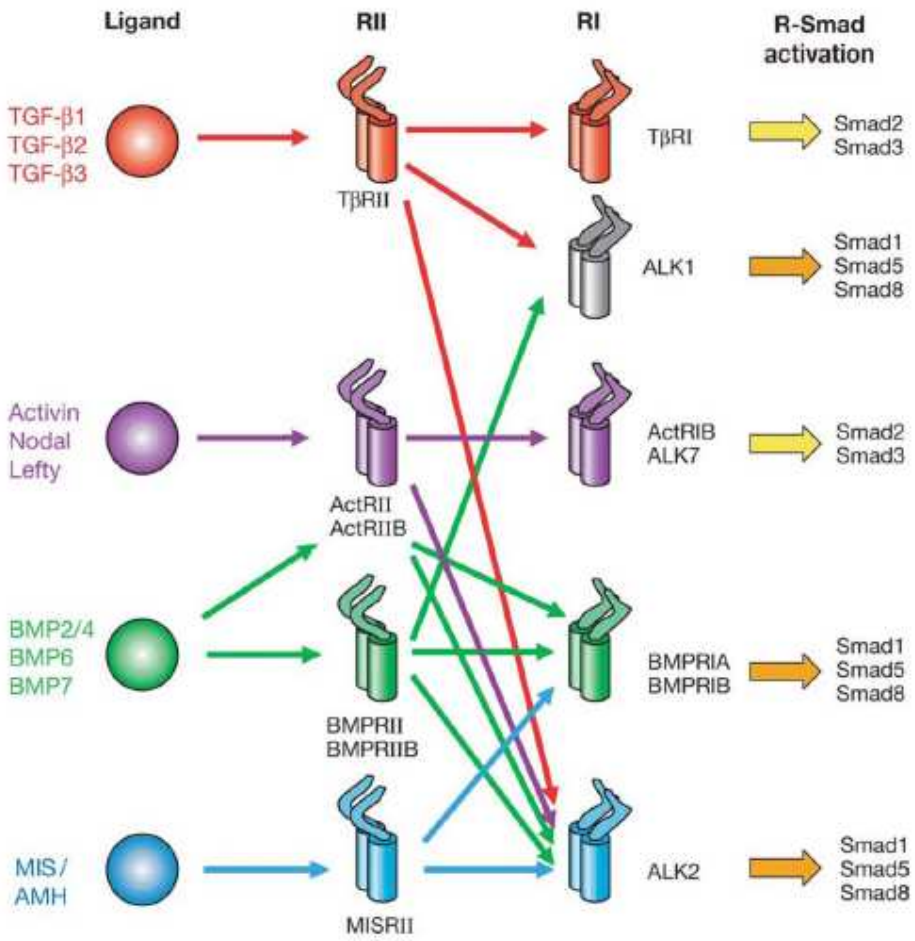

Figure 4: TGF-β superfamily ligands, receptor isoforms and corresponding downstream effector SMADs (downloaded from: http://www.biologie.uni-regensburg.de/Biochemie/Deutzmann/Signal_WS/TGF_SigTrans_web.pdf; accessed 2011-06-29).

3.2.3. Activins - Function

Activin signals have essential roles in a wide range of biological processes in different tissues and as consequence their deregulation can lead to tumor development, which is well documented by different research groups. In reproductive and endocrine organs activins demonstrated relation to tumorigenesis (Risbridger et al., 2001). In many processes like mesoderm induction, erythroid differentiation (Yu et al., 1987), gonadal functions, somatostatin expression (Sekiyama et al., 2009) stem cell biology, inflammation, reproductive biology, cell

death induction, fibrosis and wound healing activins are found to be involved as important regulators (Chen et al., 2006) and the list is still not complete.

Activin A, also functionally the best characterized member of the activin cytokines, arrests growth of prostate gland cells, adrenal gland cells, liver cells and mammary gland cells (Liu et al., 1996; Spencer et al., 1990; Wang et al., 1996; Zauberman et al., 1997) and is involved in regulation of hippocampal long term potentiation (Shoji-Kasai et al., 2007). Additionally, activin A stimulates cell growth of fibroblasts, osteoblasts and keratinocytes (Chen, Lui et al. 2002). In neuronal cells activins A and B behave as survival factors (Kupershmidt, Amit et al. 2007). Due to the expression of activin A by various immune cell types during inflammatory processes, mediator functions in immune responses count to the widespread actions of activin A (Ebert et al., 2007; Eramaa et al., 1992; Phillips et al., 2009; Scutera et al., 2008).

Cripto, which is implicated in the TGF-β signaling pathway, has been shown to inhibit activin signaling and to be highly overexpressed in breast cancer, a cancer cell model, which has low levels of activin and its receptors by down regulation (Liu et al., 1996). Another activin antagonist, follistatin-like 3 also called follistatin–related gene (FLRG) has high expression levels in breast cancer compared to healthy tissue and silencing of FLRG expression inhibits breast tumor growth and at the same time restores responsiveness to activin A (Razanajaona et al., 2007). In melanoma cell lines and liver cancer follistatin is detectable at high levels and at the same time the responsiveness to activin is reduced (Rossmanith et al., 2002; Stove et al., 2004). Follistatin was able to suppress metastasis formation in small cell lung cancer cells (Ogino et al., 2008) and was shown to be involved in v-src connected oncogenic transformation of fibroblasts in chicken embryos (Masker et al., 2007) and in gastric cancer (Kang et al., 2008). Although activin A up-regulation is found in many tumor models, it is not a general observation. Thus the pro- or antitumorigenic character of activin A depends on the cancer tissue type and activins and their antagonists are closely connected to tumor development in several organs. Activin βA knock-out

mice showed craniofacial defects and postnatal lethality. Activin βB knock-out mice had defects in female reproduction and the development of eyelids was disturbed (Schrewe et al., 1994; Vassalli et al., 1994).

Activin C, which acts as an opponent of activin A is increased in testis, prostate and liver tumors (Gold et al., 2009). Activin C overexpressing transgenic mice demonstrated infertility, enlarged livers and prostate diseases with decreased SMAD2 levels in the affected organs, indicating inhibition of activin A signaling in vivo (Gold et al., 2009). Mice lacking activin βC or βE developed normally and the liver was not malfunctioning (Lau et al., 2000). Since βC expression is high in the liver, activin βC might act as a regulator of hepatic activin βA levels (Butler et al., 2005). Briefly, in vitro βC overexpression induced contradictory consequences in growth of different cell lines (Butler et al., 2005; Mellor et al., 2003; Mellor et al., 2000; Vejda et al., 2003; Wada et al., 2004) which is not surprising considering the fact that contradictory effects on growth were also demonstrated for other TGF-β members.

3.3. Activin βE – Signaling and Function

Activin βE, was the latest activin subunit to be discovered and filed into the activin branch of the TGF-β superfamily, of which the common roles have yet to be defined *(Figure 5).* It was first described and detected in the mouse (Fang et al., 1996), followed by identification of orthologs in rat (O'Bryan et al., 2000) and human (Hashimoto et al., 2002). In addition to homodimeric activin E, previous studies suggest that the βE subunit can also form the heterodimers CE and AE (Vejda et al., 2002). The formation of inhibin E (α:βE) and activin BE has not been demonstrated so far.

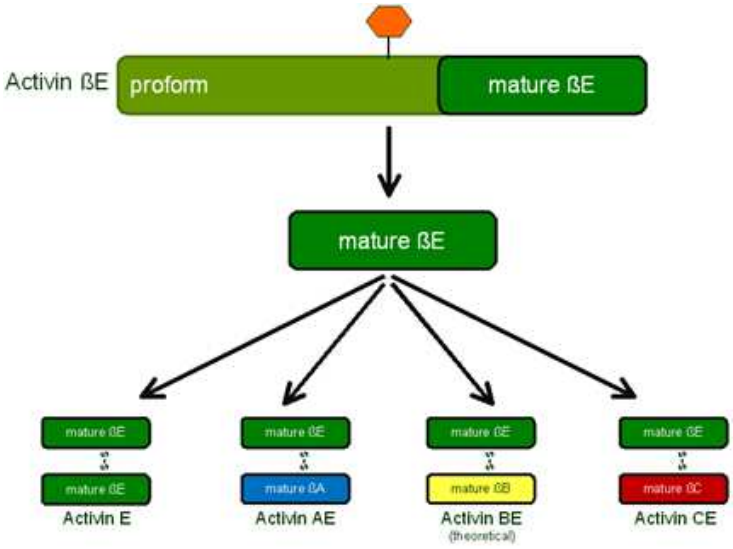

Figure 5: Synthesis of activin E and dimerization possibilities with other activin subunits. (Emanuel Kreidl, Diploma Thesis at the University of Vienna, 2008).

Activin βE signaling mechanisms have not been identified till now. Previous discoveries suggest that activin E does not signal via activin A receptors in contrast to activin A (Emanuel Kreidl, Diploma Thesis at the University of Vienna, 2008). Furthermore activin E does not block activin A signaling (Emanuel Kreidl, Diploma Thesis at the University of Vienna, 2008). In the course of investigating the signaling mechanisms of activin βE, conditioned media from cells with high transient expression of activin βE did not activate SMAD2 phosphorylation in HepG2 cells and VM48 melanoma cells. Studies demonstrated that βC expression in cells co-expressing other activin subunits including βA lead to more heterodimerization and less homodimeric activin A and thus alterations in induction of signal transduction (Mellor et al., 2003). Similar mechanisms might also apply to activin βE. In addition, activin βE is a target for RASSF1A, a tumor suppressor which is often epigenetically silenced in several tumor entities and which leads to decreased cell proliferation after reexpression in cancerous cells (Chow et al., 2006). Overexpression of RASSF1A led to activin βE expression stimulation, whereas RASSF1A knockdown led to INHBE down regulation (Chow et al., 2006). Chow, Lam et al. 2006 demonstrated also that

Inhibitor of DNA binding 2 (Id2), a potential oncogene which is known as a TGF-β target (Lasorella et al., 2001), was downregulated when activin βE levels were elevated. Also in case of activin βE a crosstalk with different signaling pathways has to be considered, due to the fact that the INHBE gene was e.g. a reported target for hedgehog signaling (Katoh et al., 2008). In connection with activin βE regulation, important transcription factor SP1 binding sites for basal activin βE expression were identified in previous studies of our group (Alev Deli, Diploma Thesis at the University of Vienna, 2008). Besides, Trichostatin A and sodium butyrate were found to act as potent inducers of activin βE, whereas dexamethasone and interferon (IFN) gamma prevented the expression of activin βE.

The screening of activin appearance in many tumor entities led to the observation that in multiple leukemia cell lines activin βE is highly expressed, most notably in the K562 CML leukemia cell line (Rodgarkia-Dara personal communication and manuscript in preparation). Screening of human peripheral blood mononuclear and healthy bone marrow cells revealed that βE was nearly undetectable in bone marrow, whereas elevated levels of βE were found in leukemia cell lines.

Investigation of βE expression indicated main expression in hepatocytes and decreased expression levels in multiple hepatoma cell lines (Vejda et al., 2002; Vejda et al., 2003). After liver damage activin βE mRNA was upregulated and in hepatocellular carcinoma (HCC) βE is downregulated. At this point it has to be mentioned that activin A is contrarily expressed in case of liver damage, where its mRNA levels are decreased (Deli et al., 2008). Observation of developing mouse liver revealed the interesting fact that activin βE was undetectable until very late embryonic development stages and the peak was at birth (Lau et al., 2000). Previous data of our research group from a study focusing on the relationship between activin expression and feeding conditions of rats demonstrated noticeable changes in activin βA and βE expression whereas βC mRNA levels hardly changed. Fasting led to higher activin βE and βC mRNA levels and lower activin βA levels in fed controls

(Rodgarkia-Dara et al., 2006). Several studies show that activin βE is abundantly expressed in hepatocytes, whereas it is reduced in dedifferentiated hepatoma cells. Overexpression of activin βE in rat AML12 cells and human hepatoma cell lines HepG2 and Hep3B induced apoptosis through caspases and reduced proliferation rates (Vejda et al., 2003; Wada et al., 2005). Furthermore in cultured hepatocytes, in exocrine pancreas by inhibiting acinar cell growth (Osamu Hashimoto) and in mouse liver cells the pro-apoptotic behavior of activin βE was observed indicating a role in regulation of cell number (Chabicovsky et al., 2003; Hashimoto et al., 2002; Wada et al., 2005). Nevertheless, it is still an open question, how activin βE exerts this effect and which signaling receptors are involved. Transient overexpression of activin βE also led to inhibition of DNA synthesis (Chabicovsky et al., 2003). In connection with hypoxia, gene chip analysis illustrated changed INHBE mRNA levels in HepG2 cells (Fisher et al., 2005). INHBE gene mutation is additionally observed in human breast and colorectal cancer (Sjoblom et al., 2006). Lau et al. demonstrated that mutant mice lacking βE expression grew normally and had no abnormalities compared to wild-type mice. After partial hepatectomy the liver regenerated as in non-mutant mice, questioning an essential role of activin βE in liver growth regulation. This consideration is confirmed by βE overexpressing transgenic mouse studies, where neither macroscopic nor microscopic liver aberrations emerged (Hashimoto et al., 2006). Studies focusing on the inflammation-stimulating behavior of activin βE illustrated significantly increased levels of βE after injection of lipopolysaccharide (LPS) into rats (O'Bryan et al., 2000). Activin βE expression seems to be fine tuned in many regulatory processes, as applies to all activins. Induction of osteogenic differentiation in human mesenchymal cells led to strongly elevated INHBE expression together with TGF-β1 and TGF-β2 increase (Martin et al., 2010). Sekiyama et al. used βE overexpressing transgenic mice for behavior research and concluded, that male and female activin βE overexpressing mice had less anxiety and more combativeness. Subsequently, stress resistance differences in wild-type and βE overexpressing mice were investigated. The number of c-Fos positive cells in the

hypothalamic paraventricular nucleus (PVN) was reduced in transgenic mice as it is in response to acute stress, indicating an activin βE influence on the hypothalamic-pituitary-adrenal axis (Sekiyama et al., 2009). Endoplasmic reticulum (ER) stress triggered e.g. by protein load of unfolded or misfolded proteins necessitates ER differentiation. Dombroski et al. investigated gene expression after ER stress induction in human B cells and registered INHBE and very low density lipoprotein receptor (VLDLR) augmentation. Subsequent expression analysis after ER stress in human fibroblasts with likewise results confirmed the previous observations (Dombroski et al., 2010).

In the course of assessing possible functions of activin βE in glucose metabolism in liver cells, more precisely the effects of insulin on activin βE, Hashimoto et al. noticed stimulatory effects of insulin on βE expression (Hashimoto et al., 2009). These observations differ from previous studies, which illustrated higher activin βE levels in fasting mice (Rodgarkia-Dara et al., 2006), where insulin levels could be expected to be decreased. Such findings suggest a complex regulation of activin βE and highlight the necessity of more knowledge about this cytokine. Hashimoto et al suggested that these converse observations indicate that not only insulin but also other factors control activin βE expression and synthesis. Interestingly, Brown et al. demonstrated that combined loss of follistatin and follistatin-like 3 in mice resulted in augmentation of body fat and resistance to insulin in spite of more insulin synthesis (Brown et al., 2011).

As described above reproductive functions are one of the most prominent involvements of activins. Mylonas et al. investigated the evidence of activin E in human endometrial tissue and arrived at the conclusion that the presence of activin E in human endometrium might have important functions for endometrial maturation and the implantation of blastocyst (Mylonas et al., 2010).

These observations underline the importance to elucidate the biological functions of the gene products of *INHBE* in mammalian physiology and the investigation of their signaling mechanisms.

3.4. vβE - an alternative transcript

In the course of βE analysis an alternative transcript was found to be expressed from the gene encoding βE and was termed vβE. This transcript gives rise to a protein of unknown function lacking a signal peptide and consequently localized to the cytoplasm and nucleus. (Alev Deli, Diploma Thesis at the University of Vienna, 2008). For none of the other activins similar alternative transcripts have been described so far. A chimeric vβE and yellow fluorescent protein transfected in hepatoma cell lines indicated localization to the nucleus and cytosol and stable clones from these cells tended to lose expression of vβE by and by. It is strongly suggested that vβE has completely unrelated functions to activins (Alev Deli, Diploma Thesis at the University of Vienna, 2008) which, however, have not been defined yet.

3.5. Aim: Elucidation of activin beta E functions and signaling mechanisms

Due to the fact that activin βE may contribute to malignant growth, the central aim of this diploma thesis was to clarify, how activin βE affects malignant cells and its signaling mechanisms which have still to be identified. Thus, we used a dual approach, where, on the one hand we carried out a knockdown of activin βE in high endogenous activin E expressing cell lines K562 and HepG2. On the other hand we constructed expression vectors for stable overexpression of activin βE and vβE in Hep3B cells with low βE levels, and in HepG2 cells. For phenotypical characterization of activin E function, several in vitro assays were carried out with stable clones generated from these cell lines. Subsequently, to find potential pathways in which activin E is involved, transcriptome analyses were carried out using genome wide expression arrays with the generated subclones with elevated or decreased activin βE levels. Additionally, a baculovirus expression system was used for production of recombinant activin E. Due to the fact that vβe expression gets gradually lost after transfection, a tetracycline- inducible gene expression system was implemented for overexpression analysis in hepatoma cells.

4. Materials and Methods

4.1. Molecular Cloning

4.1.1. Gel electrophoresis

DNA fragments were separated or analyzed by agarose gel electrophoresis consisting of respectively 1 or 2 % (w/v) agarose (StarLab) in 0.5 x TBE buffer (5.4 g/l tris (Fluka) 2.75 g/l boric acid (Sigma), 1 mM EDTA). Samples were mixed with Vistra-Green loading dye (0.5 µl/ml 10 000 x Vistra-Green (GE Healthcare), 333 µl/ml 6 x loading dye (Fermentas), 66.5 µl/ml 0.5 M EDTA, 250 µl/ml 80% glycerol (Merck)) prior to loading onto the gel. *GeneRuler* 1 kb DNA Ladder (Fermentas) was used as marker to determine the length of fragments. The gel was run in 0.5 x TBE at a voltage of 55 V for 10 minutes (min) followed by an increase to 90 V until the bands were separated properly (power supply: Bio-Rad).

4.1.2. RT-PCR

Control PCRs were performed using *Taq* Polymerase and all steps were conducted on ice. The PCR reactions contained 17.375 µl nuclease-free H_2O, 5 µl of 5 x PCR buffer, 0.5 µl of dNTP mixture (10 mM), 0.5 µl of 5´primer (0.4 pmol), 0.5 µl of 3´primer (0.4 pmol), 0.125 µl of *GoTaq*- DNA polymerase (1.25 units, Fermentas) and 1 µl template DNA. All PCR amplifications were carried out with a protocol of denaturation at 95°C for 2 min, followed by annealing at 50°C for 50 s, and polymerization at 72°C for 1 min, for 30 cycles in a DNA thermal cycler (Biorad).

***Pfu-* PCR** was used to produce insert DNA for vector constructs, due to the proofreading capability of *Pfu*-Polymerase. The PCR reactions contained 40.5 µl nuclease-free H_2O, 5 µl of 10 x PCR buffer with $MgSO_4$, 1 µl of dNTP mixture (10 mM), 1 µl of 5´primer (0.4 pmol), 1 µl of 3´ primer (0.4 pmol) and 0.5 µl of Pfu DNA polymerase (Fermentas) and 1 µl template. All PCR amplifications were carried out with a protocol of denaturation at 95°C for 2 min, followed by annealing at 50°C for 2 min, and polymerization at 72°C for 1 min, for 30 cycles in a DNA thermal cycler.

Colony PCR was used to analyze if bacmid constructs contained the insert of interest. The following approach has been used: 5 µl 10 x Buffer with $MgSO_4$, 1 µl dNTPs (10 mM), 0.5 µl Pfu-Polymerase, and 40.5 µl nuclease-free H_2O. A colony was picked from the plate and diluted in 1 x PBS, whereof 1 µl was used as template for PCR. Above all 1µl upstream primer (0.4 pmol) and 1 µl downstream primer (0.4 pmol) were added to every reaction, spinned down and placed into the thermocycler (40 cycles, 30 sec 95°C, annealing: 2 min 50°C , elongation: 2 min 70°C). DNA was stored at 4°C.

Primers used for RT-PCR procedures are shown in table 1.

Table 1: Primers used for molecular cloning

Primersequences	**Comments**
5´CCCGAATTCCGCCATGCTAGAAATAAAGAGACCAGA-3´	Forward primer for amplification of human vβE, adding an *EcoRI* restriction site upstream of the ATG.
5´TTTGGATCCTAGCTGCAGCCACAGGCCTC-3´	Reverse primer for amplification of hvβE with stop codon and adding a BamHI restriction site.
5´CATCATCATCATCATCATTTGGAGTGTGATGGCAAGG-3´	His_Tag_AbetaA_mat: forward primer for mature form of His_INHBA
5´GTCGTCGTCGAATTCCAGGATGCCCTTGCTTTGGCTGAG-3´	HsActivinbetaA_for: forward primer for proform of INHBA_His
5´ATGATGATGAGGCCTTGGGCTGGGCAACTCTATG-3´	HsActivinbetaA_rev: reverse primer for mature form of His_INHBA
5´ATGATGATGATGATGATGGCCCCGCCGACGCCGGCGAT-3´	pro_betaA_His_rev: reverse primer for proform of INHBA_His
5´CATCATCATCATCATCATCCCACCTGTGAGCCTGCGA-3´	His ACTE mature: forward primer for mature form of His_INHBE
5´TATAAGCTTTAGCTGCAGCCACAGGCCTC-3´	ACTE mit stop HindIII: reverse primer for mature form of His_INHBE
5´ATGATGATGATGATGATGGGTCCTCCTCCTGGCCCGGC-3´	pro His ACTE rev: reverse primer for proform of His_INHBE
5´TTTGAATTCCAGGAGCATGCGGCTCCCTGA-3´	HsβE for around ATG with EcoRI

4.1.3. Dephosphorylation of the vector backbone

Calf intestinal alkaline phosphatase (CIAP: 1u/µg DNA, Fermentas) was used for dephosphorylation of the target vector according to the manufacturer's instructions. For the dephosphorylation procedure 1 µl CIAP was added to the restriction mix and incubated for 30 min at 37°C. Since CIAP works in almost all Fermentas buffers there was no need to change the buffer. Then again 1 µl CIAP was added and incubated for 30 min at 37°C. For inactivation of CIAP enzyme the digest mixture was incubated at 75°C for 10 min.

4.1.4. DNA concentration measurement

To determine the concentration of plasmid DNA from the respective positive clone, a nanodrop (Nanodrop 1000) measurement was performed. To initialize the instrument, 1 µl ddH_2O was loaded on the sample valve. Again 1 µl ddH_2O was loaded and measured for null-adjustment; subsequently 1 µl of the plasmid sample was loaded and OD_{260} measured.

4.1.5. Restriction digests

For diagnostic restriction digests 1 µl plasmid-DNA diluted in 7.5 µl depc H_2O (diethylpyrocarbonate-treated H_2O) was mixed with 1 µl of the respective buffer (Fermentas) and digested with 0.5 µl restriction enzyme (10 u/µl, Fermentas). The restriction mixture was incubated at 37°C for 1-2 hours on the thermoblock. For preparative digests 2-10 µg of plasmid-DNA were restricted with 10-25 units of respective restriction enzymes over night. Buffers and double digest conditions were used as recommended by Fermentas. For partial digests 2 µg DNA with 5 units of

restriction enzyme were prepared in a 50 µl restriction approach and after 5, 10, 20, 40 and 50 min of incubation time 10 µl aliquots were mixed with Vistra-Green loading dye and stored at -20°C for further gel electrophoretic analysis. Klenow Polymerase (Fermentas) was used to generate blunt ends for further blunt end ligation according to the manufacturer´s protocol.

4.1.6. DNA purification

For purification of PCR products or restricted DNA fragments, or to change the buffer of PCR products the Promega *Wizard SV Gel and PCR Clean-Up System* was used according to the instructions of the manufacturer. DNA fragments or PCR products were loaded on a preparative agarose gel and after separation via gel electrophoresis the desired fragments were excised from the gel. The slices were weighed to add subsequently 1 µl *membrane binding solution* per 1 mg gel and to dissolve the mixture through incubation at 65°C. The completely dissolved DNA was transferred to an *SV minicolumn* which was inserted into a collection tube. The tube was incubated 2´ at room temperature (RT) and centrifuged at 16 000 g for 1 min (Eppendorf Centrifuge 5417R). The flow-through was discarded and the column reinserted into the collection tube. Subsequently 700 µl *membrane wash solution* were added to the minicolumn and centrifuged likewise. The flow-through was removed and the column was washed again with 500 µl *membrane wash solution*. To eliminate excess of washing reagent another centrifugation step was performed at 16 000 g for 1 min with the empty assembly. Then the minicolumn was transferred to a 1.5 ml tube (Eppendorf), 50-100 µl nuclease-free water were added directly onto the column and incubated for 2 min. DNA was eluted by recentrifugation (16 000 g, 1 min), the column discarded and the DNA containing flow-through was stored at -20°C.

Membrane binding solution:

4.5 M	*guanidine isothiocyanate*
0.5 M	*potassium acetate (pH 5.0)*

Membrane wash solution

10 mM	*potassium acetate (pH 5.0)*
80%	*Ethanol*
16.7 µM	*EDTA (pH 8.0)*

4.1.7. Ligation

Ligation procedures were performed in 10 µl total volumes over night (o/n) at 16°C or 5-10 min at 25°C for rapid ligation. Insert DNA was in molar excess to the vector (60-100 ng) in a ratio of 3:1 or 4:1. Briefly, the ligation approach contained insert DNA, vector DNA, 1 µl 10 x *T4* DNA ligase buffer (Fermentas) or 2 µl 5 x rapid ligation buffer (Fermentas) for rapid ligation, 1 µl *T4* DNA ligase (5 u/ µl, Fermentas). The mix was then filled up to 10 µl with nuclease-free H_2O. As control for religation a sample was prepared containing nuclease-free H_2O instead of insert DNA.

4.1.8. Transformation

Heat Shock transformation protocol for JM109 *E.coli*

For the transformation procedure competent *E.coli* strains were thawn on ice. In a tube (Eppendorf) 3 µl ligation mix were mixed with 70-100 µl of competent cells (JM109 *E.coli*-strain) and stored on ice for 20 min; followed by a heat shock of exactly 1 min at 42°C and by a quick addition of 1 ml SOC Medium (Yeast extract 0.5% (w/v), trypton 2% (w/v), sodium chloride 10 mM, potassium chloride 2.5 mM, magnesium chloride 10 mM, glucose 20mM, pH 7). Subsequently bacteria were rotated for 1-2

hours (h) at 37°C on a shaking thermoblock and then plated on LB plates (for plates 15 g agar/l LB medium were added) containing the desired antibiotic. The plates were incubated at 37°C over night (Heraeus incubator).

Heat Shock transformation protocol for DH10Bac *E.coli*

For the transformation procedure competent *E.coli* strains were thawn on ice. 4 µl of ligation solution were mixed with 75 µl of competent DH10Bac *E.coli* cells and placed on ice for 20 min followed by a heat shock (42°C, 1 min) and addition of 1 ml SOC medium. Subsequently bacteria were rotated for 1-2 hours at 37°C on a shaking thermoblock and then plated on LB plates containing the desired antibiotic or additive (Table 2). The plates were incubated at 37°C over night (Heraeus incubator). After 48h blue and white colonies were visible.

SOB Medium (for 1 liter)

20 g	trypton
5 g	yeast extract
0.5 g	NaCl
+10 ml	250 mM KCl

pH was set to 7 with NaOH and the medium autoclaved

SOC Medium

SOB Medium	+ 1/100 Vol. autoclaved 1 M MgCl2-solution (10 mM MgCl2)
	+ 1/100 Vol. autoclaved 2 M glucose-solution (20 mM glucose)

Table 2: Additives for growth medium

Additives	Final concentration in growth medium
Ampicillin (Roche)	50 μg/ml
Kanamycin (Fluka)	50 μg/ml
Gentamicin (Sigma)	7 μg/ml
X-gal (Fluka)	100 μg/ml
Tetracyclin (Sigma)	10 μg/ml
IPTG	40 μg/ml

4.1.9. Quick and Dirty Miniprep

"Quick 'n' Dirty" plasmid isolation of overnight cultures:

To screen for potential positive clones, tubes (Falcon) containing 1.5 ml LB (10 g peptone, 5 g yeast extract, 5 g NaCl, in 1 l H_2O, pH 7.0) and the appropriate antibiotic (Table 2) were inoculated with single colonies and incubated on a 37°C shaker at 200 revolutions per minute (rpm) over night. Subsequently a plasmid"quick- mini preparation" was performed from overnight cultures for further control restrictions of plasmids containing the gene of interest. Cells were harvested and dissolved in 700 μl STET buffer (50 mM Tris, 50 mM EDTA, 8% Sucrose, 5% Triton-X). After adding 13 μl lysozyme (10 mg/ml) to each sample, they were inverted and boiled at 100°C for 2 min. With another centrifugation step cell debris, proteins and chromosomal DNA were pelleted and removed with a RNase A-covered toothpick. Plasmid DNA was precipitated with 700 μl isopropanol which were added to the remaining supernatant and the samples were stored at -20°C for 20 min. Subsequently the DNA was pelleted, washed once with 70% ethanol and the pellet

was air dried. The extracted plasmid DNA was resuspended in 15 µl TE-buffer (100 mM Tris, 10 mM EDTA, pH 8) and stored at -20°C.

STET- buffer (500 ml, pH 8)

25 ml 1 M Tris/HCl [50 mM Tris]
50 ml 0.5 M EDTA [50 mM EDTA]
40 g Sucrose
+ bidest. H_2O to 475 ml and then autoclave
+ 25 ml Triton X

Alkaline lysis Miniprep for bacmids (DH10 E.*coli* strain)

1.5 ml of an overnight culture were pelleted (14 000 g, 1 min) and after aspirating the supernatant the cells were gently resuspended in solution I (15 mM Tris-HCl pH 8.0, 10 mM EDTA, 100 µg/ml RNAse A, filter-sterilized and stored at 4°C). 0.3 ml of Solution II (0.2 N NaOH, 1% sodium dodecyl sulphate (SDS), filter-sterilized) was added afterwards and incubated for 5 min at RT. 0.3 ml 3 M potassium acetate was added to the now nearly translucent lysate, mixed gently and placed on ice for 5-10 min. Then the mixture was centrifuged (15 min, 14 000 g, -20°C), the supernatant transferred to a tube containing 0.8 ml isopropanol, inverted a few times and then placed on ice for 10 min. The sample was centrifuged again (14 000 g, 15 min) and the supernatant carefully removed. 0.5 ml of 70% ethanol was added to wash the pellet, the tube was centrifuged again (14 000 g, 5 min) and the supernatant discarded. Finally the DNA containing pellet was dissolved in 40 µl 1 x TE Buffer and stored at 4°C.

4.1.10. Plasmid Isolation: Miniprep

Wizard Plus SV Minipreps DNA Purification System (Promega) was used to obtain "pure" plasmid DNA from transformants. 1.5 ml of bacterial o/n culture was centrifuged (16 000 g, 5 min) and after aspiration of the supernatant the remaining

pellet was resuspended in 250 µl *cell resuspension solution*. Then 250 µl *cell lysis solution* were added, the tube was inverted 4 times and incubated for 3 min at RT. Next 10 µl of *alkaline protease solution* was added to the lysate, inverted again 4 times and the incubation repeated for 5 min at room temperature. Subsequently 350 µl *neutralization solution* were added to the mix and centrifuged at 16 000 g for 10 min. The cleared supernatant was transferred to a spin column which had been inserted into a collection tube. The lysate was incubated for 2 min and centrifuged at 16 000 g for 1 min. The flow-through was discarded and 750 µl *wash solution* was pipetted onto the column, which was recentrifuged at 16 000g for 1 min. The flow-through was discarded again. The same step was repeated with 250 µl of *wash solution*. DNA was eluted in 100 µl nuclease-free water, which was passed through by centrifugation (16 000g, 1 min) after the spin column had been transferred to a sterile 1.5 ml tube and incubated for 2 min. The eluted DNA was stored at -20°C.

Cell Resuspension Solution

50 mM	Tris-HCl (pH 7.5)
10 mM	EDTA
100 µg/ml	RNase A

Cell Lysis Solution

0.2 M	NaOH
1%	SDS

Neutralization Solution (final pH 4.2)

4.09 M	guanidine hydrochloride
0.75 M	potassium acetate
2.12 M	glacial acetic acid

Column wash solution

162.8 mM	potassium acetate
22.6 mM	Tris-HCl (pH 7.5)
0.109 mM	EDTA (pH 8.0)

4.1.11. Plasmid Isolation: Midiprep

The *PureYield Plasmid Midiprep System* (Promega) was used to perform midipreps and obtain pure plasmid DNA in high amounts. 100 ml of bacterial o/n cultures containing positive clones were harvested by centrifugation at 5 000 g for 10 min. The pellet was resuspended in 6 ml *resuspension solution* and afterwards lysed in 6 ml *cell lysis solution* by incubating for 3 min at RT. Subsequently 10 ml *neutralization solution* were added to the lysate and incubated again for 3 min. A *clearing column* was placed into a *binding column* and this assembly onto a vacuum manifold (Promega). The supernatant, which was gained after an additional centrifugation step at 15 000 g for 10 min, was transferred to the *clearing column* and vacuum was applied till the supernatant had passed through each column. The *clearing column* was removed and discarded and 5 ml *endotoxin removal wash* and after that 20 ml *column wash solution* was passed through the *binding column*. Vacuum was applied 30-60 sec longer to remove remaining liquid. 600 µl of nuclease-free water were transferred onto the column and incubated for 5 min. Finally DNA was collected with the *Eluator Vacuum Elution Device* (Promega) by vacuum application and stored at -20°C.

4.1.12. Preparation of glycerol stocks

700 µl of a bacterial o/n culture were transferred to a 1.5 ml tube (Eppendorf) and mixed with 300 µl of 80% glycerol (autoclaved). Prepared glycerol stocks were stored at -80°C for long-term storage.

4.1.13. DNA and RNA precipitation

DNA precipitation was carried out as follows: DNA solution was mixed with 3 x volume (V) 100% EtOH (Merck) and 1/10 V 3M sodium acetate pH 5.2 (Merck) and

incubated over night at -20°C. The next day the mixture was centrifuged at 4°C at 20 800 g for 15 min, the supernatant was discarded. The remaining pellet was washed with 500 µl 70% EtOH and centrifuged again at the same conditions but only for 5 min. The supernatant was aspirated and the pellet air dried for 10-15 min. The precipitate was resuspended in TE buffer in a desired volume.

4.1.14. Sequence analysis

All purified and cloned vector constructs were verified by nucleotide sequencing of the amplified region (Mycrosynth laboratory, CH-9436 Balgach) using CMV forward and reverse primer. For that purpose 0.8 µg DNA were sent to the company. Sequencing results were received via e-mail and alignment with the corresponding sequences in the Refseq database was performed with Clone Manager software.

4.2. Protein biochemistry

4.2.1. Protein precipitation from cell lysates

Cell supernatant was centrifuged at 1 500 rpm for 10 min to remove dead cells and debris. 4 x V of 100% EtOH was added and the precipitate stored at -20°C for at least 24 hours. Subsequently, the supernatant-ethanol mix was centrifuged (15 000 g, 10 min, 4 °C), the pellet was resuspended in 1 ml 100% EtOH and transferred to a 1.5 ml tube. After recentrifugation at the same conditions but only for 5 min the cell pellet was air dried and then resuspended in a desired volume, dependent on the pellet size, in Lysis Buffer II (1 mM EGTA, 150 mM NaCl, 1 mM Na_3VO_4, 1% triton X, 10 mM NaF, 50 mM Tris, complete tab (Roche)). Protein samples were stored at -20°C.

4.2.2. Protein isolation from whole cell extracts

All steps were done on ice. Cells were scratched/scraped off into 1 ml 1 x PBS and pelleted (centrifugation at 1 000 rpm for 5 min). PBS was aspirated and the cell pellet lysed by resuspending in Lysis buffer II, the volume of which depended on cell amount. Prior to usage, the cell lysate was sonicated 2 times for 5 min. Insoluble components were removed after centrifugation at 4°C and 20 800 g for 10 min. The cleared supernatant was transferred to a new tube. Protein samples were stored at -20°C.

4.2.3. Determination of protein concentration

Protein concentration was determined with Biorad Protein Assay Reagent. The protein samples were diluted 1:10 with cell Lysis buffer II. A standard curve, which had been obtained from bovine serum albumin (BSA) dilutions (0.1, 0.2, 0.4, 0.8, 1.0, 1.2 mg/ml) was used to estimate total protein concentration. The assay was performed in a 96-well microtiter plate (Greiner) and Lysis buffer II served as blank. The pipetting scheme was performed according to tables 3 and 4. BSA dilutions and protein sample dilutions were mixed with 190 µl of dilution of the assay reagent (1: 5 with water) and incubated for 10 min at RT. The absorption was measured then at 595 nm using the SynergyHT plate reader (BioTEK) and concentrations determined with Gen5 software (BioTEK).

Table 3: Pipetting scheme of Bradford assay for BSA standard curve

	ddH_2O (µl)	**Lysis Buffer (µl)**	**BSA-Standard (1µg/µl)**	**Bradford reagent (µl)**	**Concentration (µg/µl)**
Blank	9	1	0 µl	190	0
Standard 1	8	1	1 µl	190	0.1
Standard	7	1	2 µl	190	0.2

2					
Standard 3	5	1	4 µl	190	0.4
Standard 4	3	1	6 µl	190	0.6

Table 4: Pipetting scheme of Bradford assay for protein samples

	ddH$_2$O (µl)	**Sample (µl)**	**Bradford reagent (µl)**
Sample	9	1	190

4.2.4. SDS PAGE and Western Blot analysis

SDS gel electrophoresis:

10 or 12% (according to protein sizes to be investigated) discontinuous polyacrylamid (PAA) gels were prepared to separate isolated proteins (Table 5). 5 µl prestained marker (Page Ruler Plus Prestained Protein Ladder, Fermentas) was used to compare and estimate protein weights. Separating (10-12%) and stacking (5%) gels were mixed and prepared according to the table below and topped with isopropanol, which was removed after polymerization with filter paper. 40 µg of protein lysate were mixed with 5 x loading buffer (300 mM Tris/HCl pH 6.8, 60% glycerol, 10% SDS, 0.025% bromophenol blue, under denaturating conditions additionally 7% β-mercaptoethanol), incubated at 100°C for 5 min for denaturation, and loaded onto the gel. Gels were run starting with 55 V until separation of the marker and voltage was increased to 120 V for 2 hours in SDS running buffer (25 mM Tris, 192 mM glycin, 0.1% SDS).

Table 5: Preparation of separating and stacking gels: pipetting scheme

10% Separating gel (10ml)	12% Separating gel (10ml)	5% Stacking gel
3.92 ml distilled H_2O	3.25 ml distilled H_2O	3.6 ml distilled H2O
2.5 ml 1.6 M Tris-HCl, pH 8.8	2.5 ml 1.6 M Tris-HCl, pH 8.8	0.625 ml 0.5 M Tris-HCl, pH 6.8
3.35 ml 30% Acrylamid/Bis; 29:1 (Bio-Rad)	4.02 ml 30% Acrylamid/Bis; 29:1 (Bio-Rad)	0.625 ml 30% Acrylamid/Bis; 29:1
200 µl 20% SDS	200 µl 20% SDS	100 µl 20% SDS
25 µl 10% ammonium persulfate (APS, Merck)	25 µl 10% ammonium persulfate (APS, Merck)	50 µl 10% APS
10 µl Temed (Amresco)	10 µl Temed	7.5 µl Temed

Western Blotting

Separated Proteins were blotted onto a polyvinylidenfluorid (PVDF) membrane, therefore the following assembly was generated: three filter papers were soaked in Towbin transfer buffer (25 mM Tris, 192 mM glycin, 5% MeOH) and placed at the bottom, the PVDF membrane (Hypond-P, GE Healthcare) which was previously activated in methanol, was arranged on the filters, the stacking gel was laid onto the membrane and the assembly was finished by additional three filter papers on the top. Air bubbels were removed and the assembly was placed into the electrotransfer unit, which was filled with transfer buffer. Transfer procedure was carried out with 18 V at 4°C o/n or with 200 mA at 4°C for 2 hours.

The membrane was washed with distilled water and to visualize proteins, the membran was stained with ponceau S (0.5 g/l ponceau S (Sigma), 1 ml/l glacial acetic acid) for 20-30 min, which was removed after the staining procedure by rinsing the membrane with distilled water. By copying the air dried membrane, the staining was recorded. Then the membrane was reactivated with methanol. To avoid unspecific binding the membrane was blocked with TBS-T (TBS: 8 g/l NaCl, 0.2 g/l KCl, 3 g/l Tris, pH 7.4; T: 0.1% Tween 20 (Sigma)) containing 5% skimmed milk powder (Fluka)

under gentle agitation for 1 hour at RT. To remove the blocking solution the membrane was washed 3 times with TBS-T (5 min each).

Antibody incubation

Incubation with primary antibody (Table 6), which was diluted in blocking solution, was performed at 4°C o/n. The next day the membrane was washed 3 times with TBS-T (10 min each) by shaking on a shaker and incubated with the secondary antibody (all used secondary antibodies were from Dako) for at least 1 hour at RT, followed by additional three washing steps with TBS-T and one washing step with TBS (8 g/l NaCl, 0.2 g/l KCl, 3 g/l Tris, pH 7.4) to remove antibody surplus. Finally the membrane was incubated with equal amounts of enhanced chemiluminescent (ECL) solution 1 and 2 (Immun-Star WesternC Kit, Biorad) for at least 3 min and the luminescence was detected on X-ray film.

Table 6: Primary antibodies for Western Blot analysis

Antibody	Supplier	Species	Dilution
Anti - Actβ A	Vale	rabbit	1:5000
Anti - Actβ E	SDI	rabbit	1:1000
Anti - pSMAD2/3	Cell Signaling	rabbit	1:1000
Anti - TotalSMAD	Cell Signaling	rabbit	1:1000
Anti - Histidin		murine	1:1000

4.3. Cell biology

4.3.1. Cell lines and media

Cell lines in Table 7, obtained from the cell culture unit of the institute of cancer research, were cultured at 37°C under a humidified condition of 95% air and 5% CO_2, except SF9 insect cells, which were cultured at 27°C without CO_2. The cell lines were routinely subcultured and kept at subconfluency using PBS (137 mM NaCl, 2.7 mM EDTA, 10 mM Na_2HPO_4, pH 7.4) for washing and Trypsine-EDTA for detaching of the cells. Additives in table 8 were added as appropriate.

Table 7: Cell lines and media

Cell line	Origin	Medium
HEK293	Human embryo renal cortical cells (Graham et al., 1977)	DMEM; [Dulbecco's modified Eagle's medium, (Sigma)] 10% FCS (PAA)
Hep3B	Human hepatoma cell line (Knowles et al., 1980)	RPMI [Roswell Park Memorial Institute medium, (Sigma)]; 10% FCS (PAA)
HepG2	Human hepatoma cell line (Knowles et al., 1980)	MNP [MEME (Sigma)-Minimum Essential Medium Eagle-additionally 1 mM sodium pyruvate (Sigma); 1% non-essential amino acids (PAA)]; 10% FCS (PAA)
K562	Human myelogenous leukemia cell line (Lozzio et al., 1979)	RPMI; 10% FCS (PAA)
Sf9	Ovarian cell line from Spodoptera frugiperda (Vaughn et al., 1977)	Insect Express (PAA); 10% FCS (PAA)

Table 8: Additives to growth media

Antibiotic	Supplier	Final concentration
Puromycin	PAA	0.4-0.6 µl/ml (1x)
Penicillin/Streptomycin (P/S)	PAA	10 µl/ml (1x)
G418-Neomycin	PAA	500 µg/ml

Tissue culture flasks - sizes T 25 (25 cm^2), T 75 (75 cm^2) and T 175 (175 cm^2) - were bought from Greiner Bio-One and BD Falcon. 6-, 12- and 24-well plates were bought from IWAKI and 96 well-plates from PAA.

4.3.2. Freezing

For long-term storage of positive stable cell clones, cells were grown in T 25 tissue flasks in respective full medium until almost fully confluent. Subsequently cells were detached (Trypsin/EDTA), resuspended in medium with 10% serum and containing DMSO (final concentration 50 µl/ml, Amresco) and transferred quickly to cryo tubes (Greiner) each with 1 ml. Cells were cooled down to -80°C over night and then transferred into the liquid nitrogen tank.

4.3.3. Thawing

Ampoules taken out of the liquid nitrogen were thawn in a lukewarm water bath. Immediately, when the cell suspension was thawed, the content was transferred into a 15 ml tube (Falcon) containing 7-10 ml growth medium and centrifuged at 850 rpm for 4 min. The supernatant was removed and the cells resuspended in 6-7 ml fresh culture medium, which was stored at 37°C before usage. Cells were transferred to a T 25 flask and incubated in a humidified incubator, paying attention to not agitate the flasks for at least 24 hours. The next day the medium was removed and replaced with fresh full growth medium.

4.3.4. Cell counting

Cell counting was performed on the one hand via Neubauer chambers (Paul Marienfeld GmbH), on the other hand for specific assays via a multichannel Casy cell counter (Schärfe Systems, Reutlingen, Germany).

4.3.5. Transfection procedure and generation of stable clones

To introduce nucleic acids into cells and generate stable clones, mammalian adherent cells were transfected using either Lipofectamine 2000 (Invitrogen), Fugene 6 (Roche) or Turbofect (Fermentas) according to the manufacturers´ instructions. In brief, one day before transfection 5 x 10^5 cells were plated on each well of a 6-well-plate to gain a certain confluence at time of transfection. The next day a plasmid DNA – medium - transfection reagent mixture, prepared according to instructions, was distributed dropwise onto the cells. 48 hours after transfection the medium of transfected cells was changed to selection medium containing the respective antibiotic and gene expression was evaluated. Since the bicistronic vectors coded additionally for green fluorescent protein (GFP) every two or three days the cells were monitored by fluorescence microscopy. If necessary, the selective medium was changed and after forming of small GFP- expressing clones they were left to grow fully confluent for further sorting with fluorescence activated cell sorting (FACS) for GFP-positive cells. All used media contained penicillin and streptomycin (P/S) to prevent bacterial infections.

4.3.6. FACS sorting

For FACS sorting 5 l filtered 1x PBS, 2 l filtered 70% ethanol and 2 l filtered distilled water were prepared. Additionally 50 ml Falcon tubes containing 35 ml growth medium with 10% FCS were incubated over night at 4°C. Before sorting, the cells were detached (Trypsin/EDTA), pelleted and washed once with 1 x PBS. Afterwards the pellet was resuspended in 1 ml serum-free medium containing penicillin/streptomycin. The growth medium in the 50 ml Falcon tube was removed and instead 5 ml of medium containing penicillin/streptomycin were filled in each of the prepared tubes. Also untransfected cells were prepared for FACS analysis as negative controls. FACS tubes (BD Falcon) containing the cells and falcon tubes containing the growth medium were stored on ice and brought to the FACS analysis and sorting unit (Dr. Herbacek Irene). An appropriate number of GFP-positive cells was sorted and subsequently centrifuged at 800 rpm (Beckman CS-6KR Centrifuge) for 5′. The hardly observable pellet was resuspended in growth medium containing penicillin/streptomycin and G418 and transferred to a fresh culture dish, the size of which depended on the cell number.

4.3.7. RNA extraction

All steps were performed with the usage of filter tips. Total RNA isolation from tissue culture cells was performed with Trizol (Invitrogen) reagent according to the manufacturer´s protocol. After the medium was discarded cells were washed with 1 x PBS and Trizol (1 ml per T25 culture dish) was added onto the cells which were scraped into the Trizol suspension and incubated for 5 min at RT. The lysate was transferred into a 2 ml tube (Eppendorf) and incubated for 10 min with 0.2 ml chloroform/isoamylalcohol (50:1) per ml Trizol used. With a first centrifugation step

(12 000 g, 4°C, 15 min) cell debris were pelleted and the aqueous supernatant transferred into a new tube. 0.5 ml isopropanol per ml used Trizol were added to the transferred supernatant, inverted for nearly 20 seconds (sec) and incubated for 10 min at RT. The precipitate was centrifuged (16 000 g, 4°C, 10 min), the supernatant aspirated and the pellet washed with 1 ml 75% EtOH by an additional centrifugation step (15 000 g, 4°C, 7 min). The supernatant was discarded and the pellet air dried. The RNA pellet was resuspended in 15-50 µl nuclease-free water and stored at -20°C or at -80°C for long-term storage.

Nanodrop RNA measurement was used to determine RNA concentration by absorbance at 260 nm. To ensure integrity 1 µg RNA was analyzed on a 1.5% agarose gel. RNA secondary structures were resolved through treatment of diluted RNA (ad 5 µl with nuclease-free H_2O) with 5 µl urea loading buffer (2 x TBE, 7 M Urea, 13% ficoll or 15% glyecrol) and incubation at 70°C for 3 min. RNA was loaded with 2 µl Vistra-Green onto the gel and gel electrophoresis was performed as described above. The RNA was visualized by Typhoon Trio imager (GE Healthcare).

4.3.8. cDNA synthesis

2 µg RNA were diluted with nuclease-free H_2O to a total volume of 13 µl and incubated at 70°C for 10 min for denaturation. After that, samples were put on ice for 5 min. A reverse transcription mix containing 4 µl 5 x buffer (M-MLV-Promega), 1 µl M-MLV reverse transcriptase (200 u/µl), 0.5 µl ribolock RNase inhibitor (40 u/µl MBI) and 0.5 µl random hexamers (1 µg/µl working stock) was added to the sample and incubated at 42°C for 1 hour for the transcription procedure. The reaction was stopped by additional incubation at 70°C for 10 min and 20 µl nuclease-free H_2O were added to gain a total volume of 40 µl. cDNA quality was tested by performing RT-PCR with primers for a housekeeping gene followed by agarose gel electrophoresis. cDNA aliquots were stored at –20°C.

4.3.9. Expression anlaysis: quantitative RT-PCR

Quantitative real time polymerase chain reaction procedures were always carried out wearing gloves and using filter tips (Starlab).

SYBR-Green-qPCR

A mastermix containing nuclease-free H_2O, *SYBR-Green Master Mix* and respective upstream and downstream primers (each 20 µM) (Table 9) were mixed on ice. In each well of a 96-well plate 1 µl cDNA was pipetted in duplicates for each sample, in selected wells nuclease-free water was pipetted instead of cDNA and served as negative control. The prepared master mix was added to the cDNAs and the plate subjected to PCR by using an ABI 7500 Fast PCR System 1.4 according to the manuals. Used primers are listed in the table 9 below.

TaqMan-qPCR:

A mastermix containing nuclease-free H_2O, *TaqMan qRT-PCR Mastermix* and the respective *TaqMan* (Assay-ID´s in table 10) probe was prepared on ice. In each well of a 96-well plate 1 µl cDNA was layered in duplicates for each sample. In selected wells nuclease-free water was pipetted instead of cDNA and served as negative control. The prepared master mix was added to the cDNAs and the plate subjected to PCR by using an ABI 7500 Fast System 1.4 according to the manuals. The fluorescence was measured after each cycle and evaluated with ABI 7500 Fast System.

As control for cDNA integrity and for normalization, B2M (Beta-2 microglobulin) or GAPDH TaqMan probes or respective primers for SYBR-Green qPCR were used. The qRT-PCR reactions were conducted with the cycling parameters shown in table 11.

Table 9: Primer used for SYBR-qPCR

Gene	Primer sequences	Fragment size (bp)
INHBE	5′GAGACTACAGCCAGGGAGTG-3′/ 5′CCCAGTTCCTGGAAGTCTAC-3′	548
GAPDH	5′CTGGCGTCTTCACCACCAT-3′/ 5′GCCTGCTTCACCACCTTCT-3′	499

Table 10: TaqMan probes used for TaqMan-qPCR

Gene of interest	Assay ID of TaqMan probe
INHBE	Hs00368884_g1
B2M	Hs00984230_m1

Table 11: qRT-PCR parameters

Step	Temperature/Time	Cycles
Initial Denaturation	95°C/ 10 min	1 x
Denaturation	95°C/ 15 sec	40 x
Annealing	60°C/ 30 sec	
Elongation	72°C/ 30 sec	

4.3.10. Knockdown of βE with sh-lentiviruses

Lentiviral shRNA vectors were used for long-term silencing and gene knockdown studies.

Puromycin titration:

First of all a puromycin kill curve was generated for the cell lines selected for knockdown. 16 000 cells in 120 µl full medium were plated in each well of a 96-well plate. The next day various concentrations (0.1, 0.2, 0.4, 0.6, 0.8 and 1 µl/ml) of puromycin were added to selected wells. The cell viability was examined microscopically every two or three days and five days after antibiotic treatment cell

viability was examined with the usage of MTT reagent (EZ4U, Biomedica) according to the manufacturer´s instructions and as described below. The minimum concentration of puromycin that caused 90-100% cell death was used further for selection of lentivirus-transduced clones.

Lentiviral transduction

1.6 x 10^4 cells in full medium were pipetted into the wells of a 96-well plate in duplicates one day before transduction in the case of adherent cells and at the day of transduction in the case of non-adherent cells. At the day of transduction, full medium was removed (by centrifugation and aspiration in case of non-adherent cells), replaced with 110 µl medium containing 8 µg/ml hexadimethrine bromide and incubated for 10 min at 37°C. Finally cells were transduced with a range of volumes (2-5 µl) of lentiviral particles to determine the optimal transduction efficiency; selected wells were not transduced and served as control. The plate was incubated for 24 hours at 37°C in an atmosphere of 5% CO_2. The next day medium was removed and replaced with fresh medium containing puromycin. This procedure was repeated every 3 or 4 days until only resistant colonies remained. Resistant clones were subjected to qRT-PCR to examine knockdown efficiency, expanded for further analysis and frozen for long-term storage.

4.4. Functional characterization of stable clones

4.4.1. Cell vitality and proliferation

4.4.1.1. MTT

MTT cell viability assay was performed by using 3-(4,5 dimethylthiazol-2-yl)-2,5-diphenyltetrazoliumbromide (EZ4U reagent, Biomedica). Briefly, 500-1 500 cells were seeded in each well of a 96-well plate in –at least- triplicates for each clone. Cells were grown for 24 hours and medium was changed to fresh medium (0.1%, 1%, 10% serum concentrations). The cells were incubated for four or five days at 37°C, medium only served as blank control. For detection of living cells incubation with EZ4U solution was carried out for 3-5 hours and the extinction was measured at 450 nm and 620 nm as reference by using a SynergyHT microplate reader (BioTEK). The obtained data were saved and reported with Gen5 (BioTEK) software.

4.4.1.2. Proliferation

To elucidate the cumulative cell number after several times of passaging, cells were seeded in 6-well plates or T25 tissue culture flasks- dependent on their proliferation speed- at a certain density (70 000 – 150 000 cells /well of 6-well plates; 500 000 cells per T25). Every 2nd day cells were trypsinized and resuspended in full medium and an aliquot of 50 µl was subjected to analysis by the Casy cell counter. The primary seeded number of cells or a smaller number were reseeded for all samples and the cell counting and reseeding procedure was repeated every second day, trying to have at least four time points. Cumulative cell numbers were calculated from the cell counts plus diluton factors and growth curves were created with Graphpad Prism 5 software.

4.4.2. Clonogenic survival

To analyze the proliferation of adherent cells by their capability to form colonies on tissue culture plastic, clonogenic survival assays were performed. 1 000-3 000 cells were seeded in each well of a 6-well plate in 2 ml growth medium. When a desired clone sizes were reached cells were fixed and stained with crystal-violet. For this, cells were washed with 1 x PBS and fixed with methanol/acetic acid (3:1) and further stained with 0.1% crystal violet in PBS. Cells were dried and the clonogenic growth behavior documented by photography (Nikon). Clones which were above a specific threshold were counted and after solubilization of the dye with 2% SDS absorption measured photometrically at 560 nm. Unstained wells subjected to 2% SDS as well served as blank controls.

4.4.3. Cell cycle analysis: Propidium iodide (PI) staining and flow cytometry

For PI staining cells were detached, resuspended in 5 ml cold 1 x PBS and pelleted (1 200 rpm, 4°C, 5 min.). The supernatant was removed and the pellet resuspended in cold 70% ethanol for fixation. Fixation was performed either through storage for at least 30 min at 4 °C or over night at -20°C. Prior to staining, cells were pelleted (1 200 rpm, 4°C, 5 min.) and the ethanol-containing supernatant was aspirated. The cells were washed with at least 2 ml cold PBS to remove remaining ethanol with another centrifugation step at the same conditions as before. After removing the supernatant cells were stained with 0.5 ml PI staining solution (0.5 ml cold 1 x PBS, 2.5 µl RNAse A (10 mg/ml stock), 10 µl propidium iodide (2.5 mg/ml stock)) in round-bottom FACS tubes (BD Falcon) which were incubated 10 min at 4°C before measurement (Dr. Herbacek Irene).

4.4.4. Migration

4.4.4.1. Transwell assay

The migratory phenotype of cells was analyzed by transwell assays. The transwell chambers fitted into wells of 24-well plates. 800 µl medium were added into one well of the tissue culture plate. The transwell chamber was placed into the well and 20 000 cells in 200 µl medium were pipetted onto the porous membrane. Incubation time was dependent on the migratory behavior of cells and thus necessitated daily monitoring via microscopy. When a low and countable amount of cells had passed the membrane, the filter was removed and the cells were incubated 24-48 hours longer before staining with crystal violet. Staining and migration results were documented on photographs.

4.4.4.2. Wound healing assay

The migratory phenotype of cells which correlates with metastatic and invasive phenotype was also evaluated by a so called wound healing or scratch assay. The assay was performed in 6-well plates. Confluent cell monolayers were scraped with a blue pipette tip and 3 or 4 scratches of about 1 cm length were created. Subsequently cells were washed to remove detached cells and wound closure was monitored by microscopy at various time points (0 h, 24 h, 48 h, 72 h). Wound closure was recorded on photographs and analyzed with ImageJ software and Graphpad Prism software.

4.4.5. Soft Agar

Soft agar assay to analyze adherence-independent colony formation behavior was performed in 6- well plates. Two water baths were used to keep solutions at the required temperatures. Realization of the assay lasted two days and on the first day the bottom agar was prepared as follows. For a total volume of 50 ml Soft Agar medium 10 ml 10 x RPMI medium (Sigma), 2 ml $NaHCO_3$, 1 ml glutamine, 17 ml autoclaved distilled H_2O and 50 µl folic acid were mixed, brought to a pH value of 8 and then filter-sterilized. Subsequently 20 ml FCS and 1 ml P/S were added and the medium was stored in a 37°C water bath. 1.2% agar solution was prepared and solubilised by boiling and stored at 40°C. The agar solution and soft agar medium were mixed 1:1 and 1.5 ml of agar-medium dilution pipetted into each well of the 6-well plate. Attention was paid to avoid air bubbles in the bottom agar, to avoid too fast cooling of the dilutions during pipetting and to properly distribute the bottom agar through gentle agitation of the plate. Plates were incubated over night at 37°C.

The next day the top agar was prepared. 5 000 -10 000 cells were pelleted (800 rpm, 5 min, RT) and resuspended in 750 µl Soft Agar medium which had 37°C. The agar solution (1.2%) was diluted 1:1 with autoclaved distilled H_2O and 750 µl of it were added to the cell suspension which had then a total volume of 1.5 ml. Cells were distributed onto the bottom agar by gentle agitation, stored for 3 min in the fridge and then put into the incubator. Clone sizes were monitored (over 4-8 weeks dependent on the cell line), clones were counted under the microscope and documented by photography.

4.4.6. Treatment with the demethylating agent 5′-azacytidin

Due to the fact that vβE overexpressing cells lost vβe expression by and by demethylation with 5′-azacytidin was performed to evaluate epigenetic regulation of vβE. 15 x 10^4 stable transfectants, control cells (mock transfected or expressing scrambled shRNA), and not-transfected cells (NTC) were seeded per well of a 12-well plate in 1 ml full medium and incubated at 37°C for 24 hours. The next day medium was replaced with serum-free medium containing 0.5 μM 5′-azacytidin (dissolved in DMSO). Treatment was performed in duplicates and renewed every 48 hours and since the bicistronic plasmid expressed GFP the effect of demethylation was monitored with fluorescence microscopy.

4.4.7. Statistical analysis

Graphpad Prism 5.0 software (Graphpad Software Inc.) was used for statistical calculations and evaluation of significance. P-values < 0.05 were considered to be significant and were marked with an asterisk.

4.5. Transcriptome analysis: Microarray

Expression profiling was performed using microarrays (Agilent Technologies) to find potentially regulated target genes of βE. 44K whole human genome arrays which contain 44 thousand probes and are based on DNA-RNA hybridization were used. We performed two color experiments, where one of the samples was labeled with Cyanine 3-CTP (Cy3) and the other one with Cyanine 5-CTP (Cy5) fluorescent dye.

Before RNA isolation, cells were seeded in T25 tissue culture flasks at equal density and growth medium was changed at regular intervals to keep cells in optimal conditions. RNA isolation was performed using Trizol reagent and then RNA precipitation was carried out as described above. To analyze RNA integrity 150-500 ng RNA were analyzed with Agilent Bioanalyzer 2100 to determine the RNA integrity number (RIN).

Sample combinations were performed according to table 12:

Table 12: Pipetting scheme of one 4 x44 k expression array

	Array 1	**Array 2**	**Array 3**	**Array 4**
Cy3-labeling	Mock or Scrambled	Mock or Scrambled	NTC	βE overexpression or knockdown
Cy5-labeling	βE overexpression or knockdown	NTC	βE overexpression or knockdown	Mock or Scrambled

All steps were carried out on ice, using gloves and filter tips. Working with labeling dyes was performed under "dark" conditions. At first Spikes, which were used to integrate corresponding labeling dye during cDNA synthesis, were diluted according to table 13:

Table 13: Spike dilution preparation

Dilutions	**Components**
Dilution 1	2 µl Spike A or B + 38 µl Dilution buffer (1:20)
Dilution 2	2 µl of dilution 1 + 78 µl Dilution buffer (1:40)
Dilution 3	10 µl of dilution 2 + 30 µl Dilution buffer (1:4)

Spike A correlates with Cy3 and Spike B with Cy5. For 3 RNA samples (Mock, NTC and respective clone) 6 µl Spike A or Spike B of dilution 3 were mixed with 3.6 µl of T7 promoter primer. Additionally 1500 ng of each RNA sample was diluted with nuclease-free H_2O to a total volume of 8.3 µl and mixed with respectively 3.2 µl of Spike A or B. The samples were incubated for 10 min at 65°C and then for 5 min on ice. For cDNA synthesis a cDNA mastermix was prepared according to the table below:

Table 14: cDNA mastermix

Component	µl per reaction	Comments
5 x First Strand buffer	4	Prior to usage the buffer was incubated at 80°C for 3-4 min.
0.1 M DTT	2	
10 mM dNTP mix	1	
MMLV-RT	1	
RNase Out	0.5	

8.5 µl of the cDNA mastermix were added to each sample and gently resuspended. The samples were incubated at 40°C for 2 hours and then the reaction was stopped by additional incubation at 65°C for 15 min. cDNAs were stored at -20°C until needed for the transcription reaction. After cDNA synthesis the total volume amounted to 20 µl, whereof 10 µl were stored as backup at -20°C and the remaining 10 µl were used further. A transcription mix was prepared as shown in table 15.

Table 15: Transcription mastermix

Component	µl per reaction	Comments
nuclease-free water	7.65	
4x transcription buffer	10	
0.1 M DTT	3	
NTP mix	4	
50% Polyethylenglycol (PEG)	3.2	Prior usage PEG was incubated at 40°C for 1 min.
RNase inhibitor	0.25	
Inorganic pyrophosphatase	0.3	
T7 RNA Polymerase	0.4	
Cy3-CTP or Cy5-CTP	1.2	

30 µl of transcription mix were added to each 10µl "spiked" cDNA and the transcription reaction was carried out at 40°C for 2 hours. Subsequently labeled RNA was purified by RNeasy kit (Quiagen) according to the manufacturer´s instructions and the purification yielded 30 µl of RNA solution. The labeled cRNAs were quantified with a specific nanodrop measurement for labeled RNAs and the dye incorporation was calculated as follows:

Formula: $\frac{\text{Concentration of Cy3 or Cy5 (pmol/µl)}}{\text{Concentration of RNA (ng/µl)} \times 1000} = \text{pMol Cy3 or Cy5/ µg RNA}$

(cRNAs should have an incorporation value above 8 pMol dye/µg RNA for the hybridization procedure).

Before hybridization a fragmentation reaction was carried out to fragment cRNA. For better handling, cRNAs were diluted to 100 ng/µl. The following fragmentation mix was pipette (Table 16).

Table 16: Fragmentation mix

Reactant	**µl**
Cy3 cRNA	8.25 (825 ng)
Cy5 cRNA	8.25 (825 ng)
10 x blocking reagent	11
Nuclease-free H2O	25.3
25 x fragmentation buffer	2.2
Total volume	55 µl

The fragmentation reaction was incubated at 60°C for 30 min and the reaction was stopped by adding 55 µl of 2 x Gex Hyb buffer HI-RPM (Gene Expression Hybridization Kit, Agilent). The samples were put on ice and loaded on the array as fast as possible. 100 µl of each reaction were dispensed onto one of the four marked-off areas of the gasket well, which had been inserted into a chamber before. The array slide was placed onto the gasket well, so that the active side lay on the reaction suspension, and the assembly was closed. Bubbles were removed by tapping gently or mobility of bubbles was assessed by rotating the chamber. The array was hybridized in a hybridization oven at 65°C for 17 hours at 20 rpm. The next day the array slide was washed in Agilent buffers as follows: The slide was separated from the gasket well in Washing Buffer 1 and incubated in another dish containing fresh Washing Buffer 1 and a rack for 2 min while a stirrer gently mixed the solution. Then the slide, without any liquid drops on it, was transferred into Washing Buffer 2 and incubated for exactly 1 min by gently stirring. Subsequently the slide was transferred into acetonitril for exactly 1 min, dried shortly at RT (1 min) und put into a slide holder with the barcode facing up. After hybridization slides were scanned with two different lasers and detectors, one for each dye. Fluorescence signals were

captured in a TIFF picture which was extracted into a text file with Feature extraction software. This text file was loaded into Genespring GX 11 software, where a range of statistical analyses was carried out.

5. Results

5.1. Construction of expression vectors

5.1.1. βE into IRES-EGFP

The vector pIRES-HsAβE (*Figure 6*) containing the human βE coding region was used for cloning of the βE subunit into the pIRES-EGFP vector (*Figure 7*). As both the template and the target vector contained a CMV promoter upstream of the gene of interest a restriction site (*NdeI*) which cuts inside the promoter region could be used for the 5′ end. The digestion procedure for both vectors was carried out with the usage of *NdeI* and *EcoRI* restriction sites with further elution out of a 1% preparative agarose gel (Promega Kit) (*Figure 8*). The expected restriction fragments – 1771 bp and 4773 bp in the case of pIRES-HsAβE, and 395 bp and 4913 bp for pIRES-EGFP – were visible on agarose gel and nanodrop measurement resulted in 201.8 ng/µl IRES-EGFP vector DNA and 13.9 ng/µl hsβE insert DNA. After ligation and transformation into JM109 competent *E.coli* cells, a plasmid quick- mini preparation of overnight cultures and subsequent control restrictions with *SnaBI* restriction enzyme of five clones was carried out (*data not shown*). Two possible positive clones producing the expected fragment sizes – 1206 bp, 5748 bp - on an agarose gel were used to prepare again over night cultures and to conduct plasmid mini preparations with the Promega Kit. Subsequent control restrictions with *SnaBI, HindIII* and *Eco47III* resulted in the observation of nearly the anticipated fragments: *SnaBI* 1212 bp, *HindIII* 1628 bp, *Eco47III*: 967 bp (*Figure 9*). The sequencing report for the βE construct by Mycrosynth confirmed that the 1052 bp product was the open reading frame of the human βE subunit (*Figure 10*) and manual inspection of undefined bases in the chromatogram confirmed the absence of mutations. The newly constructed vector pHsβE-IRES2-EGFP is shown in *Figure 11.*

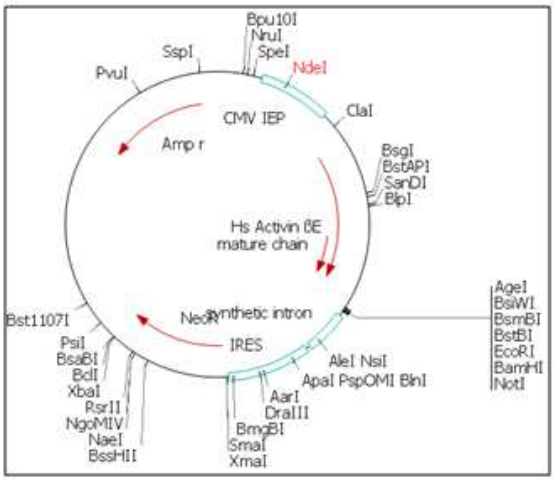

Figure 6: Template vector pIRES-HsAβE containing the human βE-subunit.

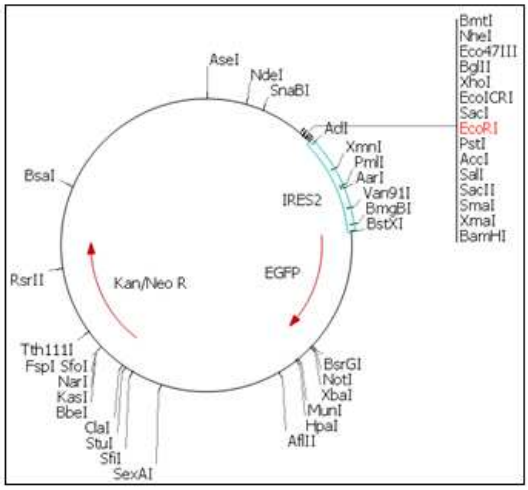

Figure 7: pIRES-EGFP target vector and mock control.

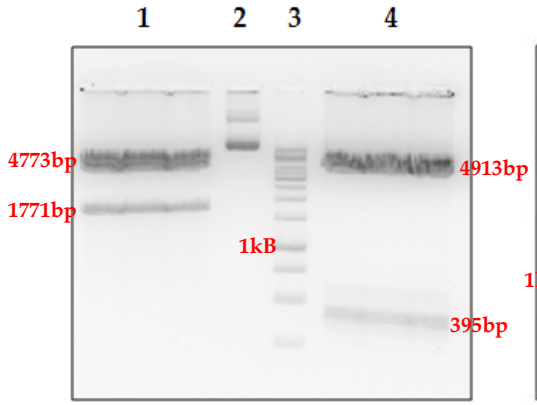

Figure 8: Preparative agarose gel: Lane 1: pIRES-HsAβE vector restricted with NdeI and EcoRI (50 µl DNA + 10 µl VistraGreen), Lane 2: pIRES-HsAβE unrestricted, Lane 3: 1kB Marker, Lane 4: pIRES-EGFP restriction by NdeI and EcoRI, (1% agarose gel in 0.5x TBE).

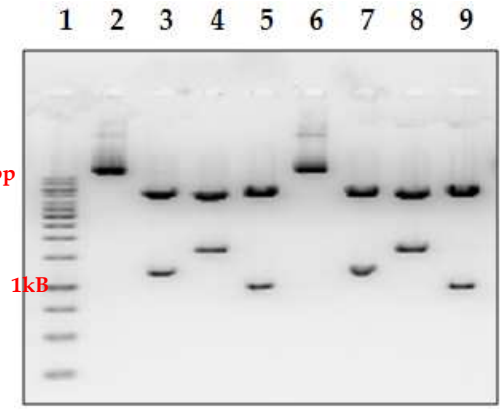

Figure 9: Plasmid preparation and restriction of two possible clones with respectively SnaBI, HindIII or EcoR47III: Lane 1: 1kB Marker, Lane 2: unrestricted plasmid DNA of clone 1, Lane 3: clone 1-SnaBI restriction, Lane 4: clone 1-HindIII, Lane 5: clone 1-Eco47III, Lane 6: unrestricted plasmid DNA of clone 2, Lane 7: clone 2-SnaBI restriction, Lane 8: clone 2-HindIII restriction, Lane 9: clone 2-Eco47III restriction (1% agarose gel in 0.5x TBE).

Figure 10: Nucleotide sequencing report: Alignment analysis based on sequencing report results and pIRES-HsAβE vector as reference, and subsequent chromatographic analysis of undefined ("n", see red arrows) bases for point mutation.

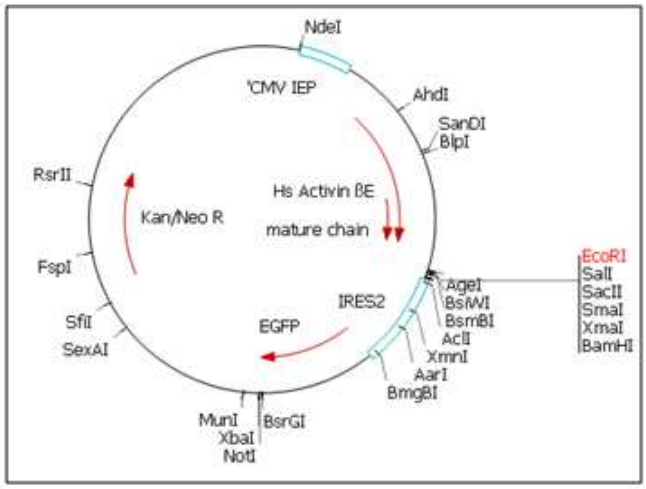

Figure 11: Cloning product vector pHsβE-IRES-EGFP.

5.1.2. vβE into IRES-EGFP

For construction of a bicistronic expression vector we amplified the coding region of the human vβE (also termed altβE for alternative transcript of the beta E gene) by PCR. The vector pCMV-Sport6-altβE (*Figure 12*) was used to design primers to amplify the coding region of vβE including the ATG and adding an *EcoRI* restriction site. The following primers were used: a 5′end specific forward primer adding an *EcoRI* restriction site upstream of the ATG (5′ CCCGAATTCCGCCATGCTAGAAATAAAGAGACCAGA- 3′) and a 3′ end specific reverse primer including the stop codon and adding a *BamHI* site (5′ TTTGGATCCTAGCTGCAGCCACAGGCCTC-3′). Before performing a *Pfu*- PCR, an amplification procedure with *Taq* polymerase was analysed by gel electrophoresis and showed bands around 1kb (*data not shown*). Repetition of the PCR procedure with *Pfu* Polymerase provided fragments with the same size on agarose gel (*Figure 13*). The PCR product was again subcloned into an IRES-EGFP vector (*Figure 6*). For ligation restriction digests with *BamHI* and *EcoRI* restriction enzymes were performed for the target vector pIRES-EGFP and the PCR samples. Subsequently they were purified out of a preparative gel (*Figure 14*). The nanodrop measurement resulted in 70 ng/µl pIRES-EGFP vector DNA and 6 ng/µl vβE insert DNA. The ligation as indicated above led to fusion of DNA molecules which were transformed into *E.coli* JM109 cells and then plated on selective media containing kanamycin for selection of plasmid-containing cells. For quick selection of potential positive clones containing the insert of interest, a "quick preparation" of plasmid DNA was performed and plasmid DNA was restricted once with *HindIII* and once with *Eco47III* and analyzed on a 1% agarose gel (*Figure 15*). *Eco47III* digested the vector two times and the expected fragments were of 170 bp and 6085 bp lengths. The fusion product contained also two *HindIII* restriction sites yielding fragments of 1216 bp and 5039 bp lengths. Two clones, 1 and 8 were identified as producing bands of the expected lengths (although the 170 bp fragment was not detectable in the gel) and

subsequently overnight cultures for minipreparation with the Promega Kit were prepared. Plasmid DNA of clone 1 and 8 was isolated and restricted again with the enzymes *BamHI* and *EcoRI* and analyzed by gel electrophoresis (data not shown). The expected fragment of 978 bp length after this restriction was received by both clones and so a sample (0.8 µg in 10 µl nuclease-free H_2O) was sent to Mycrosynth for nucleotide sequencing and screening for mutations. For sequencing, CMV forward and reverse primer were used. Nucleotide sequencing results were checked with Alignment analysis in Clonemanager (Sci-Ed Software) and subsequent manual inspection of ambiguous nucleotides in the chromatogram, which confirmed the absence of mutations (*Figure 16*). The newly constructed vector pHsvβe-IRES2-EGFP is shown in *Figure 17*.

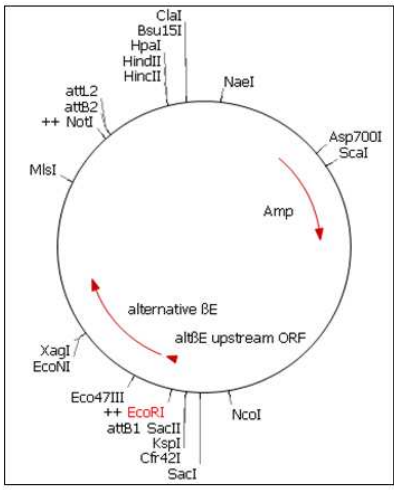

Figure 12: pCMV-Sport6-altβE vector containing the alternative βE subunit.

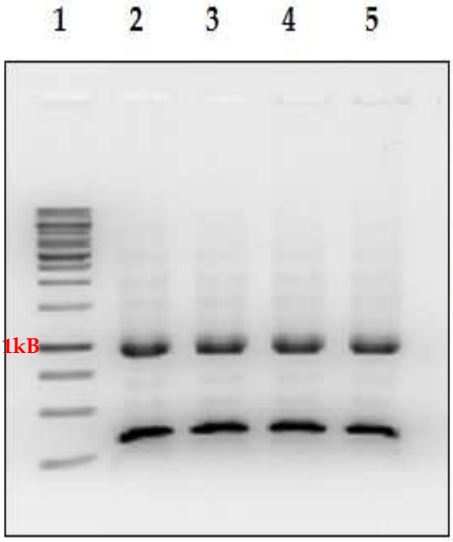

Figure 13: PCR amplification of vβE subunit with Pfu-polymerase: Lane 1: 1kB Marker, Lane 2-5: PCR product, (1% agarose gel in 0.5x TBE).

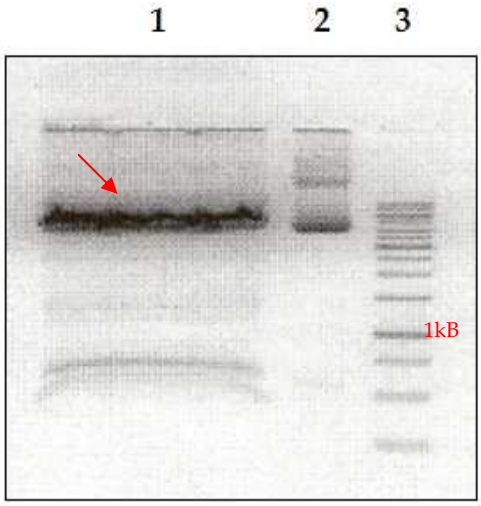

Figure 14: Vector pIRES-EGFP restriction digest with BamHI and EcoRI: Lane 1: pIRES-EGFP restriction, Lane 2: pIRES-EGFP unrestricted, Lane 3: 1kB Marker, (1% agarose gel in 0.5 x TBE)

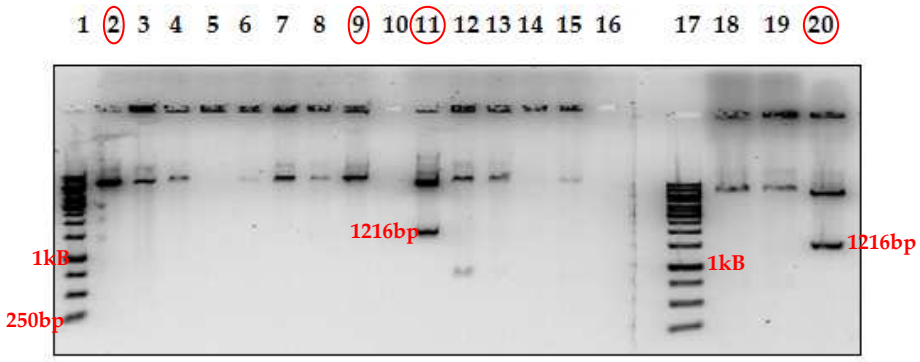

Figure 15: Plasmid "quick-preparation" of eight clones and restriction with respectively HindIII or Eco47III to screen for potential positive clones containing pvβE-IRES-EGFP vector: Lane 1: 1kB Marker, Lane 2-9: Eco47III restricted plasmids of different clones, Lane 10: empty, Lane 11-16: HindIII restriction approaches with same plasmids gained by same clones, Lane 17: 1kB Marker, Lane 18-20: HindIII restriction, (1% agarose gel in 0.5x TBE).

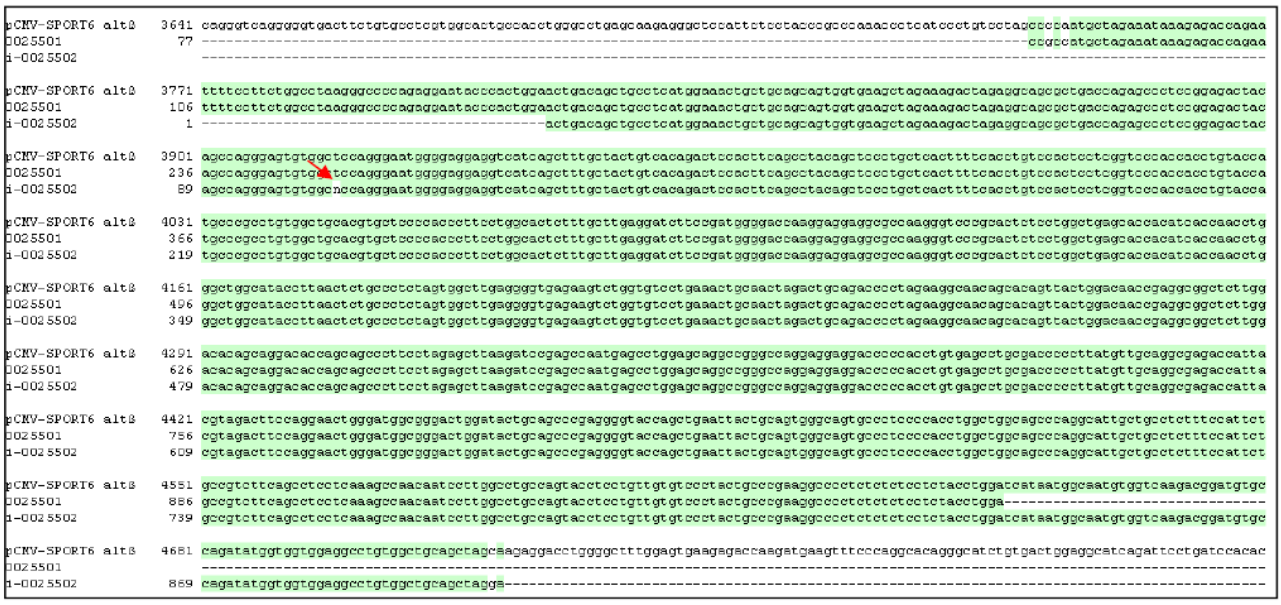

Figure 16: Nucleotide sequencing report: Alignment analysis based on sequencing report results and pCMV-SPORT6-altβE vector as reference, and subsequent chromatographic analysis of undefined ("n", see red arrows) bases for point mutation.

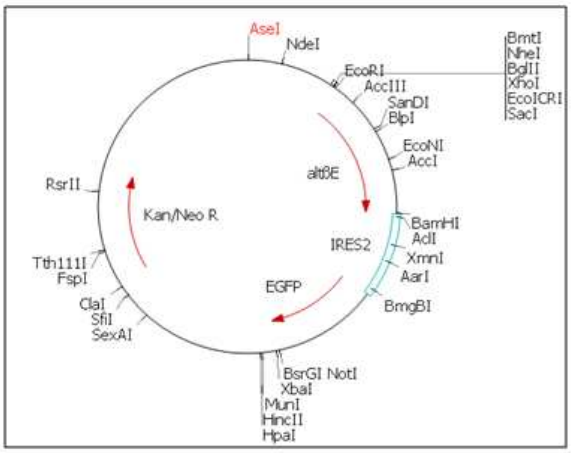

Figure 17: newly constructed fusion product: vector pHsvβE-IRES-EGFP.

5.2. Tet System reconstruction

The Tet-Off Advanced Inducible Gene Expression System (Clontech) allows inducible expression of the gene of interest, where transcription can be reversibly turned on or off in presence/absence of tetracycline.

5.2.1. inducible GFP

In a first cloning approach, which was performed to simplify the system, the vectors pTet-Off Advanced (A99, *Figure 18 a*) and pTRE-Tight (A100, *Figure 18 b*) were digested and ligated to gain one plasmid containing the transactivator and the inducible promoter sequences (p pTet-Off-TRE-Tight).

For that purpose 10 µg of the vector pTet-Off Advanced were restricted with 2.5 µl *HindIII* (10 u/µl) in buffer R (Fermentas) for 1.5 hours at 37°C. At the same time a preparative digest was carried out for 2 µg vector pTRE-Tight with *XhoI* enzyme. Both digestive approaches were inactivated by incubation at 80°C for 20 min and subjected to Klenow Polymerase reaction to create blunt ends. Vector pTet-Off was dephosphorylated additionally. Both products were loaded on an agarose gel and desired fragments were excised (*data not shown*). DNA purification yielded 14.1 ng/µl vector DNA pTet-Off and 18.8 ng/µl insert DNA containing the inducible promoter and the multiple cloning site from pTRE-Tight. Subsequently vector and insert DNA were ligated o/n at RT and then transformed into JM109 *E.coli* competent cells. The transformants were plated on ampicillin-containing agar plates. The next day colonies were picked from plates and o/n cultures were generated for further plasmid quick preparation. Prepared DNA was restricted with *HpaI* for control. One clone yielded fragment sizes of 414 bp, 2875 bp, and 4450 bp indicating the presence of the expected insert with the inducible promoter in antisense orientation with respect to the ORF of the transactivator (*Figure 19*). This clone was subjected to

plasmid Miniprep purification (Promega) which yielded 113.4 ng/µl DNA. Vector pTet-Off-TRE-tight-antisense is shown in *Figure 20*.

A second cloning procedure was performed to clone GFP into the newly generated pTet-Off-TRE-Tight vector. 7 µg of vector pEGFP-N3 (A16) and of vector pTet-Off-TRE-Tight were digested with enzymes *NotI* and *KpnI* in *BamHI* buffer. Additionally pTet-Off-TRE-Tight vector backbone was dephosphorylated. Both products were loaded on an agarose gel and desired fragments were excised (*data not shown*). The expected fragment sizes were 7695 bp and 44 bp for pTet-Off-TRE-Tight and 3981 bp and 748 bp for pEGFP-N3.

DNA purification yielded 28.4 ng/µl vector DNA (pTet-Off-TRE-Tight) and 8 ng/ul insert DNA (A16). A rapid ligation kit was used to ligate vector and insert DNA, the ligation mixture was transformed into JM109 *E.coli* cells and transformants plated on ampicillin-containing agar plates. A quick minipreparation was performed with several clones and DNA digested with *BamHI* in unique BamHI buffer (*data not shown*). For one potential positive clone two control restriction procedures were performed, the first with *EcoRI* enzyme in unique EcoRI buffer and the second one as a double digest with *NotI* and *KpnI* in BamHI unique buffer. The expected fragments of the first approach were 2216 bp and 6235 bp, of the second approach 756 bp and 7695 bp (*Figure 21*).

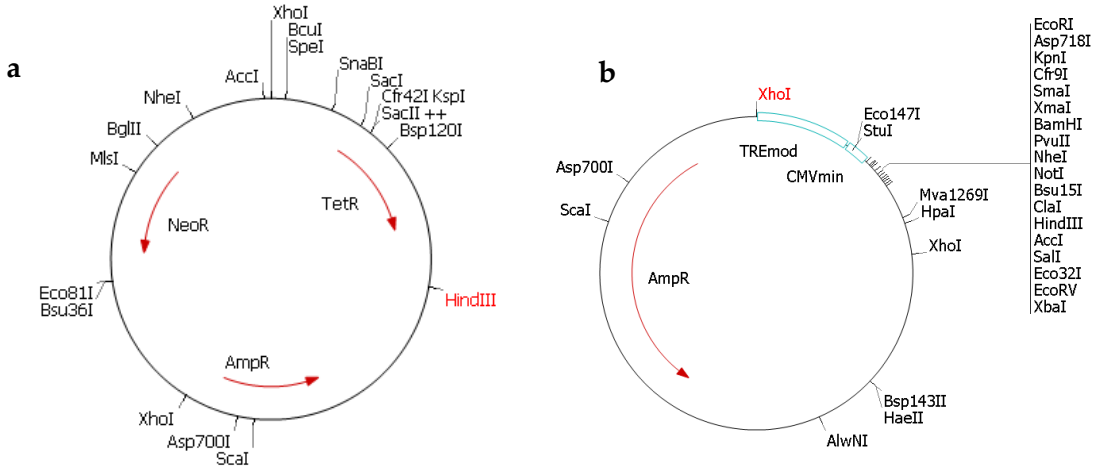

Figure 18: (a) Vector pTet-Off Advanced expresses constitutively the tetracycline-controlled transcriptional transactivator. (b) Vector pTRE-Tight contains the inducible promoter that controls the transcription of the gene of interest.

Overnight cultures were prepared from our positive clone for further preparation and glycerol stock generation. Newly generated vector pTet-Off-TRE-Tight-EGFP is shown in *Figure 22*.

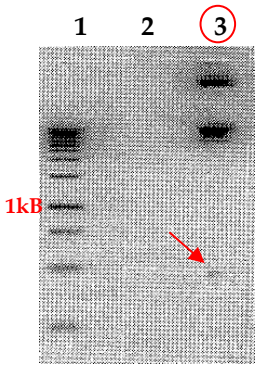

Figure 19: Control restriction of newly generated pTet-Off-TRE-Tight with HpaI: Lane 1: 1kB Marker, Lane 2: empty, Lane 3: HpaI restricted clone. Expected fragment sizes of 414 bp, 2875 bp, and 4450 bp were obtained and indicate an antisense orientation of insertion of insert DNA.

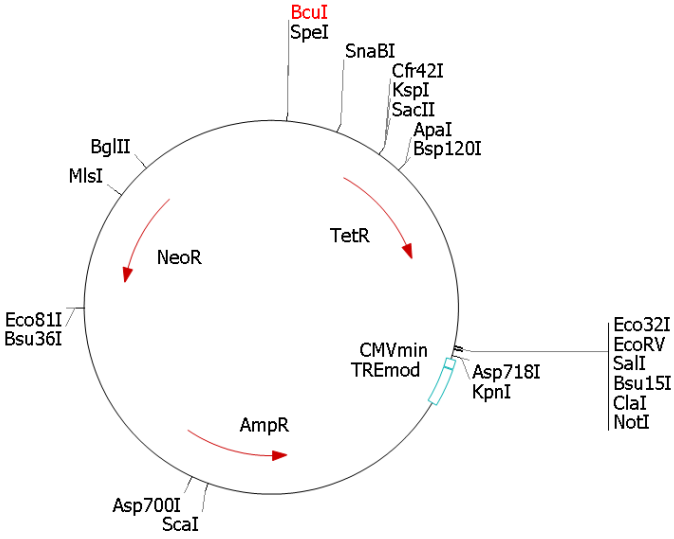

Figure 20: Newly generated vector pTet-Off-TRE-Tight.

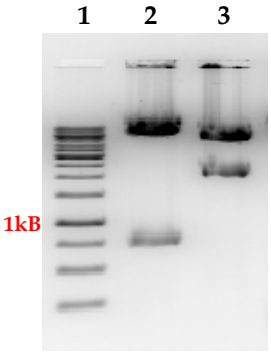

Figure 21: Control restriction of newly generated pTet-Off-TRE-Tight-EGFP: Lane 1: 1kB Marker, Lane 2: NotI and KpnI double digestion of clone with expected fragment sizes of 756 bp and 7695 bp, Lane 3: EcoRI restriction of clone with expected fragment sizes of 2216 bp and 6235 bp.

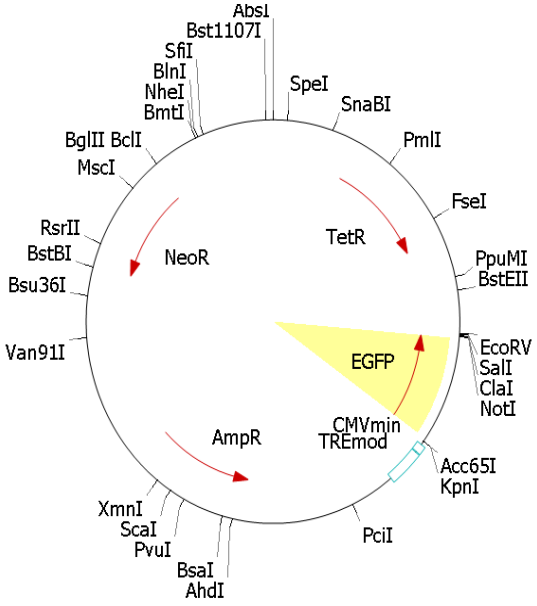

Figure 22: Newly generated vector pTet-Off-TRE-Tight-EGFP.

To investigate the activity of the newly generated vector, AKH3P cells were transfected with the vector pTet-Off-TRE-Tight-EGFP and selected with the antibiotic G418 for generation of stable clones. Expression of GFP was monitored under the microscope. Cells were expanded and after they had reached a certain density distributed to two culture flasks. In one of the culture dishes stable clones were treated with doxocyclin, which binds to the TRE sequence and blocks the transcription of the gene of interest, which was GFP in our case. 48-72 h after treatment with doxocyclin we did not observe inhibition of GFP-expression, which was due to the half-life of GFP, but gradually the GFP expression decreased and after 4 days was markedly reduced. This was an indication that our newly generated plasmid pTet-Off-TRE-Tight contained all essential parts to serve as an inducible gene expression system.

5.2.2. inducible alternative beta E

Vector pTet-Off-TRE-Tight was used as target vector for cloning of the coding region of human vβE and GFP as insert and generation of an inducible gene expression system for the alternative βE transcript. In previous transfection procedures our pHsvβE-IRES-EGFP plasmids lost expression by and by after transfection in the respective mammalian cells. Thus we decided to use an inducible expression system. The cloning strategy was performed as follows: 5 µg vector pHsvβE-IRES-EGFP containing vβE were digested with 5 µl *XhoI* (Fermentas fast enzyme) and 5 µl *HpaI* (Fermentas fast enzyme) in 10 x fast digest buffer for 10 min on 37°C, expecting fragments of 2429 bp and 7735 bp. 5µg vector pTet-Off-TRE-Tight were digested in a first approach with *EcoRV* in buffer O for 4 hours, then the enzyme was inactivated by incubation at 80°C for 20 min and then 1.5 µl *SalI* restriction enzyme were added to the approach and digested further for another 1.5 hours. The expected fragments of the *EcoRV-SalI* double restriction were 7753 bp and 4 bp. Subsequently DNAs were

loaded onto an agarose gel, excised, purified and used for rapid ligation (vector pTet-Off-TRE-Tight yielded 35.77 ng/µl and insert vβE-EGFP 16 ng/µl according to nanodrop measurement). Ligations were transformed into JM109 *E.coli* cells and plated onto ampicillin containing LB plates. Quick minipreps were performed with clones which were subsequently digested with *SnaBI* enzyme in buffer Tango (*data not shown*). Three potentially positive clones were selected and digested with *EcoRI*, expecting fragments of 3838 bp, 6235 bp and 87 bp lengths (*Figure 23*). Clone number one was subjected to a minipreparation with the Promega kit and yielded 80.5 ng/µl. The newly generated vector pTet-Off-TRE-Tight-HsvβE is shown in *Figure 24*. For vector pTet-Off-TRE-Tight-HsvβE a glycerol stock was generated for long-term storage for further investigation of the alternative βE transcript in future studies, but no additional experiments were conducted during this diploma thesis.

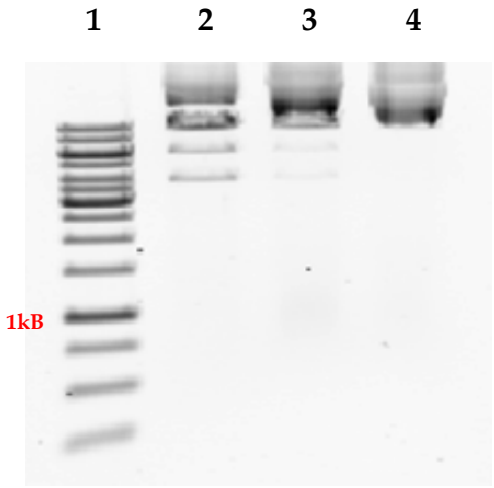

Figure 23: Control restriction with EcoRI enzyme: Lane 1: 1kB, Lane 2-4: three different clones digested with EcoRI.

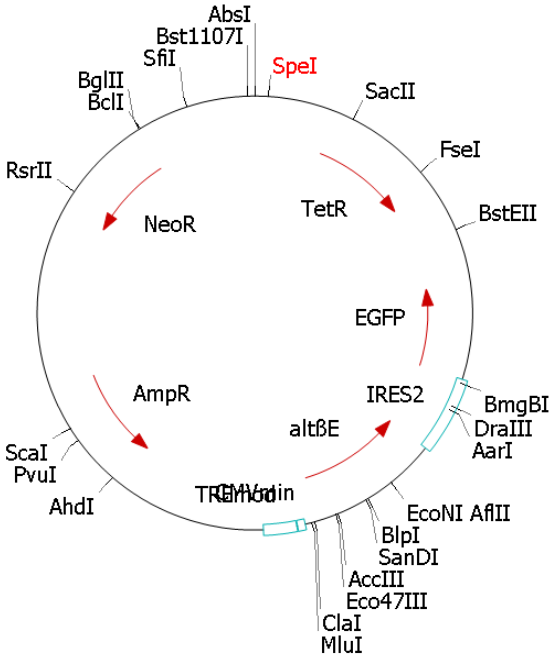

Figure 24: Cloning product vector pTet-Off-TRE-Tight-HsvβE.

5.3. Baculovirus Expression System: Construction of recombinant activins in insect cells

With the BAC to BAC baculovirus system (*Figure 25*) we created recombinant baculoviruses for high level expression of His –tagged versions of activin βA and βE (*Figure 26*) in insect cells (SF9). Integration of DNA fragments into bacmids was accomplished in E.coli hosts via recombination into a lacZ gene on the bacmid and recombinant bacmids were identified by blue/white screening (Trowitzsch et al., 2010).

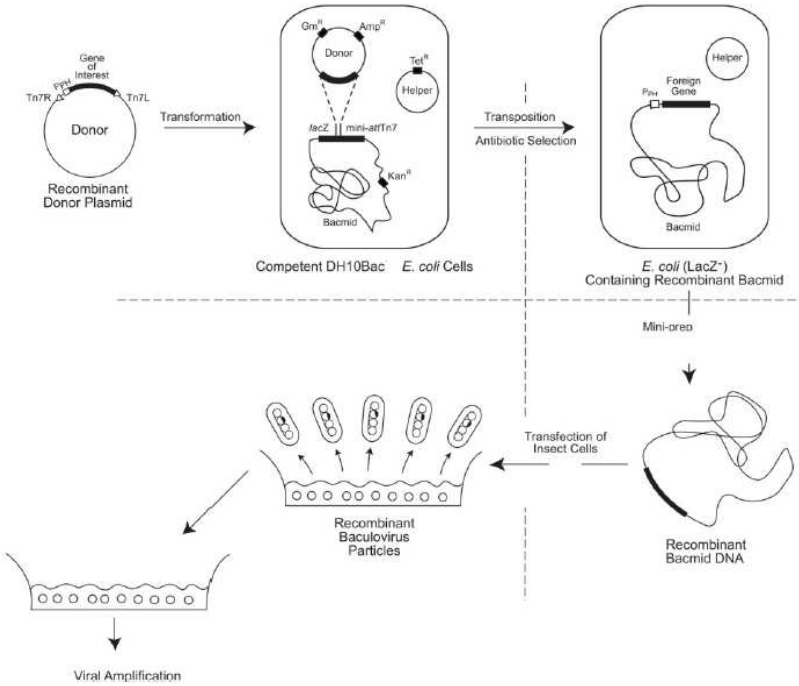

Figure 25: Schematic overview of the Bac to Bac expression system (Bac-to-Bac Expression Kit Handbook, Invitrogen life technologies).

5.3.1. Construction of Histidin-tagged activins

First, purchased primers (Table 1) were tested by *Taq*- PCR (expected fragment sizes of the mature peptides = around 400 bp; propeptides around 800 to 900 bp; INHBA_His= 1400 bp; INHBE_His = 1100 bp, *data not shown*) and after verification the PCR products generated with *Pfu*-PCR. As PCR templates for activin beta A and activin beta E expression vectors containing the respective coding region for the individual proteins were used (*Figure 27 a+b*). For activin subunits with the Histidin-tag (His-tag) in the middle (at the N-terminus of the mature peptides after proteolytic processing in the ER: His_INHBA, His_INHBE) two PCR rounds were performed to get the cassette. At first a PCR product of the propeptide with the His-tag at the C-terminal-end and one of the mature protein with the His-tag at the N-terminal-end was generated. PCR products were loaded on an agarose gel, respective bands were excised and eluted with the promega purification kit. Then the His-tagged mature peptide and propeptide were mixed in one Eppendorf tube and this mixture served as the new template. Another *Pfu*-PCR with primers binding at the n- and c-terminus of the activin cDNAs was performed where finally activin cDNAs with the His-tag in the middle were gained. For the His-tag at the C-terminal-end (INHBA_His, INHBE_His) only one *Pfu*-polymerase PCR was performed. After elution of the DNA from the gel slices the desired fragments were obtained with their concentrations: Activin A constructs: His_INHBA [23 ng/µl], INHBA_His [11 ng/µl]; Activin E constructs: His_INHBE [22 ng/µl]; INHBE_His [16 ng/µl]. The "His" at the beginning stands for the histidin tag in the middle of the construct, "His" designation at the end indicates a C-terminal histidin tag.

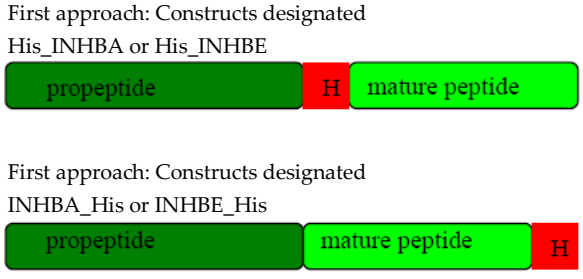

Figure 26: For production of recombinat activin E or A two different approaches were conducted. In the first approach the recombinant protein was HIS-tagged between the pro- and mature peptide, and in the second approach at the C-terminal end of the mature peptide.

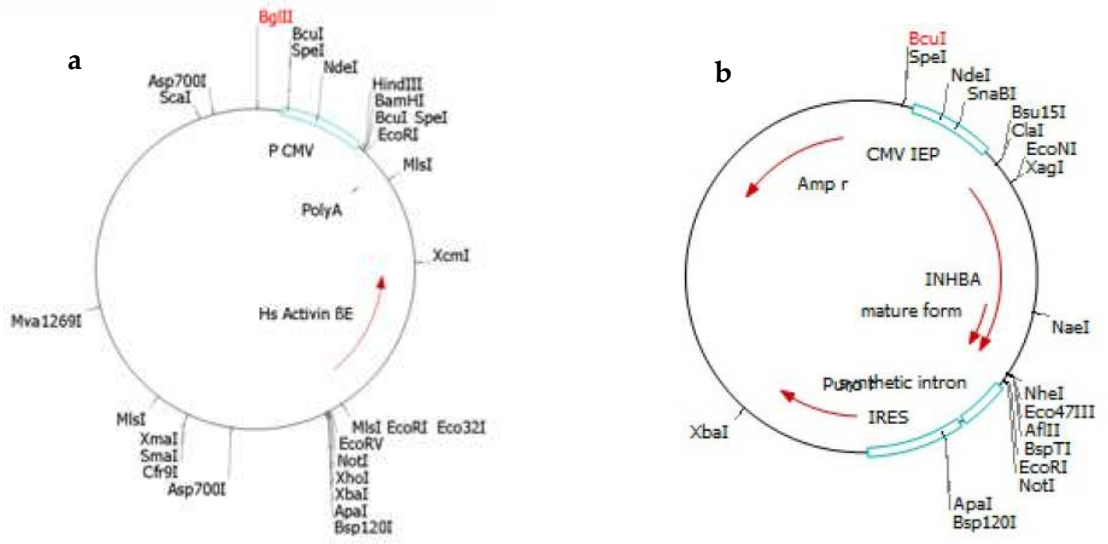

Figure 27: (a) Vector pHsaβE was used as PCR template for construction of His-tagged activin βE. (b): Vector pHsINHBA-IRES-puro was used as PCR template for construction of His-tagged activin βA.

5.3.2. Restriction digest and transformation of JM109 E.coli

The generated PCR products were cloned into the baculovirus transfer vector pFastbac-1. In fact the restriction sites *EcoRI* and *StuI* were used for further ligation with the activin A cassettes and *EcoRI* and *HindIII* with the likewise restricted activin E cassette. Restriction and ligation procedures were performed as mentioned above. The generated expression vectors were transformed into competent JM109 *E.coli* cells, which successively were plated on ampicilin containing LB - plates o/n at 37°C. For a Quick n´dirty plasmid minipreparation o/n cultures were generated and afterwards plasmids were restricted with *HindIII* for the activin βA-containing vectors and *SnaBI* for activin βE. Positive clones (marked as red arrows in the *figures*) of activin A cassettes = 1300 bp and activin E cassettes = 1100 bp *(Figure 28-30)* were identified and clean preparation of the plasmids followed. The DNA amounts of our activin vectors (His_INHBA = 4 ng/µl, INHBA_His = 9 ng/µl; His_INHBE = 9 ng/µl; INHBE_His = 8 ng/µl) were measured with nanodrop and then sent for sequencing

to Microsynth. No mutations were detected in the activin cassettes; His_INHBE had only 5 instead of the intended 6 histidines.

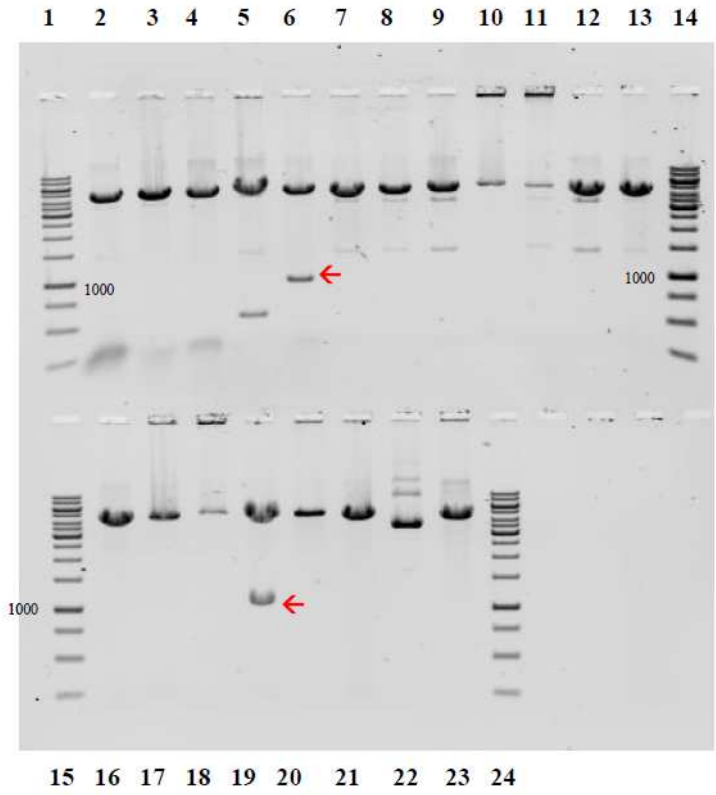

Figure 28: Control restrictions of plasmid minipreparations: Lane 1+14: 1kB Marker, Lane 2-7: His_INHBE restricted with SnaBI, Lane 8-15: INHBE_His restricted with SnaBI, Lane 16-23: INHBA_His restricted with HindIII. Red arrows indicate fragments of expected length after restriction which were 1300 bp in the case of activin A cassettes and 1100 bp in the case of activin E constructs.

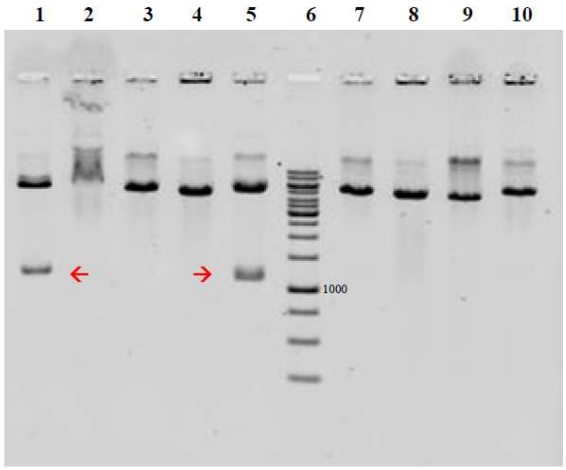

Figure 29: Control restrictions of plasmid minipreparations: Lane 6: 1kB Marker, Lane 1-5 + 7-10: His_INHBA construct restricted with HindIII. Red arrows indicate fragments of expected length after restriction which was 1300 bp.

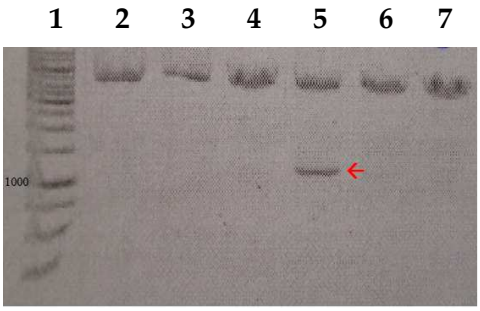

Figure 30: Control restrictions of plasmid minipreparations: Lane 1: 1kB Marker, Lane 2-7: INHBE_His construct restricted with SnaBI. Red arrows indicate fragments of expected length after restriction which was 1100 bp.

5.3.3. Transformation of the DH10Bac *E.coli* strain with activin plasmids

Correct plasmids were subsequently transformed into the DH10 *E.coli* strain, the activin cassettes were inserted into the bacmid between two transposon sites. After incubation for 48h white colonies were picked and transferred with a pipette tip to a "grid" LB-plate (kanamycin [50 µg/ml], tetracycline [10 µg/ml], gentamycin [7 µg/ml], Iptg [40µg/ml] and X-Gal [100 µg/ml]. The rest of the colony was diluted in a tube containing 15 µl PBS for colony PCR and colonies possessing the correct insert were subjected to an alkaline lysis minipreparation. The amount of bacmid DNA was analyzed by nanodrop measurement.

5.3.4. Transfection of SF9 cells with bacmids

SF9 insect cells were transfected with bacmids (Fugene6) coding for recombinant activin A or activin E. The backbones of the bacmids also expressed yellow fluorescence protein (YFP) and gradually the cells started having fluorescence under the microscope indicative of viral spread (*Figure* 31). Cells expressing the recombinant activin A construct outspeeded cells transfected with His-tagged activin E in expressing fluorescent protein. The latter took longer at many parallel transfection approaches, whereas most of the recombinant activin A transfected cells fluoresced soon.

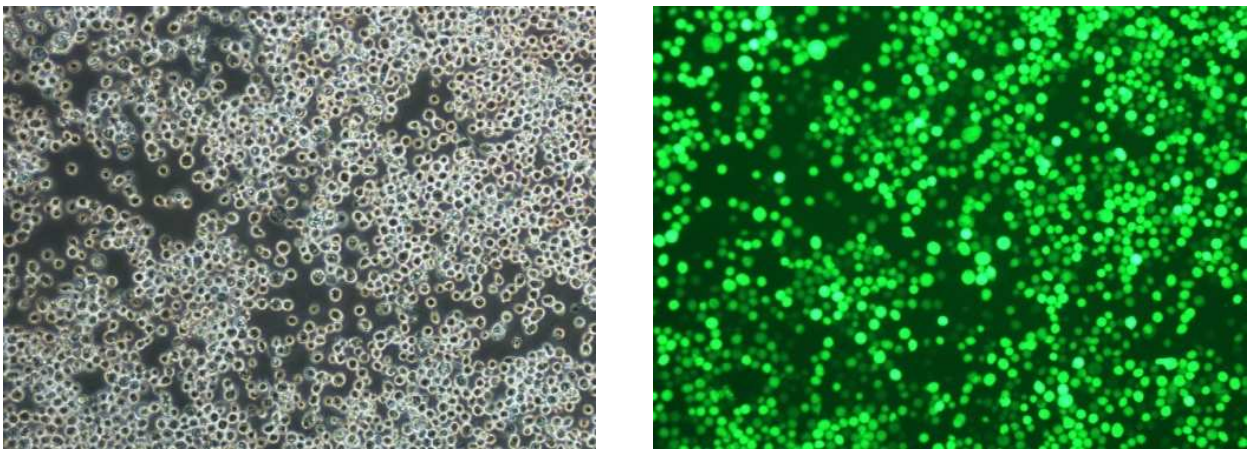

Figure 31: Microscopy of SF9 insect cells expressing recombinant activin and YFP.

5.3.5. Investigation of expression and bioactivity of recombinant activins

To analyze if the expression of recombinant proteins was detectable, protein was precipitated from SF9 cell supernatants and isolated from whole cell extracts. After determining the protein concentration with Bradford reagent assay, proteins were separated with SDS gel (12%) and detected with Western blotting. Anti-Activin A antibodies could detect activin A in samples precipitated from the SF9 cell supernatant, in the cell layer and directly in the supernatant of SF9 cells (without

precipitation) when SF9 cells were infected with activin A expressing baculovirus. The highest amount was found after ethanol precipitation of cell supernatant (data not shown). Due to the fact that there are no efficient antibodies against activin E Anti-Histidin antibodies were used to detect the His-tag of all recombinant proteins (*Figure 32*).

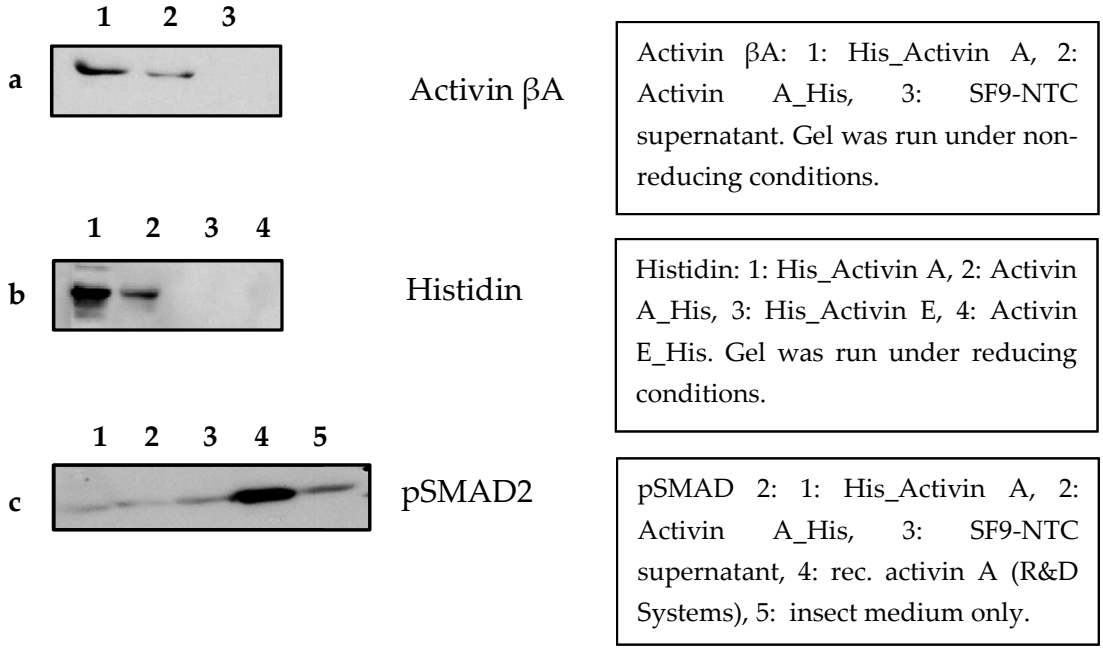

Figure 32: Western Blot analysis of recombinant activin A or E. Transfected SF9 cells were incubated in serum-free medium (SFM) and after baculovirusoutbreak, which was visible under the microscope due to YFP expression, supernatant was precipitated with EtOH and protein-samples subjected to Western Blotting. Detection of protein with activin A antibody (a) or histidin antibody (b). Supernatant of SF9 cells expressing recombinant protein into SFM medium was transferred to HepG2 cells and incubated for 30 min. Proteins were isolated from the cell layer and recombinant activin bioactivity was analyzed using anti-pSMAD2 antibody (c).

The anti-Histidin and anti-βA antibodies detected protein only in samples from baculovirus transfected cells, and not in the layer or supernatant of untransfected cells. A bioactivity of the protein, however, was not detectable; there was no pSMAD2 increase after treatment of activin A-responsive HepG2 cells with supernatant of recombinant activin A-expressing SF9 cells. SMAD2 phosphorylation

was only increased when cells were treated with a commercially available recombinant activin A (R&D Systems, dissolved in 1x PBS containing 0.1% BSA). Both activin A constructs were detectable with respective antibodies when the gel was run under reducing conditions, and only His_INHBA was traceable under non-reducing conditions (data not shown). Although we detected at least one dimerized His-tagged recombinant activin A, none of the constructs could achieve bioactivity. In the case of recombinant Activin E the histidine-tags were undetectable. As future outlook this approach has to be optimized. Mammalian cell lines have to be considered for production of recombinant activin proteins.

5.4. Generation of stable clones and confirmation of overexpression or silencing

5.4.1. Stable clones overexpressing βE and vβE

The newly constructed plasmids pHsβE-IRES2-EGFP *(Figure 11)*, pHsvβE-IRES2-EGFP *(Figure 17)* and the already existing pIRES-EGFP *(Figure 7)* as mock control were transfected into Hep3B and HepG2 cells using Lipofectamine 2000. For generation of stable clones the cells were selected with the antibiotic G418 and confluent cultures were subjected to FACS sorting for GFP expressing cells. Due to the fact that the transfection efficiency of pHsvβE-IRES2-EGFP was very low *(Figure 33)* or GFP expression was lost after a short time we further analyzed and investigated only the role of βE overexpressing cell lines.

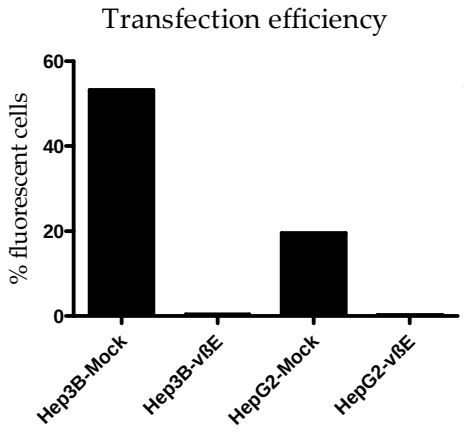

Figure 33: Transfection efficiency of pIRES-EGFP and pHsvβe-IRES2-EGFP transfected cells.

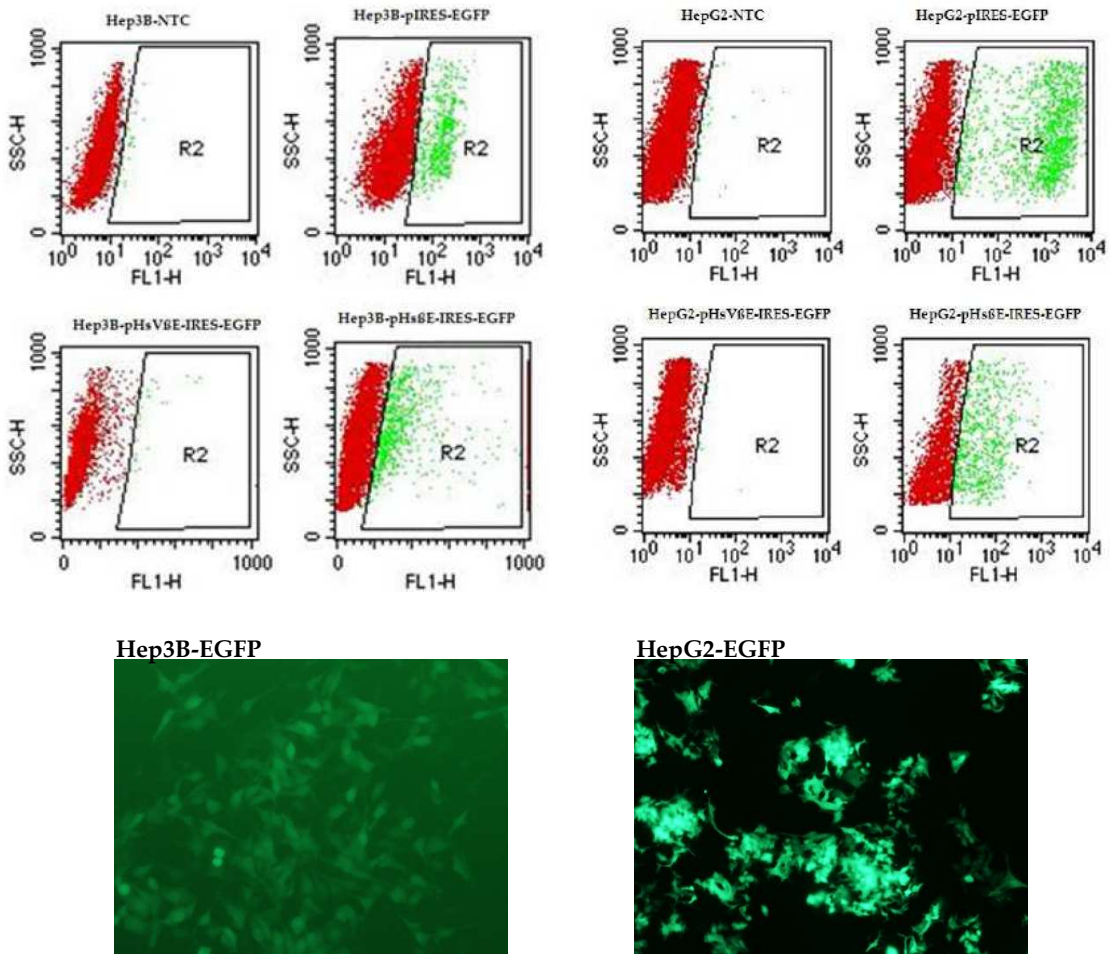

Figure 34: GFP-sort of pIRES-EGFP, pHsβE- IRES2-EGFP and pHsvβE-IRES2-EGFP transfected HepG2 and Hep3B cells. Untransfected cells (NTC) were used as negative control in order to determine GFP expressing cells. Green dots in the R2 areas of the dot blots represent GFP-positive cells. Lower panels show representative micrographs of Hep3B and HepG2 cells transfected with pIRES-EGFR after GFP-sorting.

Except for vβE transfected cells many cells of the other two transfectants showed fluorescence and it was uncomplicated to sort those which demonstrated the highest

fluorescence rates *(Figure 34)*. Sorted cells were expanded and on the one hand frozen for long term storage and on the other hand subjected to qRT-PCR for expression analysis.

5.4.2. Lentiviral transduction for long-term silencing of βE

To silence activin E in cell lines with high endogenous βE levels a lentivirus-mediated knockdown was performed. For that purpose a puromycin kill curve *(Figure 35)* was generated for the cell lines selected for knockdown and the cell viability was examined with an MTT assay. The minimum concentration of puromycin that caused 90-100% cell death was determined for selection of stable clones. We decided to use 0.6 μg/ml puromycin for HepG2 cells and 0.4 μg/ml for K562 cells.

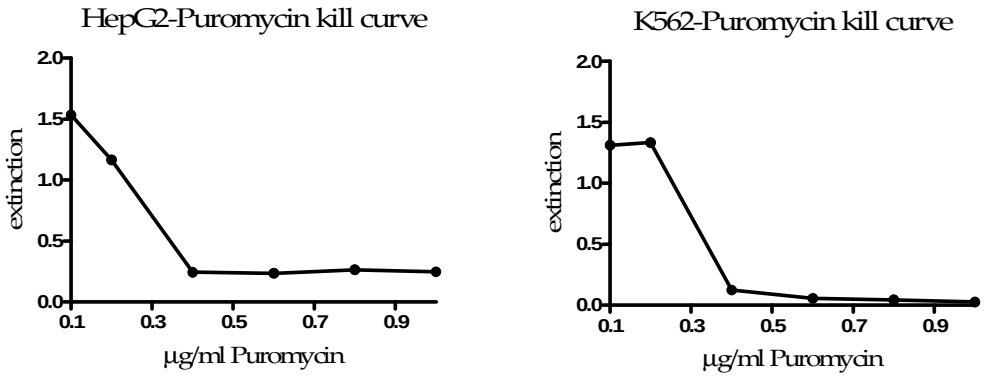

Figure 35: Various concentrations (0.1, 0.2, 0.4, 0.6, 0.8 and 1 μl/ml) of puromycin were tested on HepG2 and K562 cells to determine conditions for selection of stable clones.

After that HepG2 and K562 cells were transduced with a range of volumes (2-5 μl) of lentiviral particles for βE knockdown and with lentiviral particles expressing scrambled shRNA, which served as controls. Puromycin resistant clones were subjected to qRT-PCR to inspect the knockdown efficiency.

5.4.3. Expression anlaysis of stable clones

5.4.3.1. Analysis of βE overexpression in Hep3B and HepG2 cells

For a quantitative analysis the relative expression of Activin E in HepG2 and Hep3B cells was determined on the RNA level by qRT-PCR by either the TaqMan or SYBR green method respectively. Fold expression and Log 2 ratio values are shown in *figure 36*.

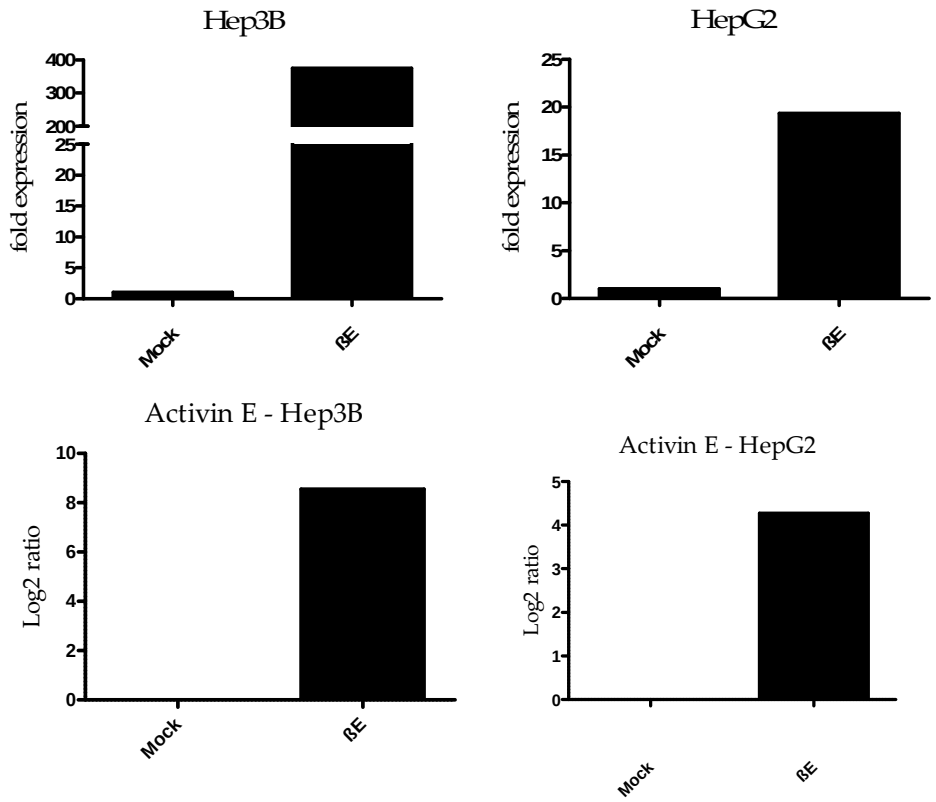

Figure 36: Expression analysis by qRT-PCR of Activin E in HepG2 and Hep3B cells after transfection, selection and establishment of stable clones.

Values were determined relative to the mock control. Activin E expression was normalized in regard to the expression level of the house-keeping gene β2M. We achieved a high over-expression of activin βE, in fact an overexpression of 400 fold in Hep3B and still 20 fold in HepG2 cells.

5.4.3.2. Analysis of βE silencing in K562 and HepG2 cells

In HepG2 and K562 cells a lentivirus mediated knockdown of activin βE was observed by means of qPCR. Relative to the scrambled control we achieved an activin βE silencing efficiency of 75% in HepG2 cells, and of 90% in K526 cells *(Figure 37)*.

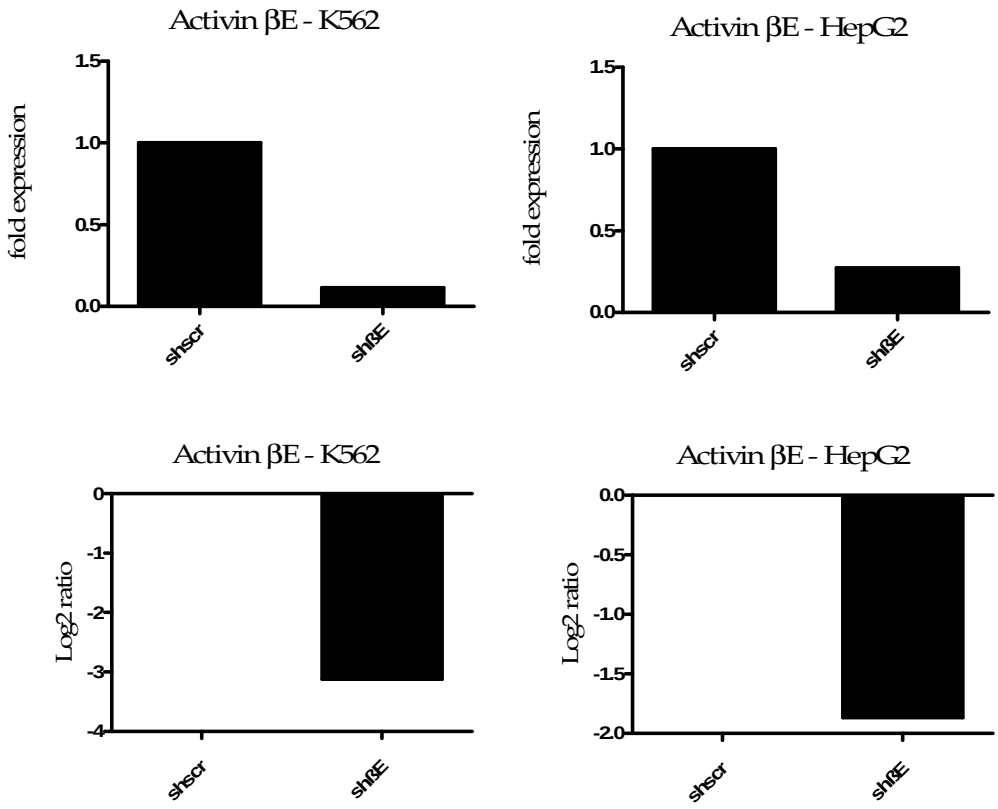

Figure 37: Expression analysis by qRT-PCR of Activin E in K562 and HepG2 cells after silencing, selection and establishment of stable clones.

HepG2 cells have compared to Hep3B and K562 cells a medium level of activin βE expression, and therefore were used for overexpression as well as for silencing of activin βE. Like in multiple other leukemia cell lines, K562 cells were reported to have elevated activin E levels compared to healthy bone marrow cells (Rodgarkia-Dara, personal communication) and therefore we selected this cell line for knockdown of activin E.

5.5. Functional characterization of stable clones

In order to determine consequences of increased or decreased activin E levels several functional assays were conducted with the generated stable clones.

5.5.1. Proliferation

5.5.1.1. MTT

For viability testing MTT assays were performed with stable clones under normal and reduced serum conditions to investigate whether activin E stimulates or inhibits proliferation. We did not observe a strong advantage or disadvantage of βE expression compared to the mock control *(Figure 38)*. There was no anti-proliferative effect obtainable in βE overexpressing Hep3B cells. Similar results were obtained for knockdown of βE, which had also no significant effect on the viability of K562 cells. Activin E silenced as well as overexpressing HepG2 cells seemed to have a reduced viability in medium with 10% FCS, but as this effect was observed in both cases it is unclear how the effect relates to the βE expression level.

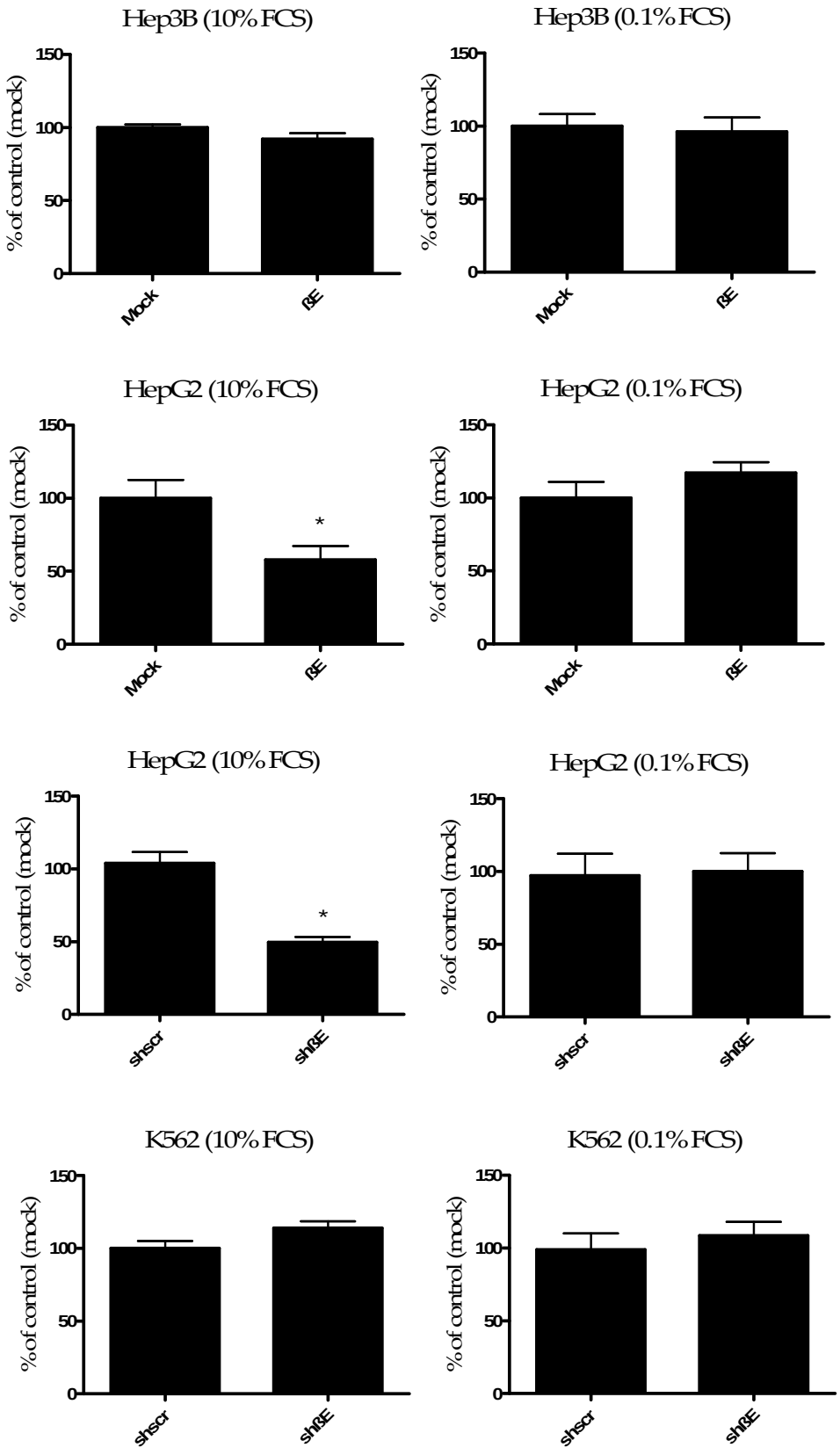

Figure 38: Cell viability of stable clones with elevated or decreased βE levels under low and normal serum concentrations.

5.5.1.2. Casy

For proliferation assay of activin E overexpressing cell lines cells were seeded at low density and cell number was determined every 2 days with the Casy cell counter. The experiment was performed in duplicates. Hep3B mock or βE transfected cells did not show any difference in the proliferation rate, similar results were observed for HepG2 cells. In *Figure 39* cell numbers of non-viable cells and viable cells are shown as determined by the Casy cell counter. HepG2 cells highly expressing activin βE seem to demonstrate a higher proliferation rate in this assay, but this effect is due to seeding of a higher number of βE transfected HepG2 cells at the beginning of the experiment. When calculated, HepG2 cells transfected with the mock vector doubled with the same factor as βE overexpressing HepG2 cells.

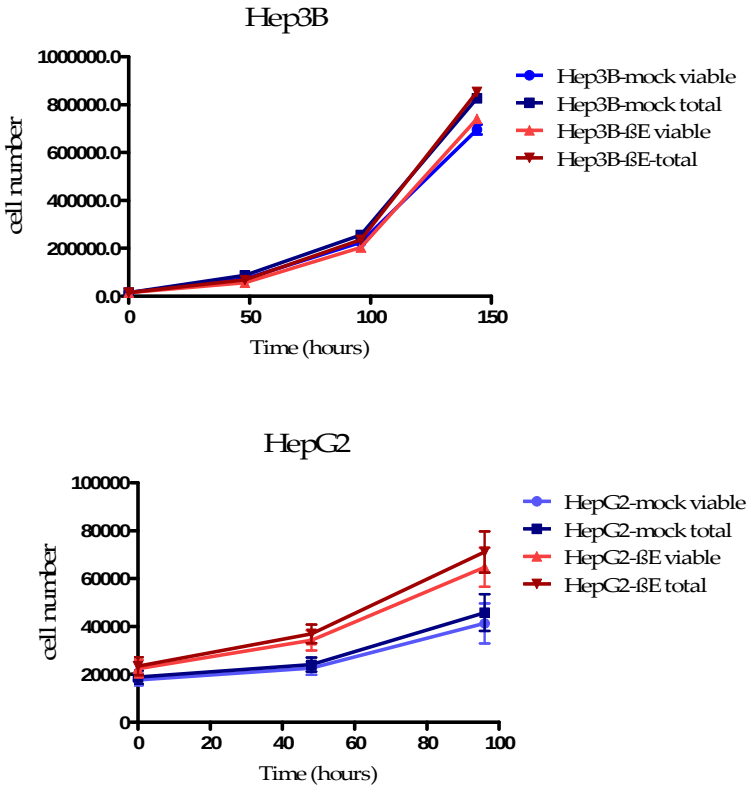

Figure 39: Investigation of the proliferation speed of HepG2 and Hep3B cells with increased βE levels compared to their respective mock control.

5.5.2. Clonogenic Survival

To analyze the capability of hepatoma cell lines overexpressing activin E or with silenced activin E to form colonies on tissue culture plastic, clonogenic survival assays were performed. After the desired clone sizes were obtained the cells were stained with crystal-violet *(Figure 40).*

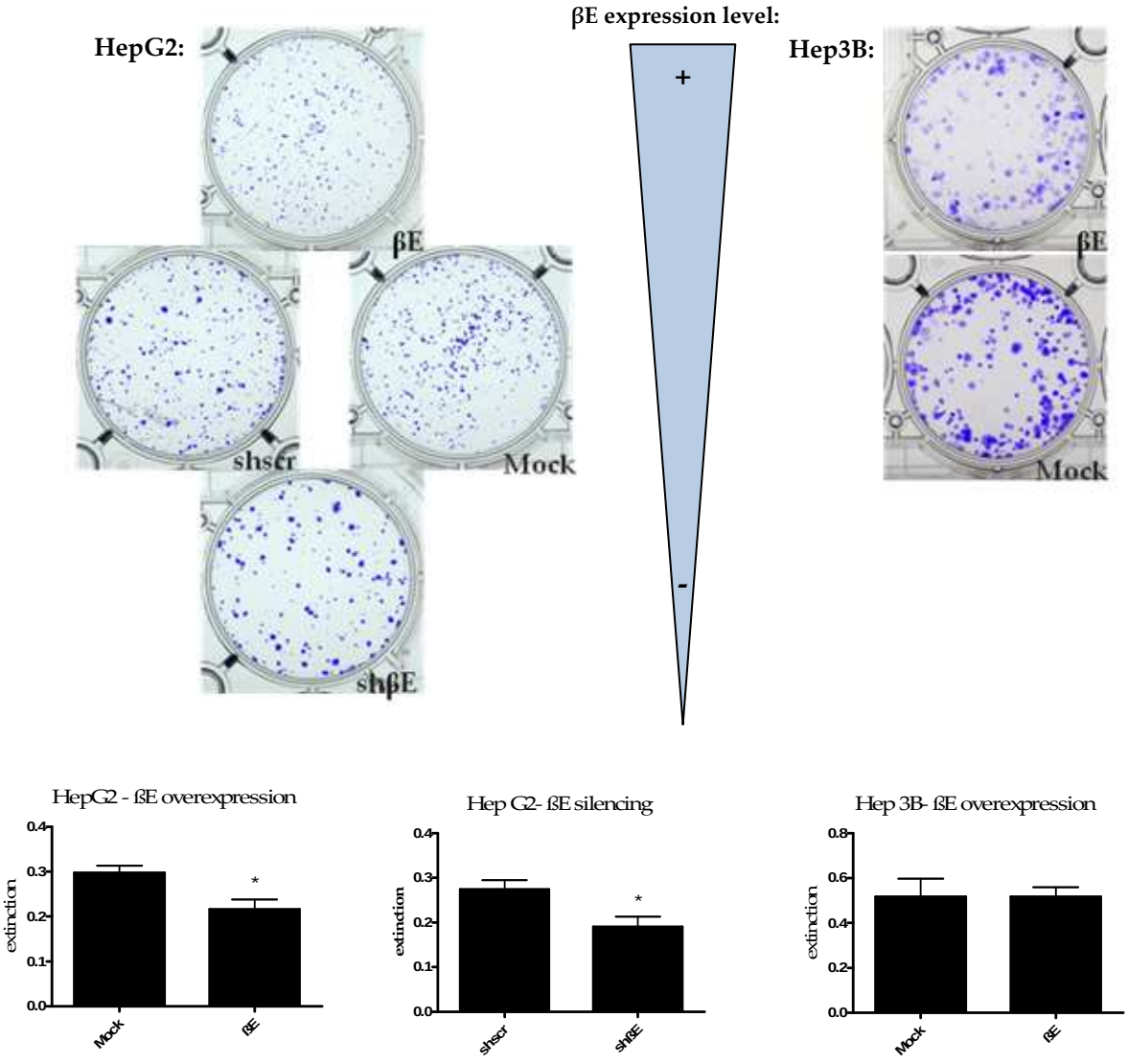

Figure 40: Clonogenicity assay of Hep3B and HepG2 cells: Activin E decreases clone size whereas silencing of activin E leads to fewer but bigger clones. Lower row: Photometrical measurement of crystal violet and extinction values.

The number and size of the clones differed, the higher the βE expression levels the smaller were the colonies. βE silenced cells showed a reduced number but bigger colonies. This effect was especially noticeable in HepG2. When we solubilized the crystal-violet for quantification and measured the absorption photometrically we could verify our findings just for the βE overexpressing Hep3B and HepG2 cells but not for βE silenced HepG2 (see Discussion section).

5.5.3. Cell cycle

To elucidate whether high activin E levels induce alterations in the distribution of the cell cycle phase, cells were stained with propidium-iodide and subjected to flow cytometric analysis. An effect of activin E overexpression in HepG2 and Hep3B cells leading to cell cycle alterations was undetectable; there was no obvious increase or decrease in any cell cycle phase compared to the mock controls *(Figure 41)*.

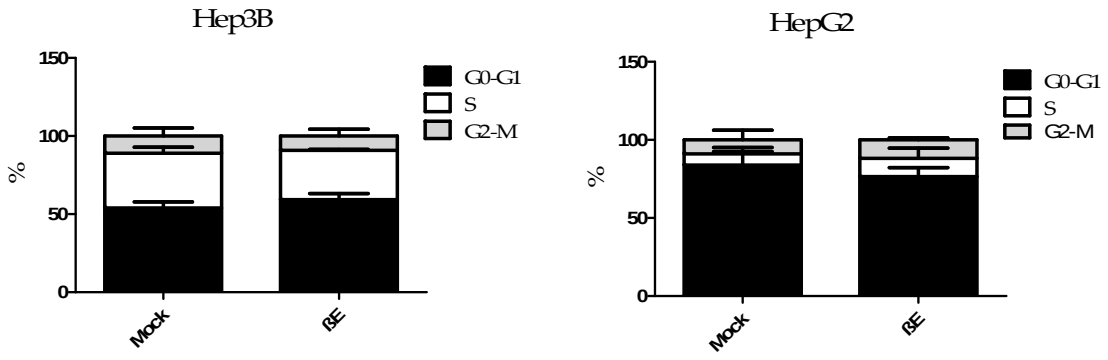

Figure 41: Influence of elevated activin E levels on the cell cycle phase distribution. Cell models are compared to mock controls. Experiments were performed in duplicates.

5.5.4. Migration

As we could not see any obvious effects of decreased or increased βE levels on proliferation and viability, we further determined the effects on migration. Migratory phenotype was analyzed by a wound healing assay and a transwell assay. For the wound healing assay confluent cell monolayers were scraped with a pipette tip and the closure of the scratches was monitored for a certain time until the scratch was completely closed. βE overexpressing cells behaved similar to mock transfected cells in the scratch assay *(Figure 42)* at the first three measuring points, and actually seemed to migrate faster than the mock control when monitored at the 8h measuring point. However after 24 hours the wound closure was still not complete compared to the mock control. Conversely, βE transfected cells showed a significant difference in the transwell assay and demonstrated a higher ability in passing the membrane *(Figure 43).* Those cells, which were able to migrate through the transwell filter and settle on the bottom were stained with crystal violet and when the dye was solubilized with SDS the results could be further confirmed.

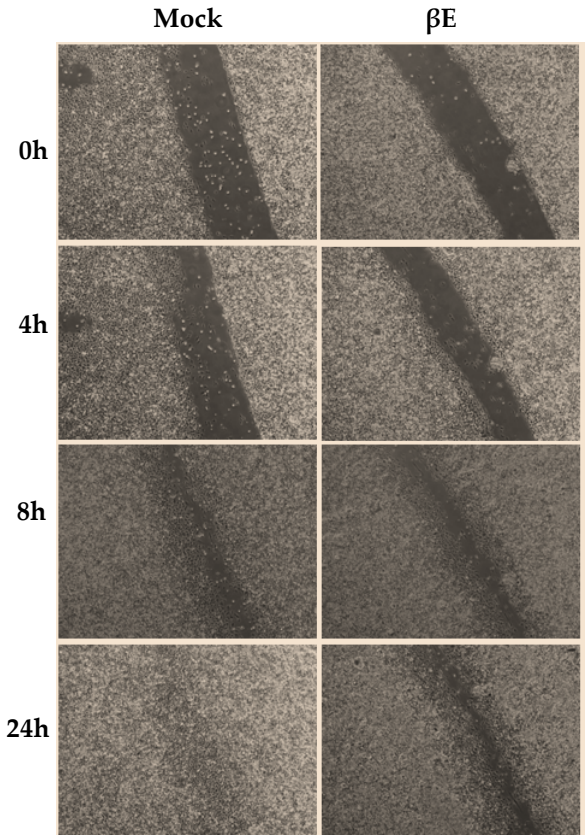

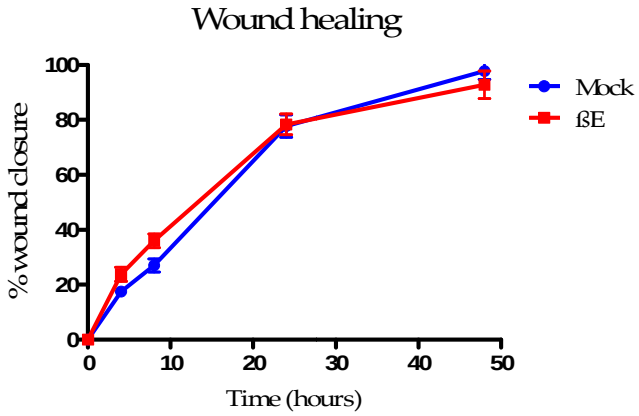

Figure 42: Hep3B cells with elevated βE levels were tested for migration in a scratch assay and compared to mock control. Wound closure in percent is depicted in the graph. Experiments were performed in duplicates.

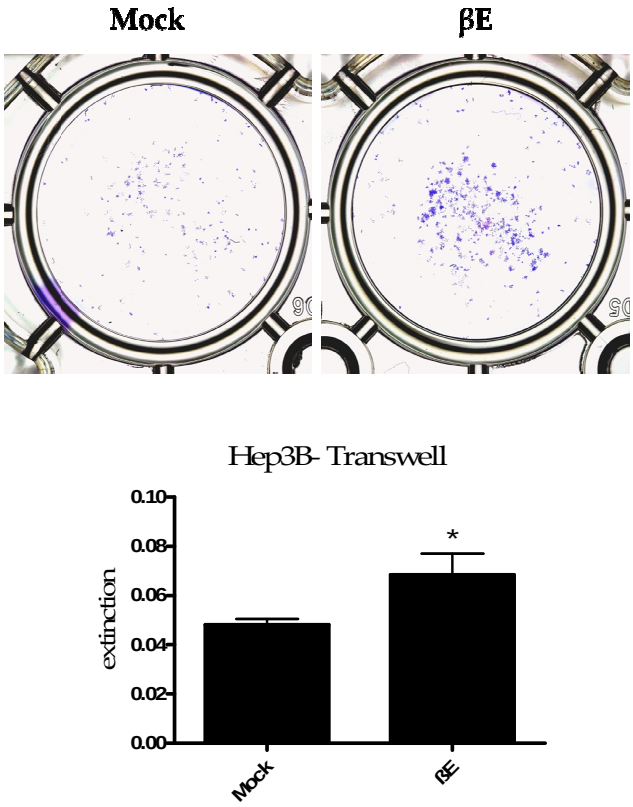

Figure 43: Hep3B cells with elevated βE levels were tested for migration through a porous membrane and compared to mock control. Cells on the bottom of the well were stained with crystal violet and documented via photography. Subsequently the dye was solubilized and absorption determined photometrically. Experiments were performed in duplicates.

5.5.5. Soft Agar

The Soft Agar assay which was performed to investigate anchorage-independent growth in three-dimensional culture revealed similar results as the clonogenicity assay. Cells were incubated for one month and clone formation was monitored by microscopy. Results showed significant differences in anchorage independent growth. Higher βE levels led to reduced clone sizes *(Figure 44)*. Again this effect was stronger in HepG2 cells where the βE silenced clones were able to create even bigger clones. Results clearly showed the impact of activin βE on anchorage independent growth behavior of hepatoma cell lines.

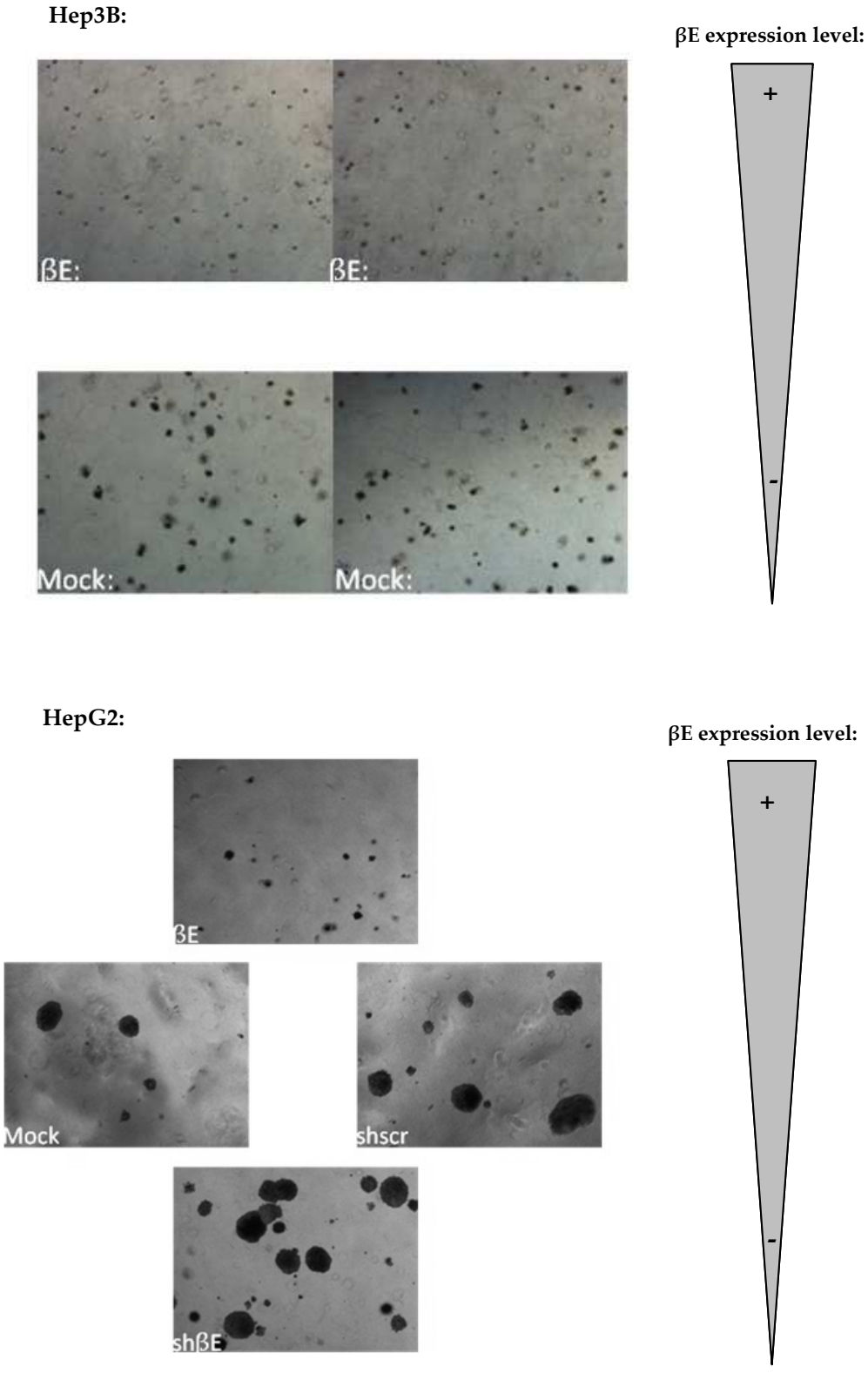

Figure 44: Two hepatoma cell lines with elevated or decreased activin E levels investigated for anchorage independent growth in a soft agar assay. Experiments were done twice in duplicates.

5.6. Transcriptome analysis: Microarray

Previous discoveries of our research group suggested that activin E does not signal via activin A receptors in contrast to activin A. For that purpose HepG2 cells were treated with activin E- or activin A-containing conditioned medium. SMAD2 phosphorylation was analyzed by Western blotting and was only achieved after treatment with Activin A-conditioned medium. Thus we performed expression arrays to investigate potential activin E target genes and potential pathways activin E might be involved in.

Tables 17-23 show the most strongly upregulated or downregulated genes in βE overexpressing or silenced cells.

Table 17: Genes with the strongest upregulation in βE overexpressing Hep3B cells compared to mock control (p-cut off: 0.005)

Fold change	Gene Symbol	Gene Name
72.192.326	TNFSF10	tumor necrosis factor (ligand) superfamily, member 10
58.520.384	SPON2	spondin 2, extracellular matrix protein
37.972.121	ALDH2	aldehyde dehydrogenase 2 family (mitochondrial)
29.477.897	LOC284561	hypothetical protein LOC284561
29.218.118	DOK3	docking protein 3
28.554.983	INPP4B	inositol polyphosphate-4-phosphatase, type II, 105kDa
25.692.537	NNMT	nicotinamide N-methyltransferase
25.187.178	OAS3	2'-5'-oligoadenylate synthetase 3, 100kDa
24.525.285	RFTN1	raftlin, lipid raft linker 1
22.899.847	C1S	complement component 1, s subcomponent
22.878.456	C11orf86	chromosome 11 open reading frame 86
22.334.228	PTPRE	protein tyrosine phosphatase, receptor type, E
20.989.166	SERPINB9	serpin peptidase inhibitor, clade B (ovalbumin), member 9
20.125.532	C9orf150	chromosome 9 open reading frame 150
16.620.596	HNMT	histamine N-methyltransferase
14.762.904	PRDM13	PR domain containing 13
14.063.863	CCL2	chemokine (C-C motif) ligand 2
8.138.984	PACSIN1	protein kinase C and casein kinase substrate in neurons 1
7.682.129	IGFBP2	insulin-like growth factor binding protein 2, 36kDa
6.502.067	RAC2	ras-related C3 botulinum toxin substrate 2 (rho family, small GTP binding protein Rac2)
5.219.576	VAV3	vav 3 guanine nucleotide exchange factor
4.341.417	KLRK1	killer cell lectin-like receptor subfamily K, member 1

3.608.239	HBE1	hemoglobin, epsilon 1
2.599.615	CD33	CD33 molecule
2.422.848	SERPINB8	serpin peptidase inhibitor, clade B (ovalbumin), member 8

Table 18: Genes with the strongest down regulation in βE overexpressing Hep3B cells (p-cut off: 0.005) compared to mock control

Fold change	Gene Symbol	Gene Name
-78.594.337	PID1	phosphotyrosine interaction domain containing 1
-75.120.435	KIF26B	kinesin family member 26B
-73.797.584	INHBA	inhibin, beta A
-66.683.493	SLC16A14	solute carrier family 16, member 14 (monocarboxylic acid transporter 14)
-62.050.586	CHSY3	chondroitin sulfate synthase 3
-56.006.455	TBC1D8B	TBC1 domain family, member 8B (with GRAM domain)
-48.262.563	PLIN2	perilipin 2
-47.573.543	CRYAB	crystallin, alpha B
-44.932.456	LY6D	lymphocyte antigen 6 complex, locus D
-43.962.555	MME	membrane metallo-endopeptidase
-42.843.037	FBN1	fibrillin 1
-41.815.395	OLFML2A	olfactomedin-like 2A
-38.130.786	NEBL	nebulette
-37.900.813	TWIST1	twist homolog 1 (Drosophila)
-36.724.718	TARSL2	threonyl-tRNA synthetase-like 2
-34.989.972	MGC5566	hypothetical protein MGC5566
-34.399.617	PSG2	pregnancy specific beta-1-glycoprotein 2
-34.361.622	EPHX2	epoxide hydrolase 2, cytoplasmic
-34.034.517	MAP1B	microtubule-associated protein 1B
-33.903.515	COMP	cartilage oligomeric matrix protein
-30.832.744	TOX	thymocyte selection-associated high mobility group box
-29.068.193	MYLK	myosin light chain kinase
-26.522.336	NEO1	neogenin homolog 1
-24.479.144	PLCG2	phospholipase C, gamma 2 (phosphatidylinositol-specific)
-23.219.671	TNFAIP3	tumor necrosis factor, alpha-induced protein 3
-23.146.129	TSPAN5	tetraspanin 5
-23.070.517	SESN3	sestrin 3
-21.198.237	GAB2	GRB2-associated binding protein 2

Table 19: Genes with the strongest regulation in βE overexpressing HepG2 cells compared to mock control (p-cut off: 0.05)

Fold change	Gene symbol	Gene name
22.154.768	NRP1	neuropilin 1
7.945.555	SHC3	SHC (Src homology 2 domain containing) transforming protein 3
-1.306.467	FGF2	fibroblast growth factor 2 (basic)
-16.511.409	PLK1S1	polo-like kinase 1 substrate 1

Table 20: Genes with the strongest upregulation in βE silenced HepG2 cells compared to scrambled control (p-cut off: 0.05)

Fold change	Gene symbol	Gene name
53.715.982	MATN3	matrilin 3
46.639.595	CXCR4	chemokine (C-X-C motif) receptor 4
44.935.265	GATA6	GATA binding protein 6
43.752.284	RASSF2	Ras association (RalGDS/AF-6) domain family member 2
38.858.762	AREG	amphiregulin
36.046.255	FGB	fibrinogen beta chain
35.110.023	ATP10A	ATPase, class V, type 10A
34.767.532	LPA	lipoprotein, Lp(a)
34.471.867	ARSI	arylsulfatase family, member I
33.723.102	PLG	plasminogen
30.969.763	TMSL3	thymosin-like 3
30.884.955	BIK	BCL2-interacting killer (apoptosis-inducing)
29.993.558	SOX8	SRY (sex determining region Y)-box 8
28.197.937	ODAM	odontogenic, ameloblast asssociated
25.075.233	PDLIM3	PDZ and LIM domain 3
23.881.536	CSGALNACT1	chondroitin sulfate N-acetylgalactosaminyltransferase 1
23.362.124	CCDC90B	coiled-coil domain containing 90B
23.251.696	C20orf114	chromosome 20 open reading frame 114
23.064.346	FXYD2	FXYD domain containing ion transport regulator 2
22.119.942	SLCO4A1	solute carrier organic anion transporter family, member 4A1
21.999.533	SLC7A10	solute carrier family 7, (neutral amino acid transporter, y+ system) member 10
21.594.415	UGT1A6	UDP glucuronosyltransferase 1 family, polypeptide A6
20.894.046	RCN1	reticulocalbin 1, EF-hand calcium binding domain
20.676.708	COL5A2	collagen, type V, alpha 2
20.158.842	DOCK8	dedicator of cytokinesis 8
20.044.498	RCN1	reticulocalbin 1, EF-hand calcium binding domain
16.679.701	CDK6	cyclin-dependent kinase 6
16.627.996	KLF9	Kruppel-like factor 9

Table 21: Genes with the strongest down regulation in βE silenced HepG2 cells compared to scrambled control (p-cut off: 0.05)

Fold change	Gene symbol	Gene name
-58.684.335	FSTL5	follistatin-like 5
-39.372.344	KRTAP3-1	keratin associated protein 3-1
-37.429.242	CDO1	cysteine dioxygenase, type I
-37.132.442	FGF13	fibroblast growth factor 13
-36.014.829	COBL	cordon-bleu homolog (mouse)
-35.948.849	LCN15	lipocalin 15
-35.048.552	AGTR1	angiotensin II receptor, type 1
-34.252.439	AQP3	aquaporin 3 (Gill blood group)
-32.355.046	ANKRD1	ankyrin repeat domain 1 (cardiac muscle)
-31.746.798	C8G	complement component 8, gamma polypeptide
-27.005.363	GSTA2	glutathione S-transferase alpha 2
-26.594.753	GSTA5	glutathione S-transferase alpha 5
-25.916.007	LGALS3	lectin, galactoside-binding, soluble, 3
-25.829.594	EFR3B	EFR3 homolog B (S. cerevisiae)
-24.957.435	ROR1	receptor tyrosine kinase-like orphan receptor 1
-23.343.658	AOX1	aldehyde oxidase 1
-22.928.731	KNG1	kininogen 1
-22.612.743	GSTA1	glutathione S-transferase alpha 1
-22.089.303	ROR1	receptor tyrosine kinase-like orphan receptor 1
-22.022.758	FRZB	frizzled-related protein
-21.941.109	IL17B	interleukin 17B
-21.870.906	HSD17B6	hydroxysteroid (17-beta) dehydrogenase 6 homolog (mouse)
-21.806.164	ADORA2A	adenosine A2a receptor
-21.768.827	CYP1A1	cytochrome P450, family 1, subfamily A, polypeptide 1
-21.271.157	DYDC2	DPY30 domain containing 2
-21.041.977	PPARGC1B	peroxisome proliferator-activated receptor gamma, coactivator 1 beta
-21.002.278	KIAA1211	KIAA1211
-19.917.067	AKR1B10	aldo-keto reductase family 1, member B10 (aldose reductase)

Table 22: Genes with the strongest upregulation in βE silenced K562 cells compared to scrambled control (p-cut off: 0.05)

Fold change	Gene symbol	Gene name
87.152.605	TF	transferrin
78.592.567	BCHE	butyrylcholinesterase
69.152.646	ZBTB20	zinc finger and BTB domain containing 20
67.465.143	ALPK1	alpha-kinase 1
66.925.416	BMP7	bone morphogenetic protein 7
65.463.476	LOC728148	hypothetical LOC728148
61.355.886	FCRLA	Fc receptor-like A
61.327.147	ZNF862	zinc finger protein 862
57.661.138	TM6SF1	transmembrane 6 superfamily member 1
53.973.117	ATL1	atlastin GTPase 1

47.718.244	FAM9B	family with sequence similarity 9, member B
45.223.513	FMN2	formin 2
43.956.585	CASP4	caspase 4, apoptosis-related cysteine peptidase
43.190.796	CSTA	cystatin A (stefin A)
43.172.073	C17orf108	chromosome 17 open reading frame 108
42.813.964	RGS3	regulator of G-protein signaling 3
41.411.753	LOC550643	hypothetical LOC550643
41.039.014	MAGEA9	melanoma antigen family A, 9
40.224.156	SCAND3	SCAN domain containing 3
39.737.864	SLC16A9	solute carrier family 16, member 9 (monocarboxylic acid transporter 9)
38.575.401	TPD52	tumor protein D52
38.520.043	CHAC1	ChaC, cation transport regulator homolog 1 (E. coli)
38.081.455	CLIC3	chloride intracellular channel 3
37.325.654	CDNF	cerebral dopamine neurotrophic factor
37.228.332	MAGI2	membrane associated guanylate kinase, WW and PDZ domain containing 2
37.002.301	ZNF618	zinc finger protein 618
36.347.253	A2LD1	AIG2-like domain 1
36.286.764	NEBL	nebulette
36.170.127	SCAND3	SCAN domain containing 3

Table 23: Genes with the strongest down regulation in βE silenced K562 cells compared to scrambled control (p-cut off: 0.05)

Fold change	Gene symbol	Gene name
-44.321.256	ARHGAP22	Rho GTPase activating protein 22
-41.625.404	ABCC3	ATP-binding cassette, sub-family C (CFTR/MRP), member 3
-34.202.886	MYBBP1A	MYB binding protein (P160) 1a
-31.906.345	PRG2	proteoglycan 2, bone marrow (natural killer cell activator, eosinophil granule major basic protein)
-31.674.523	TRMT61A	tRNA methyltransferase 61 homolog A (S. cerevisiae)
-28.635.979	POLR3H	polymerase (RNA) III (DNA directed) polypeptide H (22.9kD)
-27.985.365	SLC19A1	solute carrier family 19 (folate transporter), member 1
-27.255.046	NOLC1	nucleolar and coiled-body phosphoprotein 1
-26.329.486	COL1A2	collagen, type I, alpha 2
-25.463.548	DNAJA1	DnaJ (Hsp40) homolog, subfamily A, member 1
-24.092.095	LYPLA2	lysophospholipase II
-22.458.973	POLR2L	polymerase (RNA) II (DNA directed) polypeptide L, 7.6kDa
-21.855.948	AQP3	aquaporin 3 (Gill blood group)
-21.246.884	RASGEF1A	RasGEF domain family, member 1A
-20.812.352	POLR1E	polymerase (RNA) I polypeptide E, 53kDa
-20.643.992	PUS7	pseudouridylate synthase 7 homolog (S. cerevisiae)
-20.553.267	CTRL	chymotrypsin-like
-20.490.353	PPRC1	peroxisome proliferator-activated receptor gamma, coactivator-related 1
-19.739.822	FYB	FYN binding protein (FYB-120/130)
-19.581.864	ZC3HAV1	zinc finger CCCH-type, antiviral 1
-19.254.731	CTSC	cathepsin C
-19.162.354	QRSL1	glutaminyl-tRNA synthase (glutamine-hydrolyzing)-like 1

-18.998.454	WDR36	WD repeat domain 36
-18.882.649	FOXRED2	FAD-dependent oxidoreductase domain containing 2
-18.870.491	CXorf15	chromosome X open reading frame 15
-18.863.871	RRN3	RRN3 RNA polymerase I transcription factor homolog (S. cerevisiae)
-18.391.569	NOL12	nucleolar protein 12
-18.222.562	FBXO45	F-box protein 45
-18.150.611	SURF6	surfeit 6

6. Discussion

6.1. Establishment of activin E expression vectors for generation of stable clones

The central aim of this diploma thesis was to clarify how activin E functions in malignant cells. For that purpose on the one hand we carried out overexpression of activin E in low endogenous activin E-expressing Hep3B cells and HepG2 cells with medium activin E levels. Prior to transfection bicistronic expression vectors were generated containing an IRES sequence and verified by molecular sequencing which confirmed the absence of mutations. On the other hand we knocked down activin E in K562 leukemia cells with high endogenous activin E levels and in HepG2 cells. Thus in HepG2 we could compare knockdown and overexpression in the same cell model. Knockdowns were performed by sh-lentiviruses which were purchased commercially.

HepG2 and Hep3B hepatoma cell lines were transfected with vectors pHsβE-IRES-EGFP, pHsvβE-IRES-EGFP and the empty vector control pIRES-EGFP via lipofection to generate stable clones, because most of the previous data till now were gained by transient overexpression. Unlike untransfected cells, successfully transfected HepG2 and Hep3B cells were GFP-positive as all vector constructs (except the commercial shRNA expression constructs) carried the GFP-gene. Hence it was possible to determine the transfection efficiency via fluorescence microscopy and subject clones for selection to GFP-sort. The transfection efficiency was high of the empty vector and the βE construct. It could be observed that for the used hepatoma cell lines transfection efficiencies of 30-50% for pIRES-EGFP and pHsβE-IRES-EGFP respectively were obtained, but 0-1% for pHsvβe-IRES-EGFP. In previous experiments it was shown that cloning of vβE was not an easy task (Michael Grusch,

personal communicaiton), even when we sorted almost 1% GFP positive cells and expanded them, the cells lost GFP expression shortly afterwards. For this reason we treated vβE transfected cells with 5′azacytidine, which is a demethylating agent, and investigated if there is an epigenetic regulation of this gene. vβE transfected cells were treated with 5′azacytidine and non-treated vβE-expressing cells served as controls. Subsequently fluorescence was monitored for several days. Cells slightly gained back their fluorescence but also untreated control cells fluoresced at a very low rate. This effect might be due to the fact that the cells were not subjected to splitting during the experiment; however the fluorescence rate of vβE-transfected cells was still not indicative of a significant expression of the bicistronic transcript. Hence we decided to focus on the βE overexpressing and silenced cells.

After successful cloning and sorting, expression of βE in stable clones was verified by using qPCR and we achieved an overexpression of 400 fold in Hep3B and 20 fold in HepG2 cells. The differences in the overexpression levels might be due to the fact that the HepG2 cell line expresses endogenously far more Activin E than Hep3B cells. Untransfected HepG2 cells have an Activin E CT value of 25 whereas Hep3B cells have a CT of 30 (the CT values of the respective housekeeping genes range between 20-21 for both cell lines). However even in the cells with the highest ectopic overexpression (Hep3B) we do not exceed the level found in cells endogenously expressing high levels of activin βE such as normal hepatocytes.

For silencing, K562 leukemia cells and HepG2 hepatoma cells were cultured and transduced with sh-lentiviruses targeting activin βE and with scrambled sh control. After transfection, stable clones were obtained by antibiotic selection and the expression level was determined by qRT-PCR which demonstrated a successful knockdown of activin E.

6.2. Expression of Histidin-tagged activin E and A

Successful purification and quantification of activin E is a prerequisite for testing of potential target receptors. In order to investigate the effects of activin E, an expression system was created for a 6xhistidin-tagged version, since activin E protein is not available commercially. Expression of activin A in SF9 cells was shown previously by Wuytens et al. (1999) but this approach has not been tested for activin E. Our results suggest that SF9 cells as expression system are not suitable for the synthesis of recombinant activins. We did not achieve bioactivity of His-tagged activin A proteins, although they were able to form dimers and were detectable by Western Blot analysis. A CHO expression system could be more capable to produce activin E, based on previous reports of the production of bioactive activin A by the CHO expression system (Wada et al., 2004; Arai et al., 2006). In fact production and EtOH precipitation of activin A was not a complicated task, as with commercially available antibodies against either the histidin tag or against activin A the produced proteins were detectable. However 6xhistidin was detectable in activin E expressing cells only when gels were run under reducing conditions before immunoblotting. It has to be evaluated which factor is responsible for the lack of bioactivity in our system. Based on these findings we reason that another expression system may be required for optimizing an approach to produce and purify recombinant activin E.

6.3. Biological effects of activin E overexpression or silencing

Stable clones with decreased or increased activin E levels were consequently used for functional tests and the whole transcriptome was analyzed via expression arrays. The phenotypic differences when activin E levels lessen or were increased were analyzed by different assays. Phenotypic properties such as proliferation (obtained by CASY measurement), viability (MTT assay), clonogenicity (clonogenic survival assay), cell

cycle status (FACS analysis), migration (by wound healing and transwell assay) and anchorage independent growth (Soft agar assay) were monitored and investigated for different time periods.

Results of functional tests assessing short-term viability and proliferation did not demonstrate any obvious effects of decreased or increased βE levels, the proliferation rate was quite similar. When we incubated stable clones under reduced serum compared to normal serum conditions we did not monitor a strong advantage or disadvantage of βE expression compared to the mock control. By contrast experiments assessing anchorage-independent growth in three-dimensional cultures clearly demonstrated that the higher the βE expression levels the smaller were the colonies. This effect was stronger in HepG2 cells where the βE silenced clones could create bigger clones in contrast to βE overexpressing cells which could not build up clones about a certain threshold. The soft agar assay, which can be considered to be an in-vivo-like assay, illustrates the tumorigenic properties of cells. Similar results were obtained when we analyzed the capability of single cells to form colonies on tissue culture plastic. In these so called clonogenic survival assays we found that the number as well as clone sizes differed between mock transfected and βE transfected cells, in fact βE silenced cells showed a reduced number but bigger size of clones. This effect was again stronger in assays performed with HepG2 cells. When we measured crystal violet photometrically we could verify our findings only for the βE transfected HepG2 and Hep3B cells but not for our silenced HepG2 cells. To solubilize crystal violet from HepG2 cells was not an easy task due to the growth of HepG2 cells in tight multilayered colonies. This can be considered as one reason for our photometric results. On the other hand the observation was that the more βE the cells expressed the higher the number of (small) obtained clones was. The clonogenic assay addresses on the one hand survival at low density and on the other hand the ability to form colonies due to proliferation fitness. Even when βE silenced clones created bigger clones due to their proliferation advantage they might have difficulties in adhering and to survive at low density.

Latter results don't confirm our findings in proliferation and viability gained by Casy measurement and MTT assays where we could not detect differences between clones and controls. Reasons for that could be on the one hand that in the proliferation and viability assays cells were monitored only for a relatively short time period of 5-8 days compared to the clonogenic assay which was incubated 2 weeks and the soft agar assay which was allowed to develop for at least 4 weeks. The longer the assay lasted the stronger were the effects. On the other hand it has to be considered that during investigation of the cumulative cell number the possibility for technical problems is higher, cells might have responded differently due to repeated splitting and reseeding. Conflicting results regarding the impact of activin E on proliferation were also found in previous results from other research groups, e.g. HepG2 cells treated with activin E-conditioned medium did not demonstrate any effects on cell proliferation (Hashimoto et al., 2009), whereas transient expression of βE in HepG2 reduced cell number and induced apoptosis (Vejda et al., 2003).

Interestingly we also see a slight impact of activin βE on the migration of cells. When confluent cell monolayers were scraped with a pipette tip and the closure of the scratches was monitored for a certain time, βE overexpressing cells seemed to fill the gap more rapidly, when quantified in percentage there was a difference of more than 10% gap closure after 8 hours of incubation. This trend was not sustained, however, since after 24 hours the mock control but not the βE overexpressing cells could close the gap completely. Significant differences between mock and βE transfected cells were observed in the transwell assay, where βE overexpressing cells showed a higher ability in passing the membrane. If we solubilized the crystal violet with SDS the results could be further confirmed. Here it has to be kept in mind that the transwell assay is incubated only for a relative short time, especially in the case of the highly proliferative Hep3B cells, to allow only a low number of cells to drop into the well, and thus might demonstrate short term effects. Additionally it has to be distinguished between the ability of cells to pass through a membrane and to migrate laterally as in the wound healing assay.

6.4. Transcriptome analysis and investigation of target genes of activin E

As already mentioned in the introduction Activin A, B and heterodimers AB initiate their biological activity, like most members of the TGF-β superfamily, through type I and type II transmembrane (serine/threonine) kinase receptors whereof various isoforms exist. Further they activate downstream signaling effectors the so called SMADs and regulate target gene expression. These findings could not be demonstrated for activin E in previous results of our research group and thus signaling mechanisms of activin E need further investigation.

Expression analysis revealed some strongly regulated genes when βE overexpressing and silenced cells were compared to their respective controls. When activin E levels were elevated in Hep3B cells genes involved in apoptosis were strongly regulated. TNFSF10 (tumor necrosis factor (ligand) superfamily, member 10) for instance, which belongs to the tumor necrosis factor family induces apoptosis in tumor cells. Additionally it triggers the activation of caspase 8, caspase 3 and MAPK8/JNK (Kuribayashi et al., 2008). We obtained a 70 fold upregulation of TNFSF10 in Hep3B cells with elevated βE levels. As another indication of apoptosis regulation we detected that TNFAIP3 (tumor necrosis factor, alpha-induced protein 3) gene expression was 23 fold downregulated. This gene, which is regulated by TNF is known to inhibit TNF-mediated apoptosis and NF-kappa B activation (Nino Fong et al., 2011). These observations support the thesis that activin E overexpression leads to reduced proliferation and induction of apoptosis (Vejda et al., 2003; Wada et al., 2005). Gab 2 (GRB2-associated binding protein) was also one of the strongly down regulated genes in βE overexpressing Hep3B cells (21 fold). Gab2 down-regulation by RNA interference is known to strongly abrogate cell growth in soft agar (Mira A. et al., 2009), consistent with our soft agar experiments where βE overexpressing cells demonstrated reduced proliferation. Interestingly TWIST1 (twist homolog 1) is

strongly downregulated in βE expressing Hep3B cells. Twist is known to promote EMT (epithelial to mesenchymal transition) and tumor metastasis together with Snail 2. EMT is a process, which leads in vivo to metastatic growth, because of increased motility and invasiveness of the cells (van Zijl et al., 2011). Although we could not observe a less migratory capability of βE overexpressing cells in the transwell assay, we observed impaired motility of βE transfected cells in the wound healing assay, where βE transfectants could not completely fill the gap in contrast to the mock control. Nevertheless it has to be kept in mind that EMT is not the only mechanism of migration.

NEO 1 (neogenin homolog 1) is also strongly decreased in activin E overexpressing cells. Neogenin is a known receptor of bone morphogenetic proteins and consequently modulates SMAD signaling (Hagihara et al., 2011). The most interesting gene which was heavily downregulated in Hep3B cells when βE levels were elevated is activin βA where we obtained a 74 fold down regulation. This could mean that there is a feed-back loop connecting these two activin subunits, despite the fact that in previous results of our research group activin E did not block activin A signaling. The crosstalk between these two cytokines has to be further investigated.

In HepG2 cells overexpressing activin E some members of the VEGF signaling pathway were upregulated. Unlike in activin E silenced HepG2 cells we did not obtain many regulated genes in βE transfected HepG2. Activin E silenced HepG2 cells demonstrated elevated levels of GATA 6 (gata binding protein 6) which promotes survival and angiogenesis in endothelial cells. Additionally GATA 6 protects from apoptosis, and it was shown that overexpression of GATA 6 suppressed the activity of the TGF-beta 1 promoter (Froese et al., 2011). Amphiregulin (AREG) which is a EGF-receptor ligand and related to TGF-α, is strongly upregulated in activin E silenced HepG2 cells. AREG expression in cancerous tissue is connected to apoptosis-resistance, high replication rate, metastasis and invasive behavior to mention some (Busser et al., 2011). Elevated AREG

expression could contribute to the increased anchorage-independent growth observed for HepG2 cells with silenced βE in this study.

K562 leukemia cells have elevated levels of activin E in contrast to hepatoma cells. By this reason we were interested in the phenotype of these cells when we knocked down activin E. As shown in Hep3B cells which in contrast were brought to overexpress activin E, also in silenced K562 cells we found the same observation that apoptosis inducing genes such as Casp4 were upregulated. Additionally we found that bone morphogenetic protein 7 (BMP7), which is a member of the TGF-β family, was strongly upregulated (66 fold). Regulation of the expression of other TGF- β family members is suggested as one of the roles of activin E.

The determination of the functions of activin E is still rather difficult. Taking all results together activin E crosstalks with various signaling pathways but cannot be connected to a certain receptor. Activin E seems to modulate signaling of related cytokines, and reduce proliferation in hepatoma cells, which was also shown for the related cytokine activin A (Deli et al., 2008). However the expression arrays need further evaluation, genes regulated in the expression arrays have to be validated with other methods and a new approach to produce recombinant activin E has to be established.

7. Appendix

7.1. List of figures

7.2. List of abbreviations

ALK	activin receptor-like kinase
B2M	beta-2 microglobulin
BMP	bone morphogenetic protein
BSA	bovine serum albumin
CIAP	Calf intestinal alkaline phosphatase
DMSO	Dimethyl sulfoxide
EDTA	ethylenediaminetetraacetic acid
FACS	fluorescence-activated cell sorting
FCS	fetal calf serum
FLRG	follistatin-related gene
FSH	follicle stimulating hormone
Fst	Follistatin
GAPDH	glyceraldehyde-3 phosphate dehydrogenase
GDF	growth and differentiation factor
HCC	hepatocellular carcinoma
MIS	Muellerian inhibiting substance
MTT	dimethyl thiazolyl diphenyl tetrazolium salt
PBS	phosphate buffered saline
PVDF	Polyvinylidene fluoride
PVN	paraventricular axis
RT-PCR	reverse transcriptase polymerase chain reaction
SDS	sodium dodecyl sulfate
SDS-PAGE	sodium dodecyl sulphate polyacrylamide gel electrophoresis
TBS	Tris buffered saline

TBST	Tris buffered saline with 0.1% Tween-20
TE	Tris EDTA buffer solution
TEMED	N,N,N′,N′–tetramethylethylenediamine
TGF-β	Transforming growth factor beta
VLDLR	very low density lipoprotein receptor

7.3. List of tables

8. References

Abe, Y., Minegishi, T., and Leung, P.C. (2004). Activin receptor signaling. Growth factors (Chur, Switzerland) *22*, 105-110.

Attisano, L., Wrana, J.L., Montalvo, E., and Massague, J. (1996). Activation of signalling by the activin receptor complex. Molecular and cellular biology *16*, 1066-1073.

Bedossa, P., Peltier, E., Terris, B., Franco, D., and Poynard, T. (1995). Transforming growth factor-beta 1 (TGF-beta 1) and TGF-beta 1 receptors in normal, cirrhotic, and neoplastic human livers. Hepatology (Baltimore, Md *21*, 760-766.

Brown, M.L., Bonomi, L., Ungerleider, N., Zina, J., Kimura, F., Mukherjee, A., Sidis, Y., and Schneyer, A. (2011). Follistatin and Follistatin Like-3 Differentially Regulate Adiposity and Glucose Homeostasis. Obesity (Silver Spring, Md.

Busser, B., Sancey, L., Brambilla, E., Coll, J.L., and Hurbin, A. (2011). The multiple roles of amphiregulin in human cancer. Biochimica et biophysica acta *1816*, 119-131.

Butler, C.M., Gold, E.J., and Risbridger, G.P. (2005). Should activin betaC be more than a fading snapshot in the activin/TGFbeta family album? Cytokine & growth factor reviews *16*, 377-385.

Chabicovsky, M., Herkner, K., and Rossmanith, W. (2003). Overexpression of activin beta(C) or activin beta(E) in the mouse liver inhibits regenerative deoxyribonucleic acid synthesis of hepatic cells. Endocrinology *144*, 3497-3504.

Chen, Y.G., Wang, Q., Lin, S.L., Chang, C.D., Chuang, J., and Ying, S.Y. (2006). Activin signaling and its role in regulation of cell proliferation, apoptosis, and carcinogenesis. Experimental biology and medicine (Maywood, N.J *231*, 534-544.

Chow, L.S., Lam, C.W., Chan, S.Y., Tsao, S.W., To, K.F., Tong, S.F., Hung, W.K., Dammann, R., Huang, D.P., and Lo, K.W. (2006). Identification of RASSF1A modulated genes in nasopharyngeal carcinoma. Oncogene *25*, 310-316.

Cook, R.W., Thompson, T.B., Jardetzky, T.S., and Woodruff, T.K. (2004). Molecular biology of inhibin action. Seminars in reproductive medicine *22*, 269-276.

de Winter, J.P., ten Dijke, P., de Vries, C.J., van Achterberg, T.A., Sugino, H., de Waele, P., Huylebroeck, D., Verschueren, K., and van den Eijnden-van Raaij, A.J. (1996). Follistatins neutralize activin bioactivity by inhibition of activin binding to its type II receptors. Molecular and cellular endocrinology *116*, 105-114.

Deli, A., Kreidl, E., Santifaller, S., Trotter, B., Seir, K., Berger, W., Schulte-Hermann, R., Rodgarkia-Dara, C., and Grusch, M. (2008). Activins and activin antagonists in hepatocellular carcinoma. World J Gastroenterol *14*, 1699-1709.

Dombroski, B.A., Nayak, R.R., Ewens, K.G., Ankener, W., Cheung, V.G., and Spielman, R.S. (2010). Gene expression and genetic variation in response to endoplasmic reticulum stress in human cells. American journal of human genetics *86*, 719-729.

Ebert, S., Zeretzke, M., Nau, R., and Michel, U. (2007). Microglial cells and peritoneal macrophages release activin A upon stimulation with Toll-like receptor agonists. Neuroscience letters *413*, 241-244.

Eramaa, M., Hurme, M., Stenman, U.H., and Ritvos, O. (1992). Activin A/erythroid differentiation factor is induced during human monocyte activation. The Journal of experimental medicine *176*, 1449-1452.

Fang, J., Wang, S.Q., Smiley, E., and Bonadio, J. (1997). Genes coding for mouse activin beta C and beta E are closely linked and exhibit a liver-specific expression pattern in adult tissues. Biochemical and biophysical research communications *231*, 655-661.

Fang, J., Yin, W., Smiley, E., Wang, S.Q., and Bonadio, J. (1996). Molecular cloning of the mouse activin beta E subunit gene. Biochem Biophys Res Commun *228*, 669-674.

Fischer, A.N.M., Blanca Herrera, Mario Mikula, Verena Proell, Eva Fuchs, Josef Gotzmann, Rolf Schulte-Hermann, Hartmut Beug, and Mikulits, W. (2005). Integration of Ras subeffector signaling in TGF-b mediated late stage hepatocarcinogenesis.

Froese, N., Kattih, B., Breitbart, A., Grund, A., Geffers, R., Molkentin, J.D., Kispert, A., Wollert, K.C., Drexler, H., and Heineke, J. (2011). GATA6 promotes angiogenic function and survival in endothelial cells by suppression of autocrine transforming growth factor beta/activin receptor-like kinase 5 signaling. The Journal of biological chemistry *286*, 5680-5690.

Gold, E., Jetly, N., O'Bryan, M.K., Meachem, S., Srinivasan, D., Behuria, S., Sanchez-Partida, L.G., Woodruff, T., Hedwards, S., Wang, H., *et al.* (2009). Activin C antagonizes activin A in vitro and overexpression leads to pathologies in vivo. The American journal of pathology *174*, 184-195.

Graham, F.L., Smiley, J., Russell, W.C., and Nairn, R. (1977). Characteristics of a human cell line transformed by DNA from human adenovirus type 5. J Gen Virol *36*, 59-74.

Groome, N., and O'Brien, M. (1993). Immunoassays for inhibin and its subunits. Further applications of the synthetic peptide approach. Journal of immunological methods *165*, 167-176.

Grusch, M., Rodgarkia-Dara, C., Bursch, W., and Schulte-Hermann, R. (2008). Activins and the liver. In TGF-ß Superfamily Members in Normal and Tumor Biology, S. Jakowlew, ed. (Totowa: Humana Press).

Hagihara, M., Endo, M., Hata, K., Higuchi, C., Takaoka, K., Yoshikawa, H., and Yamashita, T. (2011). Neogenin, a receptor for bone morphogenetic proteins. The Journal of biological chemistry *286*, 5157-5165.

Harrington, A.E., Morris-Triggs, S.A., Ruotolo, B.T., Robinson, C.V., Ohnuma, S., and Hyvonen, M. (2006). Structural basis for the inhibition of activin signalling by follistatin. Embo J *25*, 1035-1045.

Harrison, C.A., Wiater, E., Gray, P.C., Greenwald, J., Choe, S., and Vale, W. (2004). Modulation of activin and BMP signaling. Mol Cell Endocrinol *225*, 19-24.

Hashimoto, O., Sekiyama, K., Matsuo, T., and Hasegawa, Y. (2009). Implication of activin E in glucose metabolism: transcriptional regulation of the inhibin/activin betaE subunit gene in the liver. Life sciences *85*, 534-540.

Hashimoto, O., Tsuchida, K., Ushiro, Y., Hosoi, Y., Hoshi, N., Sugino, H., and Hasegawa, Y. (2002). cDNA cloning and expression of human activin betaE subunit. Molecular and cellular endocrinology *194*, 117-122.

Hashimoto, O., Ushiro, Y., Sekiyama, K., Yamaguchi, O., Yoshioka, K., Mutoh, K., and Hasegawa, Y. (2006). Impaired growth of pancreatic exocrine cells in transgenic mice expressing human activin betaE subunit. Biochemical and biophysical research communications *341*, 416-424.

Heldin, C.H., Miyazono, K., and ten Dijke, P. (1997). TGF-beta signalling from cell membrane to nucleus through SMAD proteins. Nature *390*, 465-471.

Kang, W., Saqui-Salces, M., Zavros, Y., and Merchant, J.L. (2008). Induction of follistatin precedes gastric transformation in gastrin deficient mice. Biochemical and biophysical research communications *376*, 573-577.

Katoh, Y., and Katoh, M. (2008). Hedgehog signaling, epithelial-to-mesenchymal transition and miRNA (review). International journal of molecular medicine *22*, 271-275.

Kingsley, D.M. (1994). The TGF-beta superfamily: new members, new receptors, and new genetic tests of function in different organisms. Genes & development *8*, 133-146.

Knowles, B.B., Howe, C.C., and Aden, D.P. (1980). Human hepatocellular carcinoma cell lines secrete the major plasma proteins and hepatitis B surface antigen. Science *209*, 497-499.

Kreidl, E., Ozturk, D., Metzner, T., Berger, W., and Grusch, M. (2009). Activins and follistatins: Emerging roles in liver physiology and cancer. World journal of hepatology *1*, 17-27.

Kuribayashi, K., Krigsfeld, G., Wang, W., Xu, J., Mayes, P.A., Dicker, D.T., Wu, G.S., and El-Deiry, W.S. (2008). TNFSF10 (TRAIL), a p53 target gene that mediates p53-dependent cell death. Cancer biology & therapy *7*, 2034-2038.

Lasorella, A., Uo, T., and Iavarone, A. (2001). Id proteins at the cross-road of development and cancer. Oncogene *20*, 8326-8333.

Lau, A.L., Kumar, T.R., Nishimori, K., Bonadio, J., and Matzuk, M.M. (2000). Activin betaC and betaE genes are not essential for mouse liver growth, differentiation, and regeneration. Molecular and cellular biology *20*, 6127-6137.

Lewis, K.A., Gray, P.C., Blount, A.L., MacConell, L.A., Wiater, E., Bilezikjian, L.M., and Vale, W. (2000). Betaglycan binds inhibin and can mediate functional antagonism of activin signalling. Nature *404*, 411-414.

Ling, N., Ying, S.Y., Ueno, N., Shimasaki, S., Esch, F., Hotta, M., and Guillemin, R. (1986). Pituitary FSH is released by a heterodimer of the beta-subunits from the two forms of inhibin. Nature *321*, 779-782.

Liu, Q.Y., Niranjan, B., Gomes, P., Gomm, J.J., Davies, D., Coombes, R.C., and Buluwela, L. (1996). Inhibitory effects of activin on the growth and morpholgenesis of primary and transformed mammary epithelial cells. Cancer research *56*, 1155-1163.

Lozzio, B.B., and Lozzio, C.B. (1979). Properties and usefulness of the original K-562 human myelogenous leukemia cell line. Leuk Res *3*, 363-370.

Martin, S.K., Fitter, S., Bong, L.F., Drew, J.J., Gronthos, S., Shepherd, P.R., and Zannettino, A.C. (2010). NVP-BEZ235, a dual pan class I PI3 kinase and mTOR inhibitor, promotes osteogenic differentiation in human mesenchymal stromal cells. J Bone Miner Res *25*, 2126-2137.

Masker, K., Golden, A., Gaffney, C.J., Mazack, V., Schwindinger, W.F., Zhang, W., Wang, L.H., Carey, D.J., and Sudol, M. (2007). Transcriptional profile of Rous Sarcoma Virus transformed chicken embryo fibroblasts reveals new signaling targets of viral-src. Virology *364*, 10-20.

Mason, A.J. (1994). Functional analysis of the cysteine residues of activin A. Molecular endocrinology (Baltimore, Md *8*, 325-332.

Massague, J. (2008). TGFbeta in Cancer. Cell *134*, 215-230.

McCullagh, D.R. (1932). Dual Endocrine Activity of the Testes. Science (New York, N.Y *76*, 19-20.

Mellor, S.L., Ball, E.M., O'Connor, A.E., Ethier, J.F., Cranfield, M., Schmitt, J.F., Phillips, D.J., Groome, N.P., and Risbridger, G.P. (2003). Activin betaC-subunit heterodimers provide a new mechanism of regulating activin levels in the prostate. Endocrinology *144*, 4410-4419.

Mellor, S.L., Cranfield, M., Ries, R., Pedersen, J., Cancilla, B., de Kretser, D., Groome, N.P., Mason, A.J., and Risbridger, G.P. (2000). Localization of activin beta(A)-, beta(B)-, and beta(C)-subunits in humanprostate and evidence for formation of new activin heterodimers of beta(C)-subunit. The Journal of clinical endocrinology and metabolism *85*, 4851-4858.

Muenster, U., Harrison, C.A., Donaldson, C., Vale, W., and Fischer, W.H. (2005). An activin-A/C chimera exhibits activin and myostatin antagonistic properties. The Journal of biological chemistry *280*, 36626-36632.

Mylonas, I., Bruning, A., Shabani, N., Kunze, S., and Kupka, M.S. (2010). Evidence of inhibin/activin subunit betaC and betaE synthesis in normal human endometrial tissue. Reprod Biol Endocrinol *8*, 143.

Naber, H.P., ten Dijke, P., and Pardali, E. (2008). Role of TGF-beta in the tumor stroma. Current cancer drug targets *8*, 466-472.

Nagaraj, N.S., and Datta, P.K. (2010). Targeting the transforming growth factor-beta signaling pathway in human cancer. Expert Opin Investig Drugs *19*, 77-91.

Nino Fong, R., Fatehi-Hassanabad, Z., Lee, S.C., Lu, H., Wheeler, M.B., and Chan, C.B. (2011). Uncoupling protein-2 increases nitric oxide production and TNFAIP3 pathway activation in pancreatic islets. Journal of molecular endocrinology *46*, 193-204.

O'Bryan, M.K., Sebire, K.L., Gerdprasert, O., Hedger, M.P., Hearn, M.T., and de Kretser, D.M. (2000). Cloning and regulation of the rat activin betaE subunit. J Mol Endocrinol *24*, 409-418.

Oberhammer, F., Bursch, W., Parzefall, W., Breit, P., Erber, E., Stadler, M., and Schulte-Hermann, R. (1991). Effect of transforming growth factor beta on cell death of cultured rat hepatocytes. Cancer research *51*, 2478-2485.

Oberhammer, F.A., Pavelka, M., Sharma, S., Tiefenbacher, R., Purchio, A.F., Bursch, W., and Schulte-Hermann, R. (1992). Induction of apoptosis in cultured hepatocytes and in regressing liver by

transforming growth factor beta 1. Proceedings of the National Academy of Sciences of the United States of America *89*, 5408-5412.
Oda, S., Nishimatsu, S., Murakami, K., and Ueno, N. (1995). Molecular cloning and functional analysis of a new activin beta subunit: a dorsal mesoderm-inducing activity in Xenopus. Biochem Biophys Res Commun *210*, 581-588.
Ogino, H., Yano, S., Kakiuchi, S., Muguruma, H., Ikuta, K., Hanibuchi, M., Uehara, H., Tsuchida, K., Sugino, H., and Sone, S. (2008). Follistatin suppresses the production of experimental multiple-organ metastasis by small cell lung cancer cells in natural killer cell-depleted SCID mice. Clin Cancer Res *14*, 660-667.
Osamu Hashimoto, Y.U., Kazunari Sekiyama, Osamu Yamaguchi, Kazuki Yoshioka, Ken-Ichiro Mutoh, Yoshihisa Hasegawa Impaired growth of pancreatic exocrine cells in transgenic mice expressing human activin bE subunit.
Pangas, S.A., and Woodruff, T.K. (2000). Activin signal transduction pathways. Trends in endocrinology and metabolism: TEM *11*, 309-314.
Perrien, D.S., Akel, N.S., Edwards, P.K., Carver, A.A., Bendre, M.S., Swain, F.L., Skinner, R.A., Hogue, W.R., Nicks, K.M., Pierson, T.M., *et al.* (2007). Inhibin A is an endocrine stimulator of bone mass and strength. Endocrinology *148*, 1654-1665.
Phillips, D.J., de Kretser, D.M., and Hedger, M.P. (2009). Activin and related proteins in inflammation: not just interested bystanders. Cytokine & growth factor reviews *20*, 153-164.
Razanajaona, D., Joguet, S., Ay, A.S., Treilleux, I., Goddard-Leon, S., Bartholin, L., and Rimokh, R. (2007). Silencing of FLRG, an antagonist of activin, inhibits human breast tumor cell growth. Cancer research *67*, 7223-7229.
Rebbapragada, A., Benchabane, H., Wrana, J.L., Celeste, A.J., and Attisano, L. (2003). Myostatin signals through a transforming growth factor beta-like signaling pathway to block adipogenesis. Molecular and cellular biology *23*, 7230-7242.
Risbridger, G.P., Schmitt, J.F., and Robertson, D.M. (2001). Activins and inhibins in endocrine and other tumors. Endocrine reviews *22*, 836-858.
Rodgarkia-Dara, C., Vejda, S., Erlach, N., Losert, A., Bursch, W., Berger, W., Schulte-Hermann, R., and Grusch, M. (2006). The activin axis in liver biology and disease. Mutation research *613*, 123-137.
Rossmanith, W., Chabicovsky, M., Grasl-Kraupp, B., Peter, B., Schausberger, E., and Schulte-Hermann, R. (2002). Follistatin overexpression in rodent liver tumors: a possible mechanism to overcome activin growth control. Molecular carcinogenesis *35*, 1-5.
Schmierer, B., and Hill, C.S. (2007). TGFbeta-SMAD signal transduction: molecular specificity and functional flexibility. Nature reviews *8*, 970-982.
Schneyer, A.L., Rzucidlo, D.A., Sluss, P.M., and Crowley, W.F., Jr. (1994). Characterization of unique binding kinetics of follistatin and activin or inhibin in serum. Endocrinology *135*, 667-674.
Schrewe, H., Gendron-Maguire, M., Harbison, M.L., and Gridley, T. (1994). Mice homozygous for a null mutation of activin beta B are viable and fertile. Mechanisms of development *47*, 43-51.
Scutera, S., Riboldi, E., Daniele, R., Elia, A.R., Fraone, T., Castagnoli, C., Giovarelli, M., Musso, T., and Sozzani, S. (2008). Production and function of activin A in human dendritic cells. European cytokine network *19*, 60-68.
Sekiyama, K., Hashimoto, O., Ushiro, Y., Adachi, C., Kikusui, T., Tanemura, K., and Hasegawa, Y. (2009). Abnormalities in aggression and anxiety in transgenic mice overexpressing activin E. Biochemical and biophysical research communications *385*, 319-323.
Shoji-Kasai, Y., Ageta, H., Hasegawa, Y., Tsuchida, K., Sugino, H., and Inokuchi, K. (2007). Activin increases the number of synaptic contacts and the length of dendritic spine necks by modulating spinal actin dynamics. Journal of cell science *120*, 3830-3837.
Sjoblom, T., Jones, S., Wood, L.D., Parsons, D.W., Lin, J., Barber, T.D., Mandelker, D., Leary, R.J., Ptak, J., Silliman, N., *et al.* (2006). The consensus coding sequences of human breast and colorectal cancers. Science (New York, N.Y *314*, 268-274.

Spencer, S.J., Rabinovici, J., and Jaffe, R.B. (1990). Human recombinant activin-A inhibits proliferation of human fetal adrenal cells in vitro. The Journal of clinical endocrinology and metabolism *71*, 1678-1680.
Stove, C., Vanrobaeys, F., Devreese, B., Van Beeumen, J., Mareel, M., and Bracke, M. (2004). Melanoma cells secrete follistatin, an antagonist of activin-mediated growth inhibition. Oncogene *23*, 5330-5339.
Sugino, K., Kurosawa, N., Nakamura, T., Takio, K., Shimasaki, S., Ling, N., Titani, K., and Sugino, H. (1993). Molecular heterogeneity of follistatin, an activin-binding protein. Higher affinity of the carboxyl-terminal truncated forms for heparan sulfate proteoglycans on the ovarian granulosa cell. J Biol Chem *268*, 15579-15587.
Thompson, T.B., Lerch, T.F., Cook, R.W., Woodruff, T.K., and Jardetzky, T.S. (2005). The structure of the follistatin:activin complex reveals antagonism of both type I and type II receptor binding. Developmental cell *9*, 535-543.
Trowitzsch, S., Bieniossek, C., Nie, Y., Garzoni, F., and Berger, I. (2010). New baculovirus expression tools for recombinant protein complex production. Journal of structural biology *172*, 45-54.
Tsuchida, K., Arai, K.Y., Kuramoto, Y., Yamakawa, N., Hasegawa, Y., and Sugino, H. (2000). Identification and characterization of a novel follistatin-like protein as a binding protein for the TGF-beta family. The Journal of biological chemistry *275*, 40788-40796.
Tsuchida, K., Nakatani, M., Yamakawa, N., Hashimoto, O., Hasegawa, Y., and Sugino, H. (2004). Activin isoforms signal through type I receptor serine/threonine kinase ALK7. Molecular and cellular endocrinology *220*, 59-65.
Tuuri, T., Eramaa, M., Hilden, K., and Ritvos, O. (1994). The tissue distribution of activin beta A- and beta B-subunit and follistatin messenger ribonucleic acids suggests multiple sites of action for the activin-follistatin system during human development. The Journal of clinical endocrinology and metabolism *78*, 1521-1524.
van Zijl, F., Mall, S., Machat, G., Pirker, C., Zeillinger, R., Weinhaeusel, A., Bilban, M., Berger, W., and Mikulits, W. (2011). A human model of epithelial to mesenchymal transition to monitor drug efficacy in hepatocellular carcinoma progression. Molecular cancer therapeutics *10*, 850-860.
Vassalli, A., Matzuk, M.M., Gardner, H.A., Lee, K.F., and Jaenisch, R. (1994). Activin/inhibin beta B subunit gene disruption leads to defects in eyelid development and female reproduction. Genes & development *8*, 414-427.
Vaughn, J.L., Goodwin, R.H., Tompkins, G.J., and McCawley, P. (1977). The establishment of two cell lines from the insect Spodoptera frugiperda (Lepidoptera; Noctuidae). In Vitro *13*, 213-217.
Vejda, S., Cranfield, M., Peter, B., Mellor, S.L., Groome, N., Schulte-Hermann, R., and Rossmanith, W. (2002). Expression and dimerization of the rat activin subunits betaC and betaE: evidence for the formation of novel activin dimers. Journal of molecular endocrinology *28*, 137-148.
Vejda, S., Erlach, N., Peter, B., Drucker, C., Rossmanith, W., Pohl, J., Schulte-Hermann, R., and Grusch, M. (2003). Expression of activins C and E induces apoptosis in human and rat hepatoma cells. Carcinogenesis *24*, 1801-1809.
Wada, W., Maeshima, A., Zhang, Y.Q., Hasegawa, Y., Kuwano, H., and Kojima, I. (2004). Assessment of the function of the betaC-subunit of activin in cultured hepatocytes. American journal of physiology *287*, E247-254.
Wada, W., Medina, J.J., Kuwano, H., and Kojima, I. (2005). Comparison of the function of the beta(C) and beta(E) subunits of activin in AML12 hepatocytes. Endocrine journal *52*, 169-175.
Wang, Q.F., Tilly, K.I., Tilly, J.L., Preffer, F., Schneyer, A.L., Crowley, W.F., Jr., and Sluss, P.M. (1996). Activin inhibits basal and androgen-stimulated proliferation and induces apoptosis in the human prostatic cancer cell line, LNCaP. Endocrinology *137*, 5476-5483.
Wharton, K., and Derynck, R. (2009). TGFbeta family signaling: novel insights in development and disease. Development (Cambridge, England) *136*, 3691-3697.
Woodruff, T.K. (1998). Regulation of cellular and system function by activin. Biochemical pharmacology *55*, 953-963.

Yu, J., Shao, L.E., Lemas, V., Yu, A.L., Vaughan, J., Rivier, J., and Vale, W. (1987). Importance of FSH-releasing protein and inhibin in erythrodifferentiation. Nature *330*, 765-767.
Zauberman, A., Oren, M., and Zipori, D. (1997). Involvement of p21(WAF1/Cip1), CDK4 and Rb in activin A mediated signaling leading to hepatoma cell growth inhibition. Oncogene *15*, 1705-1711.
Zhang, L., Duan, C.J., Binkley, C., Li, G., Uhler, M.D., Logsdon, C.D., and Simeone, D.M. (2004). A transforming growth factor beta-induced Smad3/Smad4 complex directly activates protein kinase A. Molecular and cellular biology *24*, 2169-2180.

9. Curriculum vitae

Personal information:

First Name / Surname:	Emine Sahin
Date of Birth:	14.06.1984
Citizenship:	Austria
Address:	Jägerstr. 91/14/3, 1200 Vienna
Email:	emi_sah@yahoo.de

School & University education:

Feb. 2010 – April 2011	Diploma Thesis at the Institute of Cancer Research, Medical University of Vienna – Supervision by Dr. Michael Grusch
since 10 / 2003:	Diploma study: Genetics and Microbiology, Specialization: Molecular genetics and pathology, University of Vienna
June 2002	Matura
1994-2002	AHS Unterstufe und Oberstufe, Karajangasse 14, 1200 Vienna